

Stereospecific Capillary Electrophoresis Assays for Methionine Sulfoxide Reductases

Dissertation

To Fulfill the

Requirements for the Degree of

„doctor rerum naturalium“ (Dr. rer. nat.)



seit 1558

**Submitted to the Council of the Faculty
of Biology and Pharmacy
of the Friedrich Schiller University Jena**

by M.Sc. Qingfu Zhu

born on 16. October 1985 in Anhui, China

Date of defense: 14.09.2015

Tag der mündlichen Prüfung:

Dekan: Prof. Dr. Frank Hellwig

1. Gutachter: Prof. Dr. Gerhard Scriba (University of Jena)
2. Gutachter: Prof. Dr. Stefan Heinemann (University of Jena)
3. Gutachter: Prof. Dr. Ulrike Holzgrabe (University of Würzburg)

My Family

Table of Contents

Acknowledgements	iii
Summary	v
Zusammenfassung	vii
1 Introduction	vii
1.1 Defining oxidative stress.....	1
1.2 Methionine oxidation	3
1.3 Methionine sulfoxide reductase.....	4
1.3.1 Msr variants and cellular locations	5
1.3.2 Catalytic mechanism of Msrs	6
1.3.3 Substrate specificity	7
1.4 Assays for Msr.....	9
1.5 Capillary electrophoresis	10
1.5.1 Modes of operation.....	12
1.6 Capillary electrophoretic enzyme assays	15
1.6.1 Off-line assay	15
1.6.2 In-capillary enzyme assays	16
2 Aims and scope	19
3 Materials and methods	21
3.1 Materials	21
3.2 Instrumentation	23
3.3 CE-based analysis systems.....	24
3.4 Method validation	29
3.5 Enzyme incubations.....	29
3.5.1 Free Met(O) as substrate	29
3.5.2 Fmoc-Met(O) as substrate (off-line assay).....	30
3.5.3 KIFM(O)K as substrate	30
3.5.4 KDM(O)DK, KDM(O)NK, KNM(O)DK, KFM(O)KK as substrates	31
3.6 Experimental design	31
3.7 Molecular modeling.....	32
4 Results	33
4.1 Off-line assay using free Met(O) as substrate	33
4.1.1 Method development and optimization.....	33
4.1.2 Method validation	35
4.1.3 Enzyme incubations.....	36

4.2 EMMA assay using Fmoc-Met(O) as substrate	40
4.2.1 Separation of FMOC-Met(O) diastereomers.....	40
4.2.2 EMMA.....	41
4.2.3 Method validation	45
4.2.4 Enzyme kinetics	46
4.3 Off-line CE assay using a diastereomeric peptide substrate.....	48
4.3.1 Evaluations of initial separation conditions.....	48
4.3.2 Method optimization by experimental design	49
4.3.3 Method validation	54
4.3.4 Enzyme incubations.....	55
4.4 Off-line assay for recombinant fungal MsrA and mutants using synthetic peptide substrates	58
4.4.1 Separation of Met(O) peptide substrates	58
4.4.2 Method validation	59
4.4.3 Enzyme incubations.....	60
4.4.4 Molecular modeling	62
4.5 CE separation of Met(O)-containing pentapeptide diastereomers	65
4.5.1 Investigation of dual system of cyclodextrin and achiral crown ether.....	65
4.5.2 Separation of Met(O)-containing peptide diastereomers by CD-mediated MEKC	73
5 Discussion	77
5.1 Separation of substrate diastereomers.....	77
5.1.1 Separation of Met(O) derivatives by MEKC	77
5.1.2 Separation of Met(O)-containing pentapeptide diastereomers.....	79
5.2 Assays for Msr enzymes	85
5.2.1 Off-line assay using free Met(O) as substrate.....	85
5.2.2 Electrophoretically mediated microanalysis (EMMA)	85
5.2.3 Off-line assays using Met(O)-containing pentapeptides as substrates	87
5.2.4 Activity determination for fungal MsrA and the mutants	88
6 Conclusion	91
Reference	91
Abbreviations	xxv
List of Publications and Presentations	xxvii
Curriculum Vitae	xxix
Eigenständigkeitserklärung	xxxii

Acknowledgements

I would never have been able to finish my dissertation without the support from these people whom I would like to thank. It is also because of them that I will always cherish my doctorate as a valuable memory in my life.

Foremost, I would like to express my sincere gratitude to my supervisor Prof. Dr. Gerhard Scriba, thank you for giving me an opportunity to work in your group and the continuous support for my Ph.D study, for your patience, enthusiasm, understanding, and immense knowledge. Your guidance helped me all the time during my research and writing of this thesis.

I take this opportunity to thank Prof. Dr. Stefan Heinemann and Dr. Roland Schönherr, from Department of Biochemistry and Biophysics, FSU Jena, for the nice cooperation, and for giving me the opportunity to use your lab for reproduction and purification of Msr enzymes, fruitful discussions as well as precious comments on the writing of the manuscripts. I also would like to thank Dr. Rabab GH Abdelaleem, thanks for providing Msr enzymes, useful suggestions and constant help.

I would like to express my great appreciation to Dr. Pavel Jáč, thanks for sharing your experience of using instruments, as well as your continuous help with the project, advice and insightful comments.

I am very grateful to all past and present members in our group for creating a great lab-atmosphere and for their support all this time. Special thanks to Henrik Harnisch for the translation of the summary into German in this thesis. Many thanks to my officemate Martina Hense for her kindness and help.

Special thanks to China Scholarship Council (CSC) for the financial support for the first three years during my Ph.D study.

Finally, I would like to thank my parents for their support, selfless love and affections. The deepest gratitude goes to my dear wife, Yuemin Hu. She has always been there cheering me up and standing by me through the good times and bad. A big thanks to my little girl, Yumo, for bringing us great happiness.

Summary

Met, either bound in proteins or in its free form is easily oxidized to Met(O) by reactive oxygen species. Met(O)-containing proteins accumulate during ageing and may play a role in degenerative diseases. Because of the chirality of the sulfoxide moiety, Met(O) exists as a pair of diastereomers Met-*S*-(O) and Met-*R*-(O). For the reduction of the diastereomers, stereospecific Msr enzymes exist. MsrA reduces free and protein-bound Met-*S*-(O), while MsrB reduces protein-bound Met-*R*-(O) with little affinity for free Met-*R*-(O). The latter is reduced by fRMsr. The aim of the present study was the development of stereospecific CE assays for Msr enzymes in order to study the stereospecificity of the enzymes. The substrates included Met(O), Met(O) derivatives as well as Met(O)-containing peptides. Upon establishment of the separation conditions, the methods were validated and subsequently applied for assaying recombinant human and fungal MsrA and MsrB enzymes.

An off-line assay was developed using free Met(O) as substrate. The separation of the Met(O) diastereomers, the product Met as well as β -alanine as internal standard was achieved upon derivatization of the analytes with dabsyl chloride by a MEKC method in a SMIL-coated capillary. The capillary coating consisted of a first layer of polybrene and a second layer of dextran sulfate providing a stable strong cathodic EOF and, consequently, highly repeatable analyte migration times. The assay was subsequently applied to screen the stereospecific activity of recombinant hMsrA and fungal fRMsr enzymes as well as to determine the Michaelis-Menten kinetics. An advantage of the present assay over existing assays is the fact that free Met(O) can be used as the natural substrate. In the assay, DTT was used as reducing agent for Msr recycling instead of using the coupled reaction involving Trx and Trx reductase so that no additional enzymes were required.

An in-capillary EMMA assay was established using Fmoc-Met(O) as substrate. The separation of diastereomers of Fmoc-Met(O), the product Fmoc-Met and the internal standard Fmoc- β -alanine was also achieved in a SMIL-coated capillary by a MEKC method. The partial filling mode was applied because the BGE contained SDS, which would lead to the denaturation of the enzyme. An injection sequence of incubation buffer-enzyme-substrate-enzyme-incubation buffer was selected. The assay was optimized with regard to the mixing time with a mixing voltage and subsequently applied for the analysis of stereospecificity of human MsrA and MsrB2. The Michaelis-Menten constant, K_m , and the maximum velocity, V_{max} , were determined. Essentially identical data were determined by the EMMA mode compared to off-line incubations. Compared to the off-line assay, the EMMA assay was fully automated and required smaller amounts of enzyme and substrates, thus, reducing the overall cost of the assay.

For the development of an assay using peptide substrates, the C-terminally dinitrophenyl-labeled, *N*-acetylated pentapeptide KIFM(O)K was chosen. The separation of the KIFM(O)K diastereomers and the reduced peptide KIFMK was achieved in a BGE containing sulfated β -CD and 15-crown-5 as buffer additives. The system was optimized using experimental design with regard to the buffer pH, ionic strength, sulfated β -CD and 15-crown-5, as well as capillary temperature and separation voltage. A fractional factorial response IV design was employed for the identification of the significant experimental factors and a five-level circumscribed central composite design for the final method optimization. The assay was successfully applied for the characterization of the stereospecificity of recombinant human MsrA and MsrB2 including the determination of the Michaelis-Menten kinetic data. Using this peptide substrate, lower K_m values but significantly higher k_{cat} constants were observed as compared to literature data reported for the substrates dabsyl-Met(O) and Fmoc-Met(O). Thus, the present pentapeptide-based assay may represent Msr activities towards protein-bound Met(O) in a better way as compared to simple amino acid derivative-based assays.

In order to better understand previous data that MsrA enzyme had a preference for peptide substrates with positively charged residues flanking Met(O), a group of peptide substrates was employed in combination with wild-type fungal MsrA and three mutants. The present data were in general agreement with the previous non-stereospecific assay except that the DE mutant (Glu99, Glu134) was not found to be more active than the wild-type enzyme for the reduction of KDM(O)DK. Interestingly, a reversed substrate preference was observed between the mutants DN (Glu99, Asn134) and EQ (Gln99, Asp134) reducing KDM(O)NK and KNM(O)DK. The asymmetric negative charges in the active center may explain this behavior. Molecular modelling was performed to rationalize the specificity and indicated that the conserved residue Glu99 in the active site of MsrA was buried in the Met-S(O) binding groove, which might contribute to the right placing of Met-S(O) and, consequently, to the catalytic activity of MsrA.

Finally, the dual selector system composed of a CD and a crown ether for the separation of the Met(O) peptide diastereomers was studied systematically using a series of *N*-acetylated Met(O) pentapeptides with a Dnp label at the C-terminus. Depending on the amino acid sequence and the applied CD, the addition of crown ethers, especially of the Krpytofix[®] diaza-crown ethers, resulted in a significant improvement of the resolution of the diastereomers of peptides containing basic amino acids. Charged CD derivatives such as carboxymethyl- β -CD and sulfated β -CD were superior compared to native β -CD. In contrast, the diastereomer separation of Met(O) peptides containing uncharged amino acids was found superior in a MEKC system in the presence of CDs.

Zusammenfassung

Met, entweder als Bestandteil von Proteinen oder frei vorliegend, kann durch reaktive Sauerstoffspezies zu Met(O) oxidiert werden. Met(O)-enthaltende Proteine akkumulieren während des Alterns im Körper und können an der Entstehung degenerativer Erkrankungen beteiligt sein. Aufgrund der Chiralität der Sulfoxid-Gruppe existiert Met(O) als das Diastereomerenpaar Met-*S*-(O) und Met-*R*-(O). Für die Reduktion der Diastereomere existieren stereospezifische Methioninsulfoxid-Reduktasen (Msr). MsrA reduziert freies sowie proteingebundenes Met-*S*-(O), MsrB-Enzyme bevorzugen proteingebundenes Met-*S*-(O). Das Enzym fRMsr reduziert freies Met-*R*-(O).

Die vorliegende Arbeit beschreibt die Entwicklung stereospezifischer Untersuchungsmethoden für Msr-Enzyme mittels Kapillarelektrophorese einschließlich off-line und online Assays. Folgende Substrate wurden verwendet: Met(O), Met(O)-Derivate und Met(O)-enthaltende Peptide. Nach der Etablierung der Trennbedingungen der Met(O)-Diastereomere und Met, erfolgte die Validierung dieser Verfahren.

Für einen offline-Assay wurde Met(O) als Substrat eingesetzt. Die Met(O)-Diastereomere, Met (Reaktionsprodukt) und β -Alanin (interner Standard) wurden nach der Derivatisierung mit Dabsylchlorid in einer SMIL-Kapillare mittels einer MEKC-Methode getrennt. Die Kapillarbeschichtung bestand aus einer Hexadimethrin- und einer Dextransulfat-Schicht. Durch diese Beschichtung ergab sich ein starker und stabiler kathodischer EOF mit gut reproduzierbaren Migrationszeiten. Die Methode wurde zum Screening der stereospezifischen Aktivität von hMsrA und aus Pilzen stammender fRMsr sowie zur Bestimmung der Michaelis-Menten Enzymkinetik eingesetzt. Ein Vorteil der Methode ist, dass freies Met(O) unmittelbar als Substrat angewendet werden konnte. DTT diente zum Recycling der Msr, so dass verglichen mit anderen Methoden, bei denen Trx- und Trx-Reduktase eingesetzt wurden, keine weiteren Enzyme notwendig waren.

Für den online-Assay kam Fmoc-Met(O) als Substrat zum Einsatz. Die Trennung der Diastereomere von Fmoc-Met(O), der reduzierten Spezies Fmoc-Met und des internen Standards erfolgte ebenfalls in einer Kapillare mit SMIL-Beschichtung unter Verwendung der MEKC. Die Injektionssequenz wurde wie folgt gewählt: Inkubationspuffer, Enzym, Substrat, Enzym Inkubationspuffer. Die Methode wurde im Hinblick auf Dauer und Höhe der angelegten Spannung, die zur Mischung der injizierten Plugs notwendig war, optimiert. Die Methode wurde zur Analyse der stereospezifischen Reaktionen der humanen Enzyme MsrA und MsrB2 verwendet. Weiterhin wurden die Michaelis-Menten-Konstante, K_m , und die maximale Reaktionsgeschwindigkeit, V_{max} , bestimmt. Die Daten waren vergleichbar mit Literaturdaten. Verglichen mit einem offline-Assay, konnte der EMMA-Assay in kürzerer Zeit mit geringerem Aufwand durchgeführt werden. Aufgrund der Automatisierung wurden geringere Proben- und Enzymmengen verbraucht, was die allgemeinen Kosten des Assays verringerte.

Als Peptid-Substrat wurde ein C-terminal mit Dinitrophenyl-Gruppe markiertes, N-acetyliertes Pentapeptid, KIFM(O)K, verwendet. Für die Trennung der KIFM(O)K-Diastereomere und des reduzierten Peptids KIFMK wurde folgende Faktoren optimiert: pH-Wert des Puffers, Pufferkonzentration, Konzentration des sulfatierten β -Cyclodextrins, Konzentration des Kronenethers 15-Krone-5, Kapillartemperatur und Spannung. Ein Fractional-Factorial-Response-IV-Design kam zur Bestimmung der signifikanten Faktoren zum Einsatz. Für die Methodenoptimierung wurde ein fünf Ebenen umschreibendes Central-Composite-Design gewählt. Das CE-Verfahren wurde zur Bestimmung der Stereospezifität humaner MsrA und MsrB2 einschließlich der Bestimmung der Michaelis-Menten-Kinetik verwendet. Verglichen mit Literaturwerten für dabsyl-Met(O) und Fmoc-Met(O), wurden niedrigere K_m -Werte, aber signifikant höhere k_{cat} -Konstanten ermittelt. Folglich bildet der vorliegende pentapeptidbasierte Assay die Msr-Enzymaktivitäten für proteingebundenes Met(O) besser ab, als auf Aminosäurederivaten basierende Methoden.

In vorangegangenen, nicht stereospezifischen Untersuchungen wurde festgestellt, dass MsrA Peptide bevorzugt umgesetzt hatte, bei denen Met(O) von positiv geladenen Aminosäureresten flankiert war. Zur Verifizierung dieses Sachverhalts wurden Peptide mit von Pilzen stammender Wildtyp-MsrA sowie drei ihrer Mutanten untersucht. Die Ergebnisse bestätigten diese Beobachtung. Die DE-Mutante (Glu99, Glu131) zeigte allerdings keine stärkere Aktivität gegenüber KDM(O)DK als der Wildtyp. Interessanter Weise wurde eine umgekehrte Substratpräferenz zwischen den Mutanten DN (Glu99, Asn134) und EQ (Gln99, Asp134) bezüglich der Reduktion von KDM(O)NK und KNM(O)DK festgestellt. Die asymmetrisch verteilte negative Ladung im aktiven Zentrum könnte dieses Verhalten erklären. Mit Hilfe von Molecular Modelling Untersuchungen konnte gezeigt werden, dass die konservierte, tief im aktiven Zentrum der Met-S(O)-Bindungstasche liegende Aminosäure Glu99, einen Einfluss auf die korrekte Bindung von Met-S(O) und somit auch auf die katalytische Aktivität von MsrA hat.

Zusätzlich wurde die Trennung der Diastereomere von N-acetylierten, C-dabsylierten Met(O)-Pentapeptiden bezüglich der Selektoren Cyclodextrin und Kronenether im Trennelektrolyt systematisch untersucht. In Abhängigkeit der Aminosäuresequenz und des verwendeten Cyclodextrins führte der Zusatz von Kronenethern, insbesondere Kryptofix[®] (Diaza-Kronenether), zu signifikant verbesserten Auflösungen der Diastereomere vom Peptiden, die basische Aminosäuren enthielten. Geladene Cyclodextrine, wie Carboxymethyl- β -CD und sulfatiertes β -CD waren nativem β -CD überlegen. Für Met(O)-Peptide, die ungeladene Aminosäuren beinhalteten, wurde mit der MEKC unter Verwendung CD-haltiger Puffer ein besseres Trennverfahren gefunden.

1 Introduction

1.1 Defining oxidative stress

Molecular oxygen is essential for the survival of aerobic creature, while the use of oxygen is fundamentally dangerous to their existence [1]. Aerobic organisms produce reactive oxygen species (ROS) inevitably during oxygen metabolism, which have the ability, either directly or indirectly, to damage all biomolecules, including proteins, lipids, DNA, and carbohydrates [2]. ROS, such as superoxide anion, hydroxyl radical and hydrogen peroxide, are generated under numerous conditions *in vivo*. The main endogenous source of ROS production is the mitochondrial metabolism, i.e., the respiration, when oxygen is reduced to water. Upon incomplete reduction of oxygen, superoxide and hydrogen peroxide are generated. The latter can further react with metal ions to form hydroxyl radicals [3, 4]. Other sources for ROS are cytochrome P450 metabolism, xanthine oxidase, inflammation processes as well as exogenous sources (**Fig.1**) [2, 5, 6]. Higher eukaryotic aerobic organisms cannot survive without oxygen which makes them constantly exposed to various forms of ROS. Researches have shown that low levels of ROS are indispensable in many biochemical processes in cells, including in signaling pathways [7, 8], gene expression and pathogen elimination [9]. However, excessive amounts of ROS are harmful for cells. Given that ROS exist unavoidably under aerobic conditions, it is not unexpected that cells and tissues have developed sophisticated mechanisms such as antioxidants, enzymes as well as repair systems to counteract oxidative damage (**Fig. 1**).

Helmut Sies proposed the concept of oxidative stress as “imbalance between oxidants and antioxidants in favor of the oxidants, potentially leading to damage” [10], which was later extended to a definition that describes a disruption of redox signaling and control [11]. Under normal circumstances, the formation of oxidants is counteracted by antioxidants so that there is minimal modification of biomolecules. Oxidative stress occurs when the balance of the formation of oxidants exceeds the ability of antioxidant system to remove ROS. Thus, biomolecules become subject to attack by excess ROS and significant molecular and physiological damage will occur.

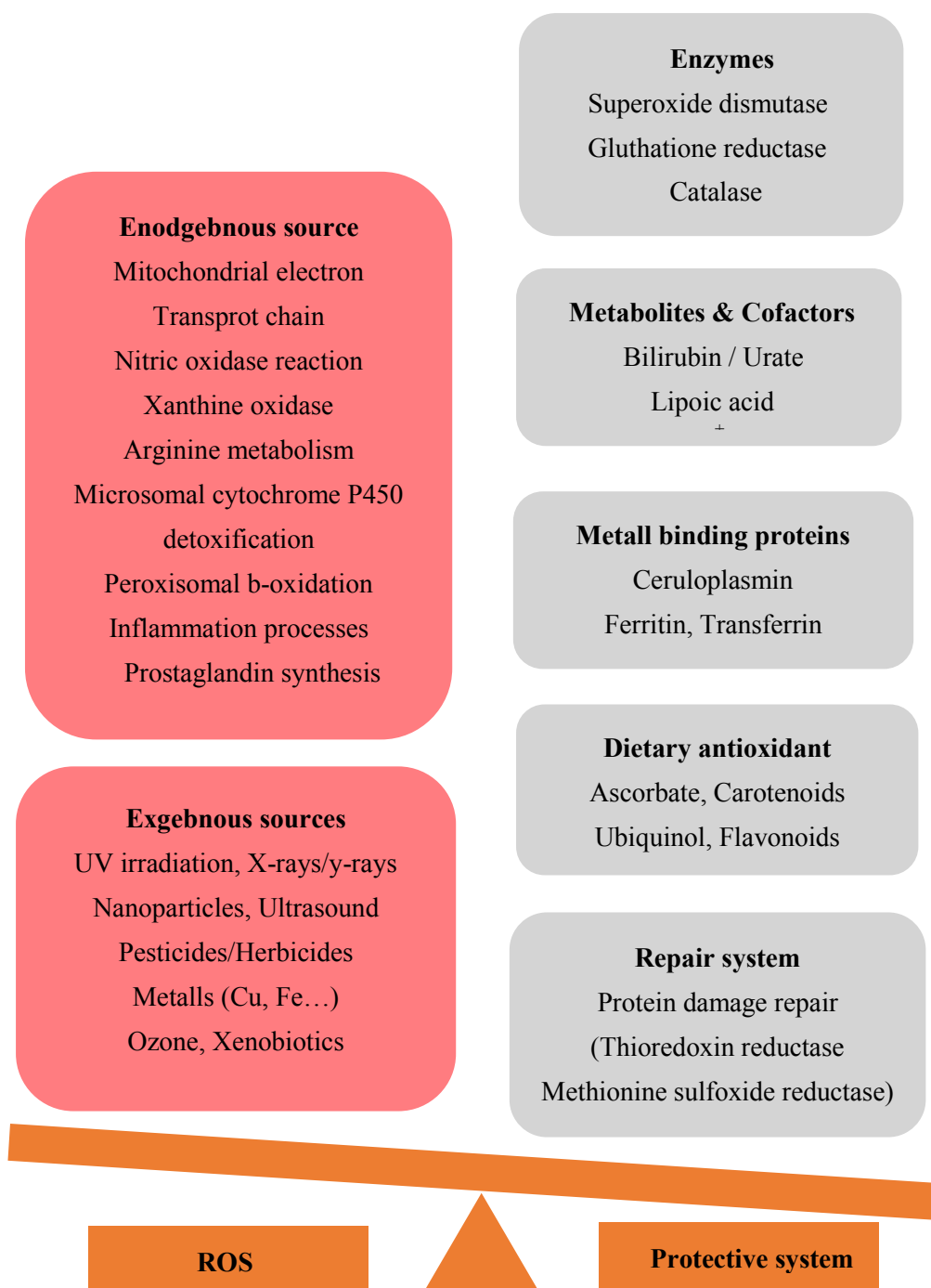


Fig. 1: The occurrence of oxidative stress depends on the interaction between the cellular antioxidative system and the formation of ROS. When the antioxidative capacity is not sufficient in detoxification of ROS products, oxidative stress appears. In this case, the balance would be in favor of ROS. Adapted from [2].

When oxidative stress happens in cells, ROS are able to damage cellular components like proteins, DNA, carbohydrates as well as polyunsaturated fatty acid [12 - 14]. Thereinto, proteins as most abundant constituent in cells are primarily attacked by ROS. Both amino acid residue side chains and the protein backbone can be targeted. Oxidative modification of proteins can involve cleavage of the polypeptide chain, modification of amino acid side chains as well as conversion of the protein to derivatives which are highly sensitive to proteolytic degradation [15 - 17]. As a result of this change, the affected proteins lose their biochemical functionality, and finally lead to protein aggregation [18, 19]. More and more evidences have shown that protein oxidation is implicated to many neurodegenerative diseases such as morbus Alzheimer [20 - 22] and Parkinson [23], as well as a wide range of age-related problems [17, 24, 25].

1.2 Methionine oxidation

Among all amino acid residues of proteins, the two sulfur-containing amino acids, cysteine (Cys) and methionine (Met), are easily oxidized even under mild conditions [26, 27]. Most Met residues are found in the hydrophobic core of proteins due to their strong hydrophobicity. Such Met residues are fairly protected from ROS, while the surface exposed Met residues are more susceptible to oxidation [28, 29]. The oxidation of Met generates methionine sulfoxide [Met(O)] which is more hydrophilic than Met, and this often results in an alternation of protein structure.

Both free Met and its protein bound form can be oxidized. Upon oxidation to the sulfoxide, the sulfur atom becomes a chiral center. Thus, Met(O) exists as a pair of diastereomers, i.e. L-methionine-(*S*)-sulfoxide [Met-*S*-(O)] and L-methionine-(*R*)-sulfoxide [Met-*R*-(O)]. There is no evidence for the preferential formation of one diastereomer of Met(O) over the other in proteins or in its free form during oxidation, except for the oxidation induced by flavin-containing monooxygenase 3 [30, 31]. Although Met(O) is a fairly stable product, the sulfur can be further oxidized to a sulfone by strong oxidants leading to an irreversible product, which occurs to a low extent also under biological conditions [32]. In contrast, cells have developed a system for Met(O) reduction. Methionine sulfoxide reductases (MsrS) are the enzymes for this function and thus are at present considered as protein repair enzymes.

1.3 Methionine sulfoxide reductase

Protein-bound as well as free Met(O) can be reduced by methionine sulfoxide reductases (Msr) [33, 34]. For the reduction of the individual diastereomers two types of Msr enzymes, MsrA and MsrB, exist. They share little sequence homology but possess mirror-like relationships of their active sites [35]. MsrA reduces Met-*S*-(O) bound in proteins or as free amino acid [36 - 38]. MsrB proteins reduce the Met-*R*-(O) but display only low activity for the reduction of free Met-*R*-(O) [38, 39]. In addition, an enzyme named free methionine-*(R)*-sulfoxide reductase (fRMsr) has been described in bacteria [40, 41] and fungi [42], which specifically reduces free Met-*R*-(O) (**Fig. 2**). Msr enzymes are considered as an important defense system to protect cells against oxidative stress [34, 43].

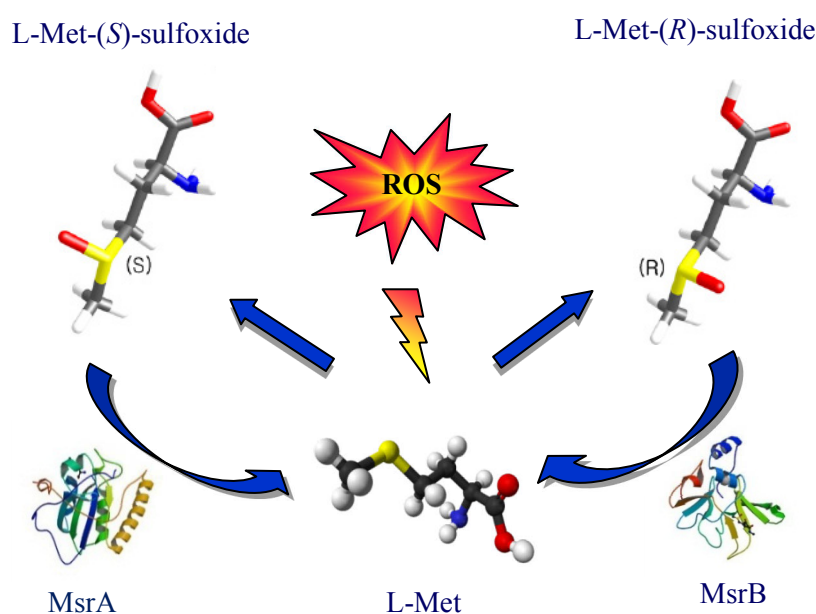


Fig. 2: Methionine oxidation and methionine sulfoxide reduction

Research suggests that MsrA concentrations decline in different rat tissues during aging [44]. In addition, lower levels of MsrA are also found in Alzheimer [45] and Parkinson [46] patients. Deletion of Msr or loss of enzyme activity reduces the lifespan in mice [33], whereas its overexpression was shown to extend the lifespan of fruit flies [47]. Furthermore, Msr may also regulate protein function by controlling the redox state of critical Met residues [48 - 50]. In terms of calcium/calmodulin ($\text{Ca}^{2+}/\text{CaM}$)-dependent protein kinase, the protein activity is enhanced by

angiotensin II-induced oxidation of paired regulatory domain Met residues in the absence of $\text{Ca}^{2+}/\text{CaM}$, while this is reversed via Met(O) reduction by MsrA [48].

Interestingly, recent studies indicate that bacterial MsrA can also function as a stereospecific oxidase which oxidize Met77 to Met-S-(O) specifically in calmodulin as well as several model substrates in the absence of reductant, whereas such behavior could not be observed for bacterial MsrB of fRMsR [51, 52]. Other studies showed that Met-S-(O) epimerase may exist. Kumar et al. observed a yeast mutant lacking MsrA and MsrB but overexpressing MsrB form *Drosophila melanogaster* was able to grow on Met-R-(O) medium as well as Met-S-(O) medium [53]. This is also indicated by the fact that MsrA and MsrB double knock-out mice showed growth deficiency when fed with Met restriction, while the deficiency can be compensated given that one gene is present [54]. This seems especially important to the endoplasmic reticulum because only MsrB can be found in this organelle [55, 56].

1.3.1 Msr variants and cellular locations

There is one gene encoding MsrA in mammals including humans [57]. The most abundant MsrA form expressed from this gene contains a typical N-terminal mitochondrial signal peptide. The mouse protein containing a mitochondrial signal peptide is found targeting to the cytosol and nucleus as well as to mitochondria [58]. In contrast to a single MsrA gene, three separate MsrB genes have been identified in mammals [43, 56]. The first known MsrB, MsrB1, is a selenoprotein and localized in mitochondria and the nucleus [56]. MsrB2 (also known as CBS-1) contains a cysteine residue instead of the selenocysteine and an N-terminal signal peptide exclusively targeting to mitochondria [56]. The third mammalian MsrB, MsrB3, also contains a cysteine residue in the active site, but develops into two forms, MsrB3A and MsrB3B by alternative first exon splicing [56]. MsrB3A contains an endoplasmic reticulum (ER) signal peptide at the N-terminal and an ER retention signal at the C-terminal, whereas MsrB3B contains a different signal peptide at the N-terminal and is targeted to mitochondria [34, 56].

Findings show that MsrA and MsrB are present in multiple cellular locations indicating that a methionine sulfoxide reduction system is maintained in different compartments in mammalian cells for the repair of oxidized methionine residues [34] (**Fig. 3**). The fact that three MsrB variants located in different cellular compartments may imply that each protein has a role in antioxidant defense [34]. The simultaneous presence of MsrA and MsrBs in multiple compartments suggests that these two enzymes complement the function of each other. Although there is no evidence for the presence of

MsrB in ER, it could be speculated that a Met-S-(O) epimerase may exist, which makes Met-S-(O) residuals accessible to MsrB [58 - 60].

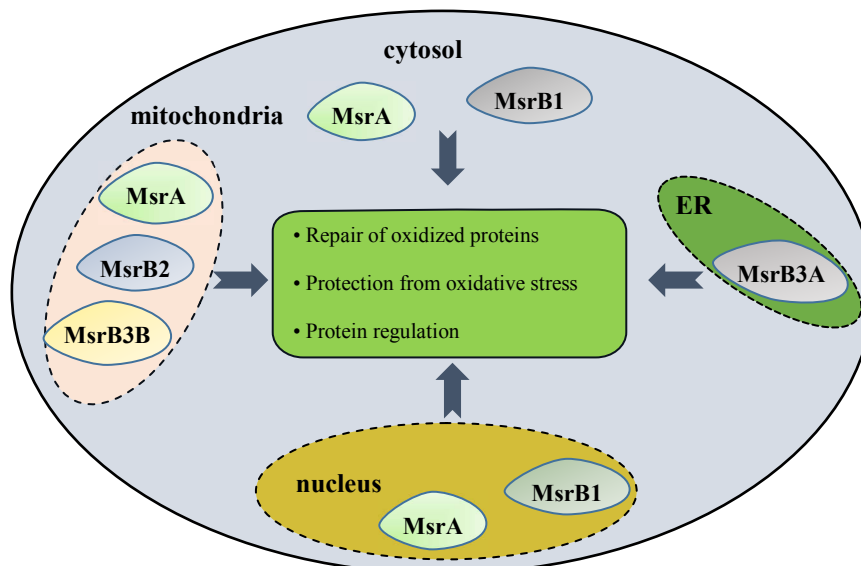


Fig. 3: Msr variants and cellular locations (adapted from Kim 2007).

1.3.2 Catalytic mechanism of Msrs

The catalytic mechanism of different Msrs is quite similar and involves the interaction of the methionine sulfoxide substrate with the catalytic cysteine residues [38, 61, 62]. The number of cysteine involved in catalytic cycle may vary between organisms. Most Msrs possess two Cys residues, one for catalysis and the other for recycling of the Msr [63, 64]. **Fig. 4** shows the general catalytic mechanism of Met(O) reduction in terms of MsrA catalysis. The catalytic process requires reductants in order to regenerate the reduced Cys residues in Msrs. The oxidoreductases thioredoxin (Trx) and glutaredoxin (Grx) are physiological reductant of Msrs. *In vitro*, dithiothreitol (DTT) also can be used to regenerate Msrs [65, 66].

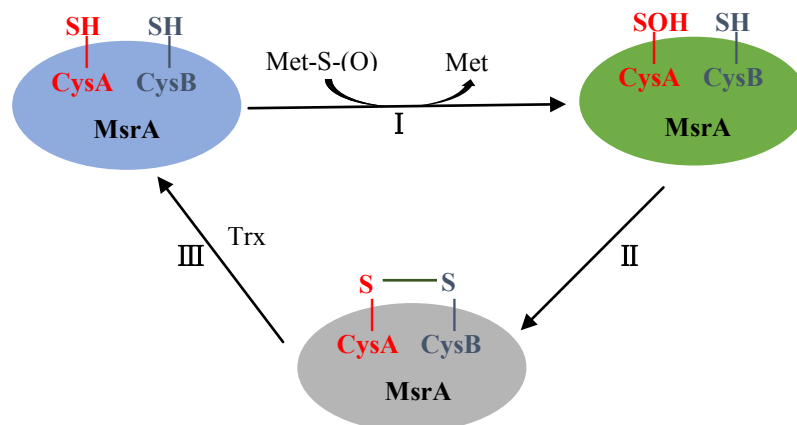


Fig. 4: General catalytic mechanisms of MsrA. In the first step (I), the substrate, Met-S-(O), is reduced by MsrA. The catalytic Cys of MsrA, CysA (shown in red), attacks the sulfur atom of Met(O) leading to a sulfenic acid intermediate. The following steps are to regenerate the enzyme. The nucleophilic attack of a recycling CysB (shown in blue) on the sulfur atom of the relatively unstable sulfenic acid intermediate results in the formation of disulfide bond (step II). Finally, the CysA-CysB disulfide bond is reduced by Trx in step III and the Msr with reduced catalytic and recycling Cys is released. DTT can be used in vitro as reductant in place of Trx. Adapted from [34].

Serine substitution of the catalytic Cys of Msrs completely inhibits enzyme activity suggesting that the essential function of the catalytic Cys in Msr function [65]. In contrast, serine substitution of the recycling Cys still allows the reduction of Met(O) but not the regeneration of the enzyme [67]. Furthermore, some Msrs have evolutionarily replaced the catalytic Cys by a selenocysteine (Sec), leading to a higher chemical reaction rate with electrophiles as well as a higher reduction potential compared to Cys [68, 69]. This may contribute to the increased redox activity of seleno-enzymes compared to the Cys-containing enzyme analogs [70].

1.3.3 Substrate specificity

Although MsrA and MsrB enzymes have distinct three-dimensional structures, determination of the protein structure from various organisms indicates a mirror-like relationship between the two enzymes active sites, in which a Trp faces the catalytic Cys and allows the docking of the substrate in the optimal position for the reduction [35, 38, 71] (**Fig. 5**). This mirror-like relationship ensures the enzymatic stereospecificity of MsrA and MsrB [38]. It should be noted that MsrA enzyme

contains two acidic residues (Asp134 and Glu99) in the active site compared to MsrB enzyme, which is thought to be related to the preference of MsrA for peptide substrates which compose positively charged residues flanking Met(O) [42, 73].

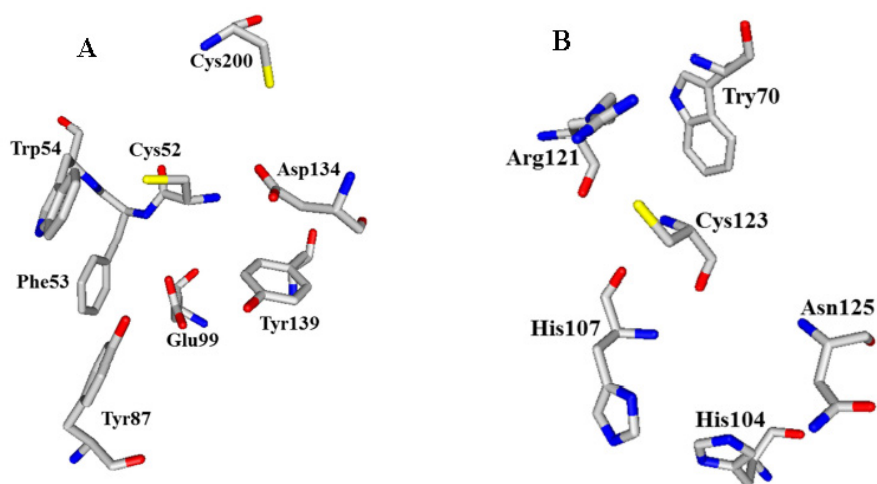


Fig. 5: Active-site models of *A. nidulans* MsrA and MsrB. (A) Stick representation of MsrA residues Cys52, Phe53, Trp54, Tyr87, Glu99, Tyr139, Asp134, and Cys200. (B) Sticks representation of MsrB active site residues Cys123, Arg121, His107, Try70 and Asn125. Atom color as follows: carbon in gray; nitrogen in blue; oxygen in red and sulfur in yellow. Adapted from [42].

MsrA has a broad substrate specificity and can reduce free Met-S(O), protein-bound Met-S(O) as well as other Met(O) derivatives, such as 4-*N,N*-dimethylaminoazobenzene-4'-sulfonyl (dabsyl)-Met-S(O) [53, 73, 74], *N*-acetyl-Met-S(O) [75], 9-fluorenylmethyloxycarbonyl (Fmoc)-Met-S(O) [76, 77] and ethionine-Met-S(O) [78]. Even dimethylsulfoxide (DMSO) can serve as a substrate for MsrA [79]. MsrB is specific for protein-bound Met-R(O) and Met(O) derivatives, but displays only low activity towards free Met-R(O) [38, 39]. Additionally, fRMsr only catalyzes the reduction of free Met-R(O) and does not reduce protein-bound Met(O) or derivatives [80, 81]. In support of the fact that MsrA and MsrB have dramatically different catalytic properties for the reduction of free Met(O), *E.coli* MsrA has been shown to possess a 1000-fold higher catalytic efficiency for the reduction of free Met-S(O) compared to *E.coli* MsrB for the reduction of free Met-R(O) [40]. Furthermore, human SK-Hep 1 cells failed to grow on free Met-R(O) supplemented media without Met, whereas they grow well on the corresponding Met-S(O) supplemented media [80].

Kinds of Met(O)-containing protein substrates have been reported recently [82]. Given the three-dimensional structures of these protein substrates, only oxidized Met residuals located on the protein surface can be reduced, unless the oxidized Met residues positioned within the three dimensional structure provoke an unfolding of the protein [83, 84].

Furthermore, some drugs containing a methylsufinyl group such as sulindac, mesoridazine or triclabendazole can only be reduced by MsrA, but not by MsrB, illustrating the broad substrate range of MsrA [85 - 88]. This also offers new insights into drug metabolism and may provide therapeutic opportunities for increased efficacy of drugs by utilizing a particular enantiomer instead of the racemic mixture.

1.4 Assays for Msr

To determine the activity of Msrs, several *in vitro* assays have been developed, including the direct detection of Met in the reduced/oxidized state and the indirect evaluation of the enzymatic activity by following the oxidation of the cosubstrate NADPH using a NADPH-coupled Trx system. A radiation assay was based on the reduction of *N*-acetyl-[³H]-Met(O) to *N*-acetyl-[³H]-Met, which is extracted into an organic solvent followed by scintillation counting [89, 90]. Reduction of [³H]-Met(O) could also be analyzed by TLC [90]. HPLC-based methods were developed utilizing labeled amino acids such as Fmoc-Met(O) [76] or dabsyl-Met(O) [36, 73, 90] as substrate and DTT as reducing agent. Dabsyl-Met(O) was also used as substrate in a photometric assay where the product dabsyl-Met was extracted into organic solvent [91, 92]. Another type of photometric assay followed the oxidation of NADPH in a coupled reaction using the Trx reduction system with various substrates [75, 79] (**Fig. 6**). This method is based on the fact that MsrA coupled with Trx reductase catalyzes the reduction of Met(O) and simultaneously initiates the oxidation of NADPH so that the enzyme activity could be evaluated by following the decrease of UV absorbance of NADPH at 340 nm. However, this indirect assay is not specific, as it involves Msr enzymes, Trx and Trx reductase, and thus reflects the total activity of the system.

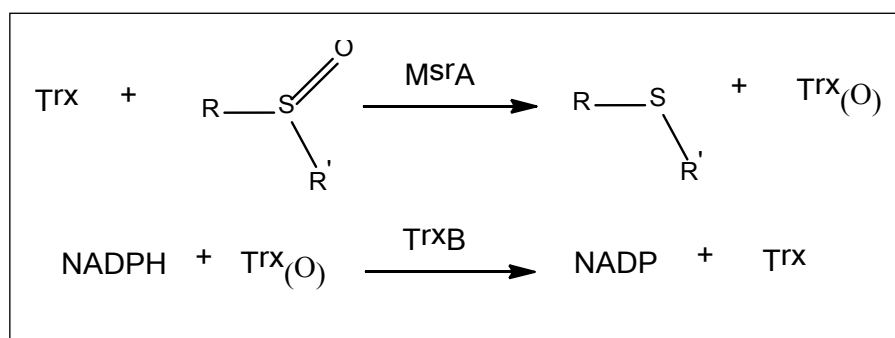


Fig. 6: Coupled reaction for the reduction of methyl sulfoxide compounds catalyzed by *MsrA*. *NADPH* is the hydrogen donor for the reduction of oxidized Trx [*Trx(O)*] by thioredoxin reductase (*TrxB*). The reduced Trx reduces methionine sulfoxide containing compounds by *MsrA* with the formation of methyl sulfide and regeneration of *Trx(O)*.

Detection methods also include mass spectrometric analysis, which is so far the only method that has been used to identify oxidized proteins and determine the extent of Met oxidation on a proteome-wide scale [65]. It should be mentioned that the unavoidable Met oxidation during MS analysis due to the ionization process makes the observed Met oxidation imprecise [93 - 95]. The oxidation of Met in proteins could be globally analyzed immunologically by western blot as well, even though the exact site of oxidation cannot be identified in this approach [65, 96 - 98].

To study the stereospecificity of Met(O) reduction by Msr enzymes, the individual diastereomers dabsyl-Met-*S*-(O) and dabsyl-Met-*R*-(O) have been frequently used as substrates [36, 73]. Recently, Uthus developed a capillary electrophoresis (CE) assay for Msr enzymes based on the separation of the dabsyl-Met(O) diastereomers [99].

1.5 Capillary electrophoresis

CE is one of most efficient separation tools and has matured as a versatile and flexible analytical technique that combines simplicity, flexibility and high reproducibility [100]. In CE, the analyte separation is carried out in a capillary with an inner diameter of 20 to 100 μm which allows the application of high voltage due to dissipation of Joule heat. UV- or the laser induced fluorescence detection is often applied as detection mode and carried out on-column. The hyphenation to a mass spectrometer to CE has become a routine as well. CE has proved useful for the separation of small

molecules such as amino acids, drugs, inorganic ions, as well as the analysis of large molecules including proteins, DNA restriction fragments, and even whole cells and virus particles.

The separation of analytes in CE is based on the difference of the electrophoretic mobilities of charged molecules upon the application of high electric field strength. The mobility of an analyte is determined by the electrophoretic mobility of a particle, μ_{ep} , as a function of charge, q , and the size of the analyte represented by the radius, r , for a spherical particle according to:

$$\mu_{ep} = \frac{q}{6\pi\eta r} \quad (1)$$

η is the viscosity of the background electrolyte. In case of acidic or basic analytes, the charge is a function of the pKa of the analytes and the pH of the electrolyte solution. The charge-to-size ratio is also generally referred to as charge density.

A fundamental constituent of CE is the electroosmotic flow (EOF), which is the bulkflow of the liquid in the capillary formed as a consequence of the surface charge on the interior capillary wall. The EOF has a plug-like flow profile compared to the parabolic flow profile of pressure driven chromatographic techniques, which makes CE a high resolution technique. The mobility of the EOF is a function of the permittivity of the electrolyte solution, ϵ , and the zeta-potential, ζ , resulting from the negatively charged capillary surface due to pH-dependent dissociation of the silanol groups:

$$\mu_{EOF} = \frac{\epsilon\zeta}{4\pi\eta} \quad (2)$$

Consequently, the effective mobility of a solute is the sum of both electrophoretic forces, μ_{ep} and μ_{EOF} , according to:

$$\mu_{eff} = \mu_{ep} + \mu_{EOF} \quad (3)$$

Under normal conditions (that is, a negatively charged capillary surface), the magnitude of EOF can be more than an order of magnitude greater than the mobility of analytes so that the EOF is able to drive the movement of nearly all species, regardless of charge, in the same direction. Modification of

the capillary wall (by pH or additives) can decrease or even reverse the EOF to achieve opposite movement direction of anions and cations.

1.5.1 Modes of operation

The versatility of capillary electrophoresis is derived from the numerous modes of operation. The main separation modes in CE are capillary zone electrophoresis (CZE), capillary electrokinetic chromatography (CEKC), capillary electrochromatography (CEC), capillary isotachopheresis, capillary gel electrophoresis and capillary isoelectric focusing. For the most part, the different modes can be realized simply by altering the buffer composition, which makes CE a very flexible and cost-effective technique. The CZE and CEKC are most commonly used CE modes and will be discussed here in more details.

1.5.1.1 CZE

CZE is the simplest form of CE, in which a capillary is filled with an electrolyte and the sample is introduced at the inlet as a narrow zone. As an electric field is applied, each component in the sample zone migrates according to its own apparent mobility, which depends on the charge-to-size ratio of this chemical compound (see equation 3). Separation of both anionic and cationic solutes is possible by CZE in one analysis.

1.5.1.2 CEKC

CEKC is based on electrophoretic migration as well as on the chromatographic separation principles. Many selectors can be added to the background electrolyte (BGE), such as surfactants [101, 102], cyclodextrins (CDs) [103 - 105], antibiotics [106], crown ethers [107], ligand exchangers [108] and proteins [109]. In this mode, the buffer additives represent a so-called pseudostationary phase that may possess its own electrophoretic mobility. The transport of the analyte and/or the analyte-additive complex to the detector is accomplished by electrokinetic phenomena. The separation is based on the different partitioning of the analytes between pseudophases and aqueous phase [110]. Therefore, the selector-based separation is a hybrid of electrophoresis and chromatography thus termed as electrokinetic chromatography. The presence of the additive in the BGE also allows a rapid change of the experimental conditions enabling rapid method development.

Micellar electrokinetic chromatography (MEKC)

MEKC is a mode of CEKC, in which surfactants such as sodium dodecyl sulfate (SDS) are added to the buffer solution. At a concentration above the critical micelle concentration (CMC), the surfactant molecule aggregates and micelles are formed. The hydrocarbon tails (hydrophobic) will be oriented toward the center of the aggregated molecules, whereas the polar head groups point outward. **Fig. 7** schematically shows a typical separation by MEKC. During the electrophoretic migration, the analytes partition differentially between the micelles and the running buffer resulting in different migration velocities so that the analytes can be separated. Therefore, MEKC is not only effective for the separation of charged species but also for neutral compounds. Furthermore, it has also been applied for the separation of diastereomers due to slight difference of distribution coefficients between micelles and aqueous phase existing for diastereomers [111 - 113].

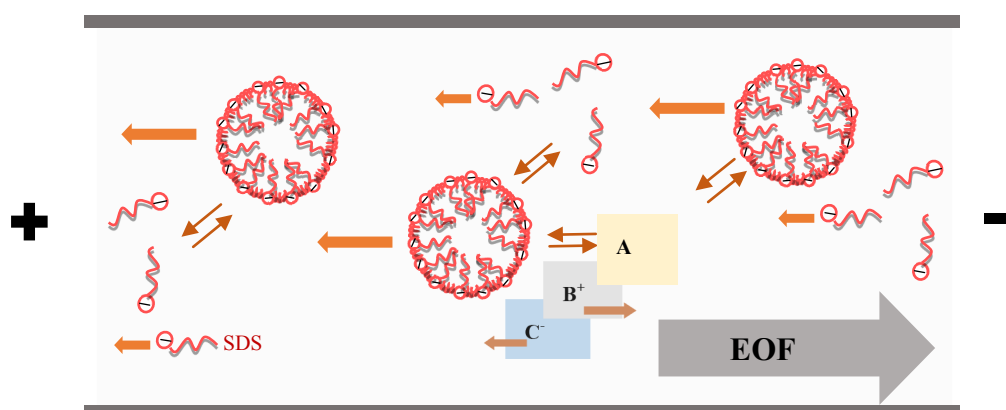


Fig. 7: Illustration of a separation by MEKC. A, B⁺, C⁻ are neutral, positively charged and negatively charged species in a sample.

CD-mediated CEKC

CDs are cyclic oligosaccharides which consist of $\alpha(1,4)$ -linked D-glucose units obtained by the digestion of starch by certain *Bacillus* strains [114]. CDs are by far the most often applied chiral selectors for the separation of stereoisomers owing to their commercial availability, UV transparency and relatively low prices. The basic structures comprise six, seven, or eight glucopyranose units attached by α -1,4 linkages and are referred to as α -, β -CD and γ -CD, respectively (**Fig. 8**).

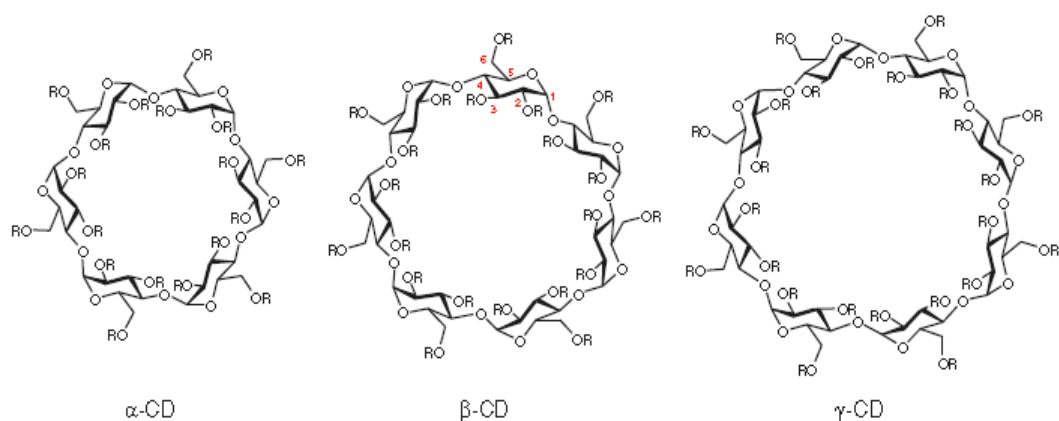


Fig. 8: Structures of native cyclodextrins.

The interior of the CD is hydrophobic. The narrow rim contains the primary 6-hydroxyl groups of the glucose molecules while the wider ring is formed by the secondary 2- and 3-hydroxyl groups. The hydroxyl groups can be derivatized resulting in a large variety of CD derivatives with uncharged or charged substituents. Complex formation is believed to occur via the inclusion of lipophilic moieties of the analytes in the hydrophobic cavity with secondary interactions including hydrogen bonding or dipole-dipole interactions with the hydroxyl groups or polar substituents [105, 115]. In case of charged CDs, ionic interactions will contribute to the binding.

Crown ethers as additives

Crown ethers are macrocyclic compounds. The polyether ring system in the structure forms a cavity which is able to include alkali and alkaline earth metal cations, ammonium and protonated alkylamines [116 - 118]. Kuhn et al. were the first to report the use of a chiral 18-crown-6 tetracarboxylic acid (18C6H4) as a chiral recognition agent to separate the enantiomers of a variety of primary amino compounds. In the subsequent study [119], an interesting synergistic effect was observed with the simultaneous use of α -CD and 18C6H4. Later, the achiral crown ethers such as 18-crown-6 (**Fig. 9A**) and Kryptofix[®] 22 (**Fig. 9B**) were also used in the combination with different CDs to improve the separation [120 - 125].

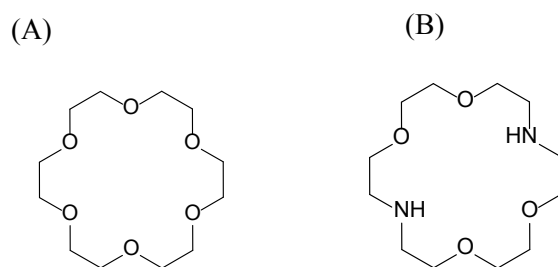


Fig. 9: Structures of crown ethers. (A) 18-crown-6 and (B) Kryptofix[®]22 (4,13-diaza-18-crown-6, 1,7,10,16-tetraoxa-4,13-diazacyclooctadecane)

1.6 Capillary electrophoretic enzyme assays

1.6.1 Off-line assays

CE has been frequently applied to enzyme analysis due to advantages such as high separation efficiency, rapid, low cost and integration of various detection modes [126 - 130]. Initially, it was used only as a separation tool in pre-capillary assay, in which the incubation of substrate, cofactor, and enzyme is carried in a separate vial and CE used for analysis (**Fig. 10**).

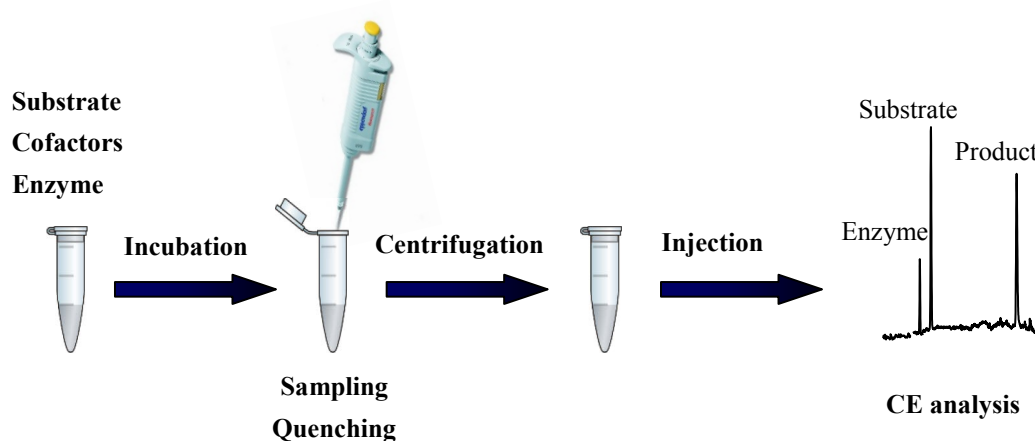


Fig. 10: Typical procedures for an off-line CE-based enzyme assay

Either the enzyme or the substrate is added to start the reaction. After incubation for an intended period of time, the reaction is most often quenched before subjected to CE analysis. Centrifugation of precipitated proteins is usually performed to prevent capillary clogging before sample injection. In pre-capillary assays, only the determination of substrate(s) and/or reaction product(s) are performed by means of CE, so that this method can be classified as an off-line assay. It is also the most frequently used method for the CE-based enzyme analysis. Since Krueger et al. used CE for the first time to determine the activity of endopeptidase Arg-C [131], numerous CE methods have been developed for many enzymes of diverse actions and origins.

1.6.2 In-capillary enzyme assays

To further miniaturize the CE assay, the incubation and the separation can be integrated into a single capillary [130, 132 - 134], because a capillary tube can serve as (i) a microreactor to carry out a reaction in a nanoliter volume, (ii) a separation column to separate the substrate and reaction product and (iii) a detection cell to quantify the substrate as well as the product. By integration of all reaction and analysis steps into a single capillary, in-capillary (on-line) assays allow a higher degree of automation and realize a further miniaturization of the analytical system.

In order to perform an in-capillary assay, the enzyme can be either immobilized onto the capillary wall or injected as plugs in solution [126, 128, 134 - 136]. In order to prepare immobilized enzyme bioreactors, many approaches can be employed including physical adsorption, ionic binding, covalent binding and sol-gel entrapment [134]. Although immobilization of the enzyme in the capillary results in a longer enzyme lifetimes, this method limits the buffer choices especially when the incubation buffer is not compatible with the separation buffer.

The first in-capillary assay by injecting enzyme plugs was described by Bao and Regnier [132] and was performed by injecting a zone of enzyme into a capillary filled with a solution of the substrate. The product is continuously formed during the electrophoretic mixing of enzyme and substrate. This method was latter defined as the long contact of electrophoretically mediated microanalysis (EMMA) [130, 137] (**Fig. 11A**), which also known as the continuous or zonal EMMA. The enzyme solution can alternatively be introduced in the capillary first followed by an injection of the substrate plug.

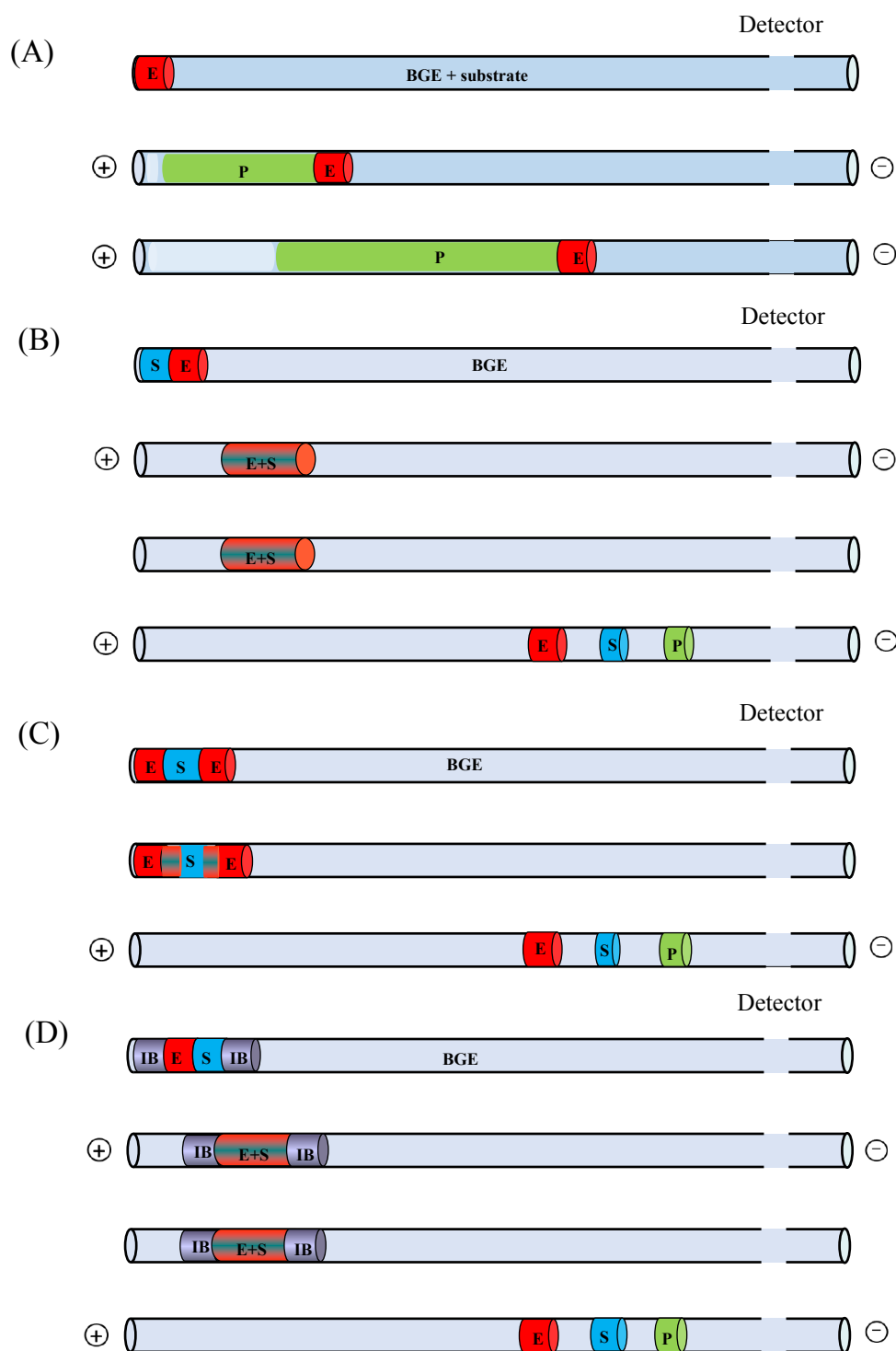


Fig. 11: Schematic illustration of the commonly used modes of EMMA for enzymatic assays. (A) Long contact mode; (B) Short contact mode; (C) At-inlet reaction mode (longitudinal diffusion) and (D) partial filling plug-plug mode. Zones of the reagents are labeled as follows: IB, incubation buffer; E, enzyme; S, substrate; P, product. Plus “ \oplus ” and minus “ \ominus ” marks mean that at the given step, voltage is applied.

In contrast to the long contact mode, the plug-plug EMMA mode was developed by injection of consecutive plugs of reactants into the capillary, which is also known as the short contact mode (**Fig. 11B**). The enzymatic reaction is initiated by the application of an electric field since the zones interpenetrate due to the difference in their electrophoretic mobilities. Normally, the first injected plug between enzyme and substrate should be the one with the lower electrophoretic mobility to ensure plug overlap [138]. After the electrophoretic mixing, the capillary is normally left for a period of time without voltage for a zero potential amplification and followed with CE separation [130, 139].

In the plug-plug mode of EMMA, the mixing of the zones could also be achieved by simple diffusion at the inlet of the capillary, in which longitudinal diffusion between short plugs (**Fig. 11C**) [135] or/and transverse diffusion of laminar flow profiles (TDLFP) [140] generated by pressure is/are contributing to the zone mixing. This is also termed “at-inlet reaction mode” and is especially suitable for enzymes not resistant to an electric field.

In many cases, the separation buffer may be incompatible with the incubation conditions due to pH, the presence of additives, etc., which may impair the enzyme. In this case, an additional plug of incubation buffer can be injected first to protect the enzyme from separation buffer. This is termed “partial filling mode” in EMMA [141] (**Fig. 11D**). The plug-plug mode has been the most commonly used EMMA mode due to the fact that less amount of reactant is required compared to the long contact EMMA mode.

EMMA offers a simple way for the study of enzyme reactions with in-capillary assays, including screening of enzyme activities, enzyme kinetics, and inhibitor studies [142 - 146]. The application of EMMA method can also be extended to in-capillary derivatizations [130] as well as investigation of chemical reactions [147].

2 Aims and scope

MsrA and MsrB are repair enzymes that reduce Met(O) residues to Met in a stereospecific manner. The enzymes have been extensively studied, and several assays have been reported for the determination of the *in vitro* activity (see chapter 1.4) However, less attention has been paid to stereospecific methods for Msr enzymes provided the fact that MsrA and MsrB work on opposite diastereomers of Met(O). As a powerful analytical technique, CE has unique advantages for the separation of structurally close compounds, which makes CE an ideal tool for the study of the stereospecificity of Msr enzymes.

Hence, the aim of this work was the development of stereospecific CE methods for Msr enzymes that allow to study and characterize recombinant enzymes. The substrates should comprise free Met(O), Met(O) derivatives as well as Met(O) containing peptides. Consequently, the specific objectives of the research included:

1. Development of an off-line assay using free Met(O) as substrate. Upon incubation, the amino acids should be derivatized with dabsyl chloride because the dabsyl-Met(O) diastereomers can be separated by MEKC [99].
2. Development of an in-capillary assay in order to further miniaturize the system. Fmoc-Met(O) should be used as substrate because it is commercially available and has been applied as Msr substrate in the literature [76, 77].
3. Development of an off-line assay using Met(O)-containing peptides as substrate. Because the separation of Met(O) peptide diastereomers has not been reported previously, the separation conditions should be also systematically studied.
4. To study the substrate specificity of MsrA mutants towards peptide substrates in comparison to the wild-type enzyme. A previous non-stereospecific HPLC-based had indicated that peptide substrates with positively charged amino acid residues adjacent to Met(O) are preferentially reduced by MsrA [42]. The enzyme mutants had been expressed in order to identify the importance of amino acids for the binding of the substrates [42]. Molecular modeling studies were intended in order to understand the substrate specificity.

3 Materials and methods

3.1 Materials

2-hydroxypropyl- β -CD	Cyclolab Ltd., Budapest, Hungary
4-Aminobenzoic acid	E. Merck, Darmstadt, Germany
15-crown-5	E. Merck, Darmstadt, Germany
18-crown-6	E. Merck, Darmstadt, Germany
acetone	VWR International GmbH, Darmstadt, Germany
ac-KDM(O)DK-dnp	Peptide Specialty-Laboratories GmbH, Heidelberg, Germany
ac-KDM(O)NK-dnp	Peptide Specialty-Laboratories GmbH, Heidelberg, Germany
ac-KEM(O)EK-dnp	Peptide Specialty-Laboratories GmbH, Heidelberg, Germany
ac-KEM(O)KK-dnp	Peptide Specialty-Laboratories GmbH, Heidelberg, Germany
ac-KFM(O)FK-dnp	Peptide Specialty-Laboratories GmbH, Heidelberg, Germany
ac-KFM(O)KK-dnp	Peptide Specialty-Laboratories GmbH, Heidelberg, Germany
ac-KIFMK-dnp	Peptide Specialty-Laboratories GmbH, Heidelberg, Germany
ac-KIFM(O)K-dnp	Peptide Specialty-Laboratories GmbH, Heidelberg, Germany
ac-KNM(O)DK-dnp	Peptide Specialty-Laboratories GmbH, Heidelberg, Germany
ac-KVM(O)VK-dnp	Peptide Specialty-Laboratories GmbH, Heidelberg, Germany
ac-NM(O)N-dnp	Peptide Specialty-Laboratories GmbH, Heidelberg, Germany
carboxymethyl- β -CD	Cyclolab Ltd., Budapest, Hungary
carboxymethyl- γ -CD	Cyclolab Ltd., Budapest, Hungary
citric acid monohydrate	Merck-Millipore, Darmstadt, Germany
dabsyl chloride	Sigma-Aldrich, Steinheim, Germany
dextran sulfate sodium salt (DS, mol. wt. > 500,000)	Sigma-Aldrich, Steinheim, Germany
DTT	Sigma-Aldrich, Steinheim, Germany
Fmoc- β -Ala	E. Merck, Darmstadt, Germany
Fmoc-Met	E. Merck, Darmstadt, Germany
Fmoc-Met(O)	E. Merck, Darmstadt, Germany
heptakis(2,6-di- <i>O</i> -methyl)- β -CD	Cyclolab Ltd., Budapest, Hungary
Kryptofix [®] 21	Merck-Millipore, Darmstadt, Germany
Kryptofix [®] 22	Merck-Millipore, Darmstadt, Germany

NaH ₂ PO ₃	Sigma-Aldrich, Steinheim, Germany
L-Met(O)	Sigma-Aldrich, Steinheim, Germany
L-Met	Sigma-Aldrich, Steinheim, Germany
methanol	VWR International GmbH, Darmstadt, Germany
methyl- β -CD	Cyclolab Ltd., Budapest, Hungary
NaH ₂ PO ₃	Sigma-Aldrich, Steinheim, Germany
polyethylene oxide	Sigma-Aldrich, Steinheim, Germany
SDS	Sigma-Aldrich, Steinheim, Germany
sulfated β -CD	Sigma-Aldrich, Steinheim, Germany
sulfobutyl- β -CD	Cyclolab Ltd., Budapest, Hungary
sulfobutylether- β -CD	Cyclolab Ltd., Budapest, Hungary
trifluoroacetic acid	AppliChem, Darmstadt, Germany
Tris	Sigma-Aldrich, Steinheim, Germany
polybrene	Sigma-Aldrich, Steinheim, Germany
β -Ala	Sigma-Aldrich, Steinheim, Germany
β -CD	Cyclolab Ltd., Budapest, Hungary
γ -CD	Cyclolab Ltd., Budapest, Hungary

Dabsyl chloride was recrystallized from acetone prior to use. All other chemicals were of the highest purity available and used without further purification.

Enzymes

All recombinant enzymes including human MsrA enzyme (hMsrA), human MsrB2 enzyme (hMsrB2), fungal fRMsr, fungal MsrA and its mutants, EQ, DN and DE were provided from the group of Prof. S.H. Heinemann and Dr. R. Schöherr (University of Jena, Germany).

The cloning and construction of a 6xHis-Tag fusion construct of Msr enzymes were described previously [148, 149]. The proteins were overexpressed in *Escherichia coli* (strains BL21 or M15) and isolated using Ni-nitrilotriacetic acid-Agarose [150]. The QuikChange II Site-Directed mutagenesis Kit (Agilent technologies, USA) was used for the mutations. The mutant's information is shown in **Table 1**.

Table 1. Site-directed mutagenesis in the active site of fungal MsrA

MsrA	Position99	Position134
wt (ED)	Glu (E)	Asp (D)
EQ	Gln (Q)	Asp (D)
DN	Glu (E)	Asn (N)
DE	Glu (E)	Glu (E)

The purity of the enzymes was confirmed by SDS-PAGE. Solutions of the Msr enzymes were prepared at a concentration of 1 mg/mL protein in Tris buffer (pH 8.0)/glycerol (2:1, v/v) and stored at $-20\text{ }^{\circ}\text{C}$. Other information refers to [42].

3.2 Instrumentation

General instrumentation

Balances	Sartorius AG, Göttingen, Germany
Centrifuge	Eppendorf AG, Hamburg, Germany
Filters (0.2 μm)	Carl Roth GmbH, Karlsruhe, Germany
Incubator	Kisker, Steinfurt, Germany
Lyophilizer	FINN-AQUA GmbH, München, Germany
Milli-Q Direct 8 system	Millipore, Schwalbach, Germany
Modde 7.0	Umetrics, Umea, Sweden
Origin 8.5	OriginLab Corp., Northampton, MA, USA
pH meter	WTW GmbH, Weilheim, Germany
Pipettes	Eppendorf AG, Hamburg, Germany
Reacti-Thermo	Fischer Scientific, Schwerte, Germany
Ultrasonic bath	Merck Eurolab, Darmstadt, Germany

Capillary electrophoresis

CE experiments were performed on a Beckman P/ACE MDQ capillary electrophoresis system (Beckman Coulter, Krefeld, Germany) equipped with a UV-Vis diode array detector and a sample tray temperature control system set at 10 °C. Data analysis was carried out with 32 KaratTM software version 4.0. Fused-silica capillaries (BGB Analytik Vertrieb, Schloßböckelheim, Germany) with 75 µm id, 375 µm od and 50 µm id, 363 µm od were used. Prior to use a fused-silica capillary, a new capillary was successively rinsed at a pressure of 138 kPa (20 psi) with 1 M sodium hydroxide for 20 min, water for 10 min, 0.1 M sodium hydroxide for 20 min, water for 10 min, and the BGE for 10 min. At the end of each day, the capillary was rinsed with 0.1 M sodium hydroxide for 10 min, water for 10 min, the BGE for 10 min and left in the BGE overnight. Between analyses, the capillary was flushed with 0.1 M sodium hydroxide for 3 min, water for 2 min, and the BGE for 3 min was applied. For a successive multiple ionic-polymer layer (SMIL)-coated capillary, it was coated according to [151] with minor modifications. Briefly, a new capillary was rinsed at a pressure of 138 kPa with 0.1 M HCl for 15 min, 1 M NaOH for 40 min and water for 15 min. Subsequently, the capillary was rinsed with 5% (w/v) aqueous HDB for 15 min and left without application of pressure for 30 min. Finally, it was rinsed with a 3% (w/v) aqueous DS for 30 min and left for 30 min. Before the first use, the coated capillary was rinsed with the BGE for 30 min. Between runs, the capillary was flushed with water for 2 min and the BGE for 3 min.

All buffers were prepared in Milli-Q water, filtered by a 0.2 µm membrane and degassed in ultrasonic bath.

3.3 CE-based analysis systems

CE-System 1

This system served for the off-line Msr assay using free Met(O) as substrate. Met(O), Met and β-Ala were separated after derivatization by dabsyl-Cl.

Capillary:	50/60.2 cm, 75 µm id, SMIL-coated capillary
BEG:	35 mM NaH ₂ PO ₄ , pH 8.0, 25 mM SDS
Voltage/Temperature:	25 kV/20 °C
Detection:	436 nm
Sample injection:	3.4 kPa, 3 s

The buffer was prepared by dissolving 35 mM NaH₂PO₄ in 1000 mL of water, adjusted to pH 8 using 1 M NaOH followed by the addition of solid SDS to achieve a SDS concentration of 25 mM.

The derivatization of the amino acids with dabsyl chloride was performed according to [152] with minor modifications. For method development, 100 µL of standard solutions containing 1 mM Met, 3 mM Met(O) and 0.5 mM β-Ala as internal standard in 150 mM sodium bicarbonate buffer, pH 9, were mixed in a 1 mL Reacti Vial with 200 µL of a 8.5 mM solution of dabsyl chloride in acetone. The mixture was heated at 70 °C for 15 min. Subsequently, the vials were put in ice for 5 min. The organic solvent was removed by a gentle stream of nitrogen at room temperature, the residue was frozen at -80 °C and lyophilized. The residue was then reconstituted in 250 µL 20% (v/v) aqueous methanol followed by centrifugation at 5000 g for 15 min. The supernatant was analyzed or stored at -20 °C. Samples for method validation and the Msr incubations were diluted with an equal volume of a 1 mM solution of β-Ala in 150 mM sodium bicarbonate buffer, pH 9.0. The mixture was vortexed and 100 µL were derivatized as described above for the standard solutions.

CE-system 2

This system was used for the separation the mixture of Fmoc-Met(O), Fmoc-Met and Fmoc-β-Ala in both off-line and EMMA assay.

Capillary:	48/58.2 cm, 50 µm id SMIL-coated capillary
BEG:	50 mM Tris-HCl, pH 8.0, 30 mM SDS,
Voltage/Temperature:	25 kV/25 °C
Detection:	214 nm
Sample injection:	3.4 kPa, 4 s

The BGE was prepared by dissolving 50 mM Tris in 1000 mL of water, adjusted to pH 8.0 using 1 M hydrochloric acid followed by the addition of solid SDS to achieve a final SDS concentration of 30 mM.

The EMMA assay was performed in the partial filling mode. First, the capillary was rinsed with the BGE for 3 min. Subsequent plugs were injected at a pressure of 3.45 kPa (0.5 psi) in the order (i) incubation buffer for 8 s, (ii) 20 µg/mL enzyme in incubation buffer for 4 s, (iii) Fmoc-Met(O) in incubation buffer for 4 s, (iv) 20 µg/mL enzyme in incubation buffer for 4 s and (v) incubation buffer for 4 s. The internal standard was added to the Fmoc-Met(O) solution at a constant concentration of

0.4 mM. After each injection, the capillary inlet was dipped into a vial containing water to prevent cross-contamination of the solutions. The reaction was started by application of a voltage of 1 kV for 30 s with the capillary ends immersed into the running buffer in order to mix the reactant zones. Thereafter, the capillary was left without voltage for a given time at 37 °C (zero potential amplification) followed by application of a voltage of 25 kV for 1 min to separate enzyme and substrate. Subsequently, the capillary was cooled to 25 °C within 2.5 min followed by application of the separation voltage of 25 kV.

CE-system 3

This system was used for the separation of ac-KIFM(O)K-Dnp, ac-KIFMK-Dnp and Fmoc- β -Ala.

Capillary:	43/53.2 cm, 50 μ m id, fused-silica capillary
BEG:	50 mM Tris-HCl, pH 7.85, 14.3 mg/ml sulfated β -CD, 5 mM 15-crown-5
Voltage/Temperature:	25 kV/21.5 °C
Detection:	214 nm
Sample injection:	3.4 kPa, 7 s

A 50 mM Tris-HCl buffer, pH 7.8, was prepared as previously described for **CE-system 2**. The appropriate amount of 15-crown-5 was first added to 50 mL of the Tris buffer, followed with the addition of an appropriate amount of sulfated β -CD to 25 mL of the 15-crown-5-containing Tris buffer.

CE-system 4

This system was used for the separation of Met(O)-containing peptide diastereomers.

Capillary:	40/50.2 cm, 50 μ m id, fused-silica capillary
BEG:	50 mM Tris-citric acid, containing CDs and/or crown ether (buffer pH and buffer composition see the chapter 4.4)
Voltage/Temperature:	25 kV/20 °C
Detection:	214 nm
Sample injection:	3.4 kPa, 4 s

50 mM Tris-citric acid buffers were prepared by dissolving the appropriate amount of Tris in water and adjusting to the pH with 1 M citric acid before completing to the desired volume with water. For buffers containing a single selector, the appropriate amount of CD or crown ether was added to 25 mL of the respective Tris-citric acid buffer. After addition of the Kryptofix[®] diaza-crown ethers, the pH of the buffer was readjusted using a 1M solution of citric acid. For the buffers containing two selectors, the appropriate amount of the crown ether was first added to 50 mL of the Tris-citric acid buffer. As in the case of single selector-containing buffers, the pH of the buffer was readjusted using a 1M solution of citric acid after the addition of Kryptofix[®] diaza-crown ethers. Subsequently, the appropriate amount of a CD was added to 25 mL of the crown ether-containing Tris buffer.

CE-system 5

This was used for the separation of Met(O)-containing peptide diastereomers.

Capillary:	50/60.2 cm, 50 μ m id, fused-silica capillary
BEG:	50 mM Tris-HCl, containing CDs and/or SDS (buffer pH and buffer composition see the chapter 4.5)
Voltage/Temperature:	25 kV/20 °C
Detection:	214 nm
Sample injection:	3.4 kPa, 4 s

For preparation of a single selector-based buffer, the appropriate amount of CD or SDS was added to 25 mL of the respective Tris-citric acid buffer. For the buffers containing two selectors, the appropriate amount of the SDS was first added to 50 mL of the Tris-citric acid buffer followed with the addition of appropriate amount of a CD to 25 mL of the SDS-containing Tris buffer.

CE-system 6

This system was used for the analysis of the incubations of ac-KDM(O)DK-Dnp in the chapter 4.4.

Capillary:	50/60.2 cm, 50 μ m id, fused-silica capillary
BEG:	50 mM Tris-HCl, pH 8.0, 15 mg/ml sulfated β -CD, 15 mM SDS
Voltage/Temperature:	25 kV/20 $^{\circ}$ C
Detection:	214 nm
Sample injection:	3.4 kPa, 4 s

Buffer preparation refers to **CE-system 5**.

CE-system 7

This system was used for the validation and analysis of the incubation of ac-KDM(O)NK-Dnp and ac-KNM(O)DK-Dnp, respectively.

Capillary:	50/60.2 cm, 50 μ m id, fused-silica capillary
BEG:	50 mM Tris-HCl, pH 7.0, 12 mg/ml sulfated β -CD, 25 mM SDS
Voltage/Temperature:	25 kV/20 $^{\circ}$ C
Detection:	214 nm
Sample injection:	3.4 kPa, 4 s

Buffer preparation refers to **CE-system 4**.

CE-system 8

This system was used for the analysis of the incubations of ac-KFM(O)KK-Dnp.

Capillary:	50/60.2 cm, 50 μ m id, fused-silica capillary
BEG:	50 mM Tris-HCl, pH 7.5, 10 mg/ml sulfated β -CD, 25 mM SDS
Voltage/Temperature:	25 kV/20 $^{\circ}$ C
Detection:	214 nm
Sample injection:	3.4 kPa, 4 s

Buffer preparation refers to **CE-system 4**.

3.4 Method validation

The assays were validated according to the International Conference on Harmonization (ICH) guideline Q2(R1) with regard to range, linearity, limit of detection (LOD), limit of quantitation (LOQ), precision and accuracy [153]. The ratio of the corrected peak areas of the analytes and the internal standard were used for quantification. For calibration, at least six generally equally spaced concentrations were used for each analyte and each concentration was analyzed three times. Intraday and interday precision were estimated by injection a sample six times a day and three times on three consecutive days, respectively. If not indicated otherwise, the LOD was calculated from the standard deviation of the y -intercepts, σ and the slope of the calibration curve, S , according to $LOD = 3.3\sigma/S$ and $LOQ = 10\sigma/S$. The accuracy of the off-line assays was estimated in the calibration range by comparison of analytes prepared in enzyme matrix. In the EMMA assay, the accuracy was estimated also at the medium concentration level by comparison of injections of the plug sequence described in **CE-system 3** but replacing the enzyme plug by incubation buffer. Each sample was analyzed three times.

3.5 Enzyme incubations

Msr enzyme reactions were carried out in 50 mM Tris, adjusted to pH 8.0 by the addition of HCl, in the presence of 20 mM DTT. Prior to the assay, the solutions containing enzyme and substrate were preincubated separately at 37 °C for 2 min. The reaction was started by addition of an appropriate amount of substrate stock solution prepared in water to achieve the desired concentration. If not indicated otherwise, enzyme reaction mixtures were incubated at 37 °C for 15 min and stopped by freezing at -80 °C. Blank sample was obtained by incubation without addition of substrate and control samples were conducted without the addition of enzyme.

3.5.1 Free Met(O) as substrate

For screening of Msr activity 20 µg/mL of Msr enzymes and 2 mM Met(O) were employed. For the characterization of hMsrA, 2 µg/mL of the enzyme was used in the incubation mixtures. The pHdependent assays were investigated at a concentration of 1 mM Met(O) in the presence of 2 µg/mL hMsrA or fungal fRMsr and were incubated at 37 °C for 30 min. The time course was studied

at a concentration of Met(O) of 1.5 mM and the kinetic data were obtained using concentrations of Met(O) of 0.3 mM, 0.5 mM, 0.8 mM, 1 mM, 1.5 mM, 2 mM, 3 mM and 4 mM. The pH-dependent assays were conducted at a concentration of 1 mM Met(O) in the presence of 2 µg/mL hMsrA or fungal fRMsr and were incubated at 37 °C for 30 min. The samples were stored at –80 °C until derivatization for analysis.

3.5.2 Fmoc-Met(O) as substrate (off-line assay)

For screening of the Msr activity, concentrations of 20 µg/mL of Msr enzymes and 600 µM Fmoc-Met(O) were employed. The kinetic data were obtained using 5 µg/mL of Msr enzymes and Fmoc-Met(O) concentrations between 50 and 500 µM (corresponding to 25 to 250 µM of the individual diastereomers). The internal standard (4-aminobenzoic acid) was spiked to all incubations to yield a final concentration of 400 µM. Incubations were carried out at 37 °C for 10 min, quenched by the addition of 100 µL ice-cold methanol and 10 µL 3% (v/v) aqueous trifluoroacetic acid (TFA) and stored at –80 °C until analyzed.

3.5.3 KIFM(O)K as substrate

Each incubation was carried out in 100 µL volume. For screening of the Msr activity, concentrations of 15 µg/mL of Msr enzymes and 160 µM ac-KIFM(O)K-Dnp were used. The time course was studied at a concentration of 160 µM ac-KIFM(O)K-Dnp with 1 µg/mL hMsrA. Incubations were carried out at 37 °C for 9 min stopped by freezing at –80 °C. Before analysis, Fmoc-β-Ala was spiked into the thawed samples at a concentration of 70 µM. The determination of the Michaelis-Menten kinetic parameters was carried out by varying the concentration of ac-KIFM(O)K-Dnp between 40 and 400 µM (corresponding to 20 to 200 µM of the individual diastereomers) in the presence of 1 µg/mL hMsrA and 7.5 µg/mL hMsrB2.

3.5.4 KDM(O)DK, KDM(O)NK, KNM(O)DK, KFM(O)KK as substrates

Each incubation was carried out in 100 μL volume. 5 $\mu\text{g}/\text{mL}$, 10 $\mu\text{g}/\text{mL}$ and 15 $\mu\text{g}/\text{mL}$ of fungal MsrA wild-type and the mutants EQ, DN and DE were investigated. The concentration of substrates, i.e., KDM(O)DK, KDM(O)NK, KNM(O)DK and KFM(O)KK were set at 180 μM , respectively. Incubations were carried out at 37 $^{\circ}\text{C}$ for 15 min stopped by freezing at -80°C . Before analysis, Fmoc- β -Ala was spiked into the thawed samples at a concentration of 60 μM .

3.6 Experimental design

Modde 7.0 (Umetrics, Umea, Sweden) was used for the experimental design and statistical analysis. For screening and optimization models, the investigated factors were fitted using a polynomial function:

$$y = b_i + b_1x_1 + b_2x_2 + b_{12}x_1x_2 + b_{11}x_1^2 + \dots \varepsilon \quad (4)$$

where x_i represents the factors to be optimized; y represents the response functions, i.e., peak resolution, and migration time of analytes. For each response y , the intercept b_i , the main coefficients $b_{1, \dots, n}$, the interaction coefficient $b_{12, \dots, (n-1)n}$, the quadratic coefficients $b_{11, \dots, nn}$, and the residual ε are calculated. The goodness of fitting ($R^2 = (\text{total sum of squares} - \text{sum of squares for residuals})/\text{total sum of squares}$) and the goodness of prediction [$Q^2 = 1 - (\text{prediction residual sum of squares}/\text{total sum of squares})$] were subsequently optimized. R^2 and Q^2 close to 1 describe an excellent model, $Q^2 > 0.5$ a good model and $Q^2 > 0.1$ indicates a significant model [154]. A fractional factorial response IV design was used for the identification of significant variables, while a five-level circumscribed central composite design (star distance 1.682) was used for the optimization of the significant variables.

3.7 Molecular modeling

The molecular modelling was performed by the group of Prof. W. Sippl (University of Halle, Germany). The model was primary built based on the x-ray structure of Msr from *N. meningitidis* in complex with a substrate (Ac-Met-S-SO-NHMe) (PDB ID 3bqf). This template shares a 43 % sequence identity with the wild-type enzyme of *A. nidulans*. The obtained model was further refined. The C-terminus was remodeled (loop refinement) to be in better agreement with the C-terminus of yeast Msr (PDB ID 3pil), where the sequence identity of this part are higher. Docking was performed using the program GOLD 4.0 with default settings. Details about the GOLD program can be found elsewhere [155]. A scaffold constraint and an H-bond constrain were set to bias the results towards undergoing the crucial expected interactions.

4 Results

Under physiological conditions, free and protein-bound Met is readily oxidized by ROS, leading to the formation of a pair of diastereomers, i.e., Met-*S*-(O) and Met-*R*-(O). For the reduction of the diastereomers, stereospecific Msr enzymes, MsrA and MsrB exist. MsrA enzymes reduce free and protein-bound Met-*S*-(O) while MsrB enzymes reduce protein-bound Met-*R*-(O) with little affinity for free Met-*R*-(O). The latter is reduced by free Msr (fRMsr). In order to develop stereospecific CE assays for the determination of stereospecificity of Msr enzymes, three frequently used substrates, i.e., free Met(O), Fmoc-Met(O), Met(O)-containing peptide, were applied.

4.1 Off-line assay using free Met(O) as substrate

In this part, the racemic mixture of Met-*R*-(O) and Met-*S*-(O) was applied as a natural substrate for the study of stereospecificity of recombinant Msr enzymes. Separation and detection of the diastereomers as well as Met were performed by capillary electrophoresis equipped with UV detection after sample derivatization.

4.1.1 Method development and optimization

The recently reported CE method by Uthus [99], which allowed the separation of the diastereomers of dabsyl-Met(O) and dabsyl-Met, was investigated as starting point. The method employed a 50/60.2 cm, 75 μ m id, uncoated fused-silica capillary, a 25 mM KH_2PO_4 buffer, pH 8.0, containing N-laurylsarcosine as BGE and a buffer containing also 25 mM SDS as conditioning solution. Although baseline separation of the dabsyl-Met(O) diastereomers was observed applying these conditions, we were not able to achieve reproducible migration times of the analytes. Since SDS is incompatible with potassium ions and leads to the formation of a precipitate [156], KH_2PO_4 was substituted by NaH_2PO_4 , but this did not result in satisfactory reproducibility either. Upon variation of the experimental conditions, separation of the dabsyl-Met(O) diastereomers was observed in a bare fused-silica capillary using a 35 mM sodium phosphate buffer, pH 8.0, containing 25 mM SDS. Thus, the presence of N-laurylsarcosine in the background electrolyte was not essential for the separation of the Met(O) diastereomers. However, under these conditions a variation of the electroosmotic flow (EOF) and consequently varying migration times of the analytes were observed. Addition of 0.04% polyethylene oxide to the BGE improved precision of the migration times (RSD <

6%, $n = 10$) but at the expense of long migration times (more than 30 min). Since the EOF proved to be variable, successive multiple ionic-polymer layer (SMIL) coating was investigated in order to provide a stable EOF. Thus, following the procedure of Katayama et al. [151], the fused-silica capillary was first coated with a layer of polybrene followed by a second layer of dextran sulfate. In combination with a 35 mM sodium phosphate buffer, pH 8.0, containing 25 mM SDS, reproducible migration times were observed. Thus after initially rinsing the SMIL-coated capillary for 30 min with the BGE, intraday run-to-run precision (RSD%) ($n=6$) was $< 2.5\%$ for the analytes and $< 1.0\%$ for the EOF, while interday precision (RSD%) ($n = 3$) was $< 2.7\%$ for the analytes and $< 1.6\%$ for the EOF. Typical resolutions of the Met(O) diastereomers of $R_S > 3.0$ were achieved. A representative electropherogram of the separation of the Met(O) diastereomers, Met, as well as β -Ala as internal standard is shown in **Fig. 12**.

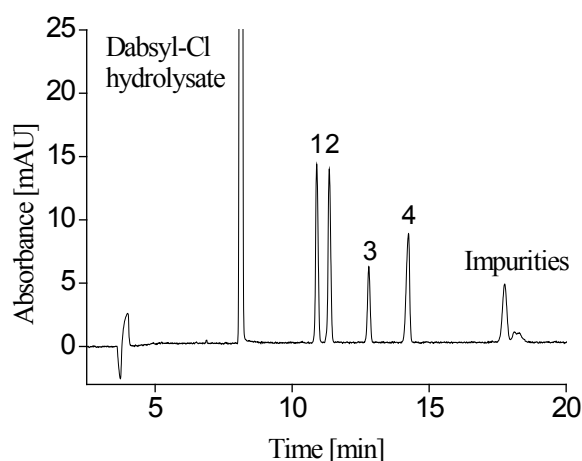


Fig. 12: Electropherogram of a standard sample derivatized with dabsyl chloride. Met-S-(O) (1), Met-R-(O) (2), β -Ala (3), Met (4). Experimental conditions: 50/60.2 cm, 75 μ m id, coated capillary; 35 mM sodium phosphate buffer, pH 8.0, containing 25 mM SDS; 25 kV; 20 $^{\circ}$ C; detection at 436 nm.

Because polybrene plays a critical role in the coating efficiency [151], different batches of polybrene were evaluated in our study. Consequently, an effect of polybrene was observed in the present study as changing the batch of polybrene while keeping identical coating conditions led to different but still highly reproducible migration times. For example, the velocity of the EOF varied between $5.2 \times 10^{-8} \text{ m}^2\text{V}^{-1}\text{s}^{-1}$ and $4.4 \times 10^{-8} \text{ m}^2\text{V}^{-1}\text{s}^{-1}$ for 4 different batches of polybrene. Subsequently, migration times in the range of 11 to 20 min were observed for the dabsyl-Met(O) diastereomers. Thus, changing the batch of polybrene in routine analysis of a validated method has to be considered with

care. Furthermore, a dependence of the EOF on the dextran sulfate coating was also observed. Using a 5% (m/v) solution of polybrene for the first coating, a faster EOF was observed when a 5% (m/v) solution of dextran sulfate was employed for the second coating compared to the EOF found for a 3% (m/v) or 1.5% (m/v) dextran sulfate solution. It may be speculated that complete coverage of the polybrene layer by dextran sulfate is necessary when using MEKC conditions because SDS may also adsorb to the polybrene layer. This may result in a change of the magnitude of the EOF as compared to a capillary with a "complete" dextran sulfate layer.

The derivatization procedure using dabsyl chloride followed a published method [152] and was performed from samples identical to the incubation mixtures. The recrystallization of the commercial reagent proved to be essential for complete dissolution of the compound in acetone and reproducible results. Derivatization was performed at 70 °C for 15 min. Under these conditions, modification of pH (pH 8-10) or derivatization time (10-30 min) did not significantly affect the yield of the dabsyl amino acids as described in the literature [157].

4.1.2 Method validation

The method was validated according to guideline Q2(R1) of the International Conference on Harmonization (ICH) [153] with regard to range, linearity, and precision. To counteract injection errors, β -Ala was used as internal standard. The ratio of the corrected peak areas of the analytes and the internal standard was used for quantification. Msr enzyme may also react with dabsyl-Cl in derivatization process, which would make calibration in standard samples inaccurate. Therefore, calibration was performed in a matrix containing hMsrA enzyme identical to the incubations. The samples were kept on ice, spiked with six different concentrations of Met(O) and Met and immediately derivatized in order to avoid reduction of Met(O). All concentrations were analyzed in triplicate. The validation data are summarized in **Table 2**.

Table 2. Assay validation data using free Met(O) as substrate.

Parameter	Met	Met-S-(O)	Met-R-(O)
Range [mM]	0.15 – 2.0	0.15 – 2.0	0.150 – 2.0
Linear equation	$y = 0.7794x - 0.0574$	$y = 0.9303x - 0.0073$	$y = 0.9147x - 0.0023$
Coefficient of determination, r^2	0.9810	0.9998	0.9999
Standard deviation of the slope	0.0003	0.0003	0.0002
Standard deviation of the intercept	0.0328	0.0154	0.0132
LOD / LOQ [μ M]	100 / 150	50 / 150	40 / 150
Repeatability (n=6)			
Migration time (RSD) [%]	3.6	1.7	1.8
Corrected peak area (RSD) [%]	2.9	1.6	1.7
Interday precision (n=3)			
Migration time (RSD) [%]	2.4	2.8	2.8
Corrected peak area (RSD) [%]	1.5	1.1	1.0
Accuracy (mean \pm SD, n=3)	77.5 ± 3.6	101.9 ± 13.3	106.9 ± 9.8

In the range 0.15 to 2.0 mM good linearity with coefficients of determination (r^2) of at least 0.9998 was observed for the Met(O) diastereomers, while only a coefficient of 0.9810 was found for Met. LODs ($3.3\sigma/\text{slope}$) were estimated at 0.04, 0.05 and 0.1 mM for the Met-R-(O), Met-S-(O) and Met, respectively. The accuracy of the analytes was estimated by comparison of analyte samples prepared in enzyme matrix immediately followed by derivatization with pure standards prepared in Tris buffer (pH 8.0). Analyte accuracy ranged between 77.5 ± 3.6 % and 101.9 ± 13.3 % at a concentration of 0.5 mM of the compounds. Because validation was performed from samples identical to the incubation conditions and not from aqueous standard solutions, accuracy is already included in the data and was, therefore, not assessed in further detail. Intraday and interday precision were estimated by injecting samples containing 0.75 mM of the individual Met(O) diastereomers [1.5 mM Met(O)], 0.5 mM β -alanine and 0.5 mM Met six times a day and three times on three consecutive days, respectively. The relative standard deviations (RSD) never exceeded 4% in case of migration times and 3% for the peak area ratio analyte/internal standard.

4.1.3 Enzyme incubations

To prove the applicability of the MEKC assay for quantitative analyses of enzymatic reactions, two Msr enzymes with inverse substrate stereospecificities, i.e. hMsrA and the fungal fRMsr protein, were investigated. Enzyme reactions were carried out in 200 μ L of 50 mM Tris-HCl, pH 8.0, in the

presence of 20 mM DTT, at 37 °C for 15 min. In standard reactions, Met(O) at a concentration of 2 mM was incubated in the presence or the absence of one of the enzymes and the reactions were stopped by freezing at -80 °C until derivatization. **Fig. 13** shows the electropherograms obtained for the enzymes in comparison to a control sample in the absence of enzyme. The blank sample was obtained by incubation without addition of substrate. The utility of the assay for the determination of the stereospecificity of the reductases towards the diastereomers of Met(O) is clearly illustrated. In accordance with the literature, hMsrA only reduced Met-S-(O) [34, 39] while the diastereomer Met-R-(O) was converted by fRMsr [40, 41]. Furthermore, the product Met could only be detected in the presence of an enzyme.

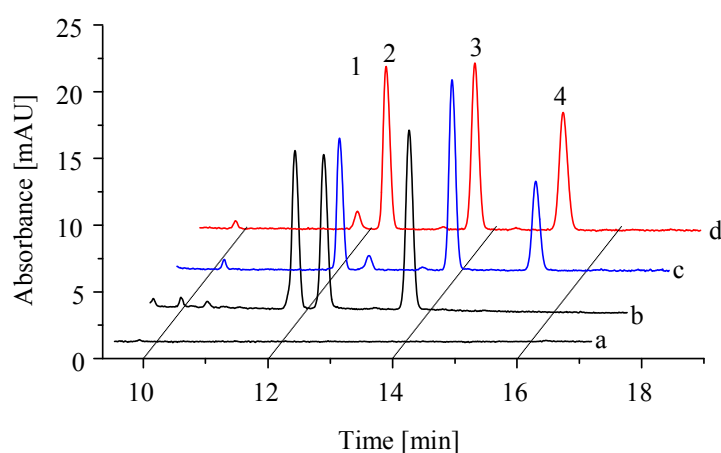


Fig. 13. Electropherograms of incubations of a blank sample in the absence of analytes (a), a control sample in the absence of enzyme (b), an incubation of fRMsr (c) and an incubation of hMsrA (d). Met-S-(O) (1), Met-R-(O) (2), β -Ala (3), Met (4). For separation conditions see **Fig. 12**.

Investigations of optimum pH for incubations

The optimum pH was screened for hMsrA and fungal fRMsr. The reactions for Msrs were carried out for 30 min at 37 °C with free Met(O) and DTT as a reductant. The incubations were performed in the pH range from 5.5 to 9.5. The reactions were stopped and derivatized before subjected to CE analysis. The data revealed that the optimum pH was 8.0 at which both, hMsrA and fungal fRMsr, showed the highest activity (**Fig. 14**). The tested Msrs were inactive at pH 6.0 or below. Human MsrA showed almost 50% activity at pH 7.5, while fungal fRMsr showed only 30% activity at this pH. Both enzymes showed a pronounced decrease of activity at a pH higher than 9.0.

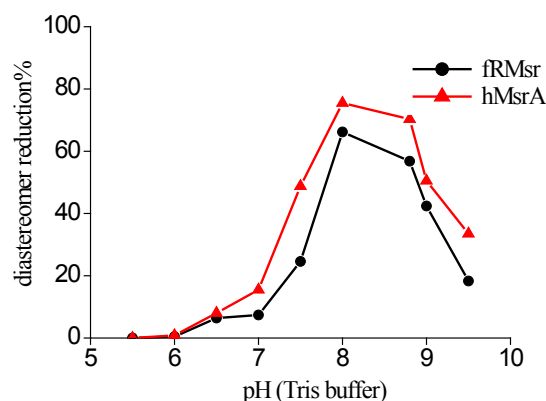


Fig. 14: pH dependent reduction of free Met(O) by hMsrA and fungal fRMsr. Reactions were carried out in 50 mM Tris-HCl at the indicated pH value using 1 mM free Met(O) as substrate in the presence of 20 mM DTT, 2 μ g/mL Msr, at 37 °C for 30 min.

Time-dependent incubation and enzyme kinetics of hMsrA

Subsequently, the assay was employed for the quantitative characterization of hMsrA. **Fig. 15** shows the time course of the incubation of 2 μ g/mL of the enzyme and 1.5 mM of Met(O). As it can be seen, in the incubations from 5 min to 25 min, the concentration of Met-S-(O) decreased with a concomitant increase of Met.

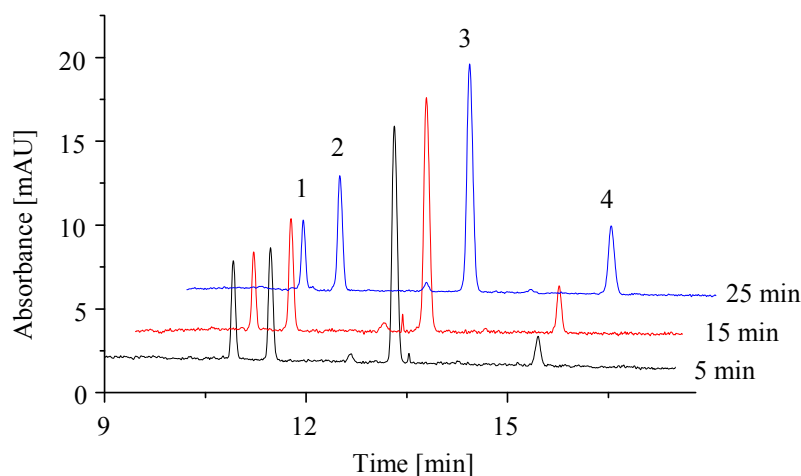


Fig. 15: Electropherograms of the time-dependent reduction of Met-S-(O) by hMsrA. 1.5 mM Met(O) was incubated in the presence of 2 μ g/mL hMsrA. Met-S-(O) (1), Met-R-(O) (2), β -Ala (3), Met (4). For separation conditions see **Fig. 12**.

Enzyme kinetics of hMsrA were subsequently determined. The plots of the initial velocities versus substrate concentration were fitted to the Michaelis–Menten equation using Origin 8.5 (OriginLab,

Northampton, MA, USA). **Fig. 16** shows the dependence of the initial velocity of the sulfoxide reduction as a function of the Met-S-(O) concentration either following the decrease of substrate or following the increase of reductive product.

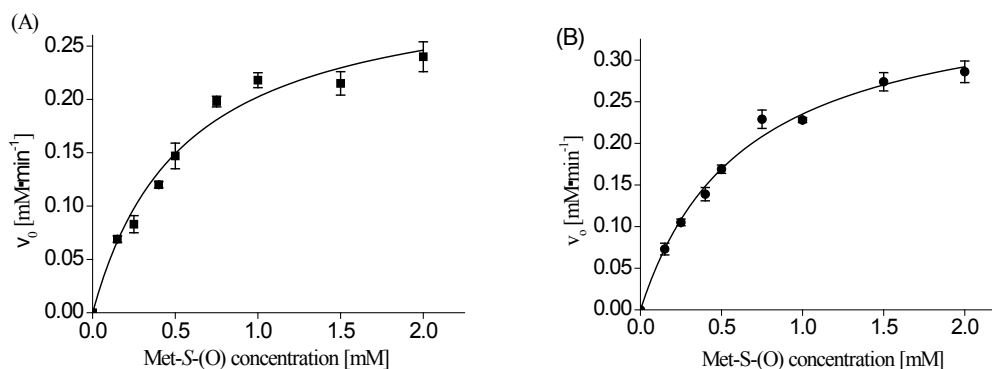


Fig. 16: Initial velocity, v_o , as a function of substrate concentration monitoring the decrease of Met-S-(O) (A) and the increase of Met (B). Each data point is the mean \pm SD ($n = 3$).

The Michaelis-Menten kinetic parameters derived from the increase of Met peak and from the decrease of the Met-S-(O) peak are summarized in **Table 3**. The corrected area ratio of the decreased Met-S-(O) was calculated according to:

$$R_{\text{decreased Met-S-(O)}} = \frac{A_{\text{Met-R-(O)}} - A_{\text{Met-S-(O)}}}{A_{\beta\text{-Ala}}} \quad (6)$$

where $A_{\text{Met-S-(O)}}$ and $A_{\text{Met-R-(O)}}$ represent the corrected peak areas of Met-S-(O) and Met-R-(O), respectively, and $A_{\beta\text{-Ala}}$ is the corrected peak area of the internal standard β -Ala. The decrease of Met-S-(O) was calculated by calibration curve according to the responsible corrected area ratio.

Table 3. Michaelis-Menten kinetic parameters of *hMsrA* using Met(O) as substrate ($n = 3 \pm$ SD).

	Met-S-(O) decrease ⁽¹⁾	Met increase
K_m [μM]	411.8 ± 33.8	390.1 ± 47.3
v_{max} [$\mu\text{M} \cdot \text{min}^{-1}$]	30.8 ± 1.9	26.1 ± 1.4
K_{cat} [s^{-1}]	6.4 ± 0.2	5.4 ± 0.3
K_{cat}/K_m [$\text{mM}^{-1} \cdot \text{min}^{-1}$]	960	840

⁽¹⁾ Calculated according to equation (5).

4.2 EMMA assay using Fmoc-Met(O) as substrate

Although the CE-based off-line enzyme assay is fast and consumes only a small amount of chemicals and enzymes, the incubation and analysis steps can be integrated into a single capillary leading to further miniaturization and automation. In order to perform on-line incubation, Met(O) derivatives are required as substrate which enable UV detection. Fmoc-Met(O) was selected because the compound is a commercially available amino acid used in peptide synthesis. Moreover, it has been reported that the compound is a substrate of MsrA [76, 77].

4.2.1 Separation of FMOC-Met(O) diastereomers

A 48/58.2 cm, 50 μ m id, SMIL-coated capillary was used in order to provide a stable EOF and, consequently, reproducible migration times as found for the CE separation of FMOC-Met(O) diastereomers. Because in chapter 4.1, incubations of Msr enzymes were performed in Tris buffer, pH 8.0, the separation of Fmoc-Met(O) diastereomers and the product Fmoc-Met was attempted in a 50 mM Tris buffer, pH 8.0. No separation of the analytes was observed under these conditions. Subsequently, MEKC was applied since it was effective for the separation of dabsyl-Met(O) diastereomers (see chapter 4.1.1). Addition of 30 mM SDS to a 50 mM Tris buffer, pH 8.0, resulted in baseline resolution of the Fmoc-Met(O) diastereomers as well as separation of Fmoc-Met within 18 min. **Fig. 17** shows a electropherogram for a standard sample spiked with 4-aminobenzoic acid as internal standard. Migration times were stable due to the use of the SMIL-coated capillary.

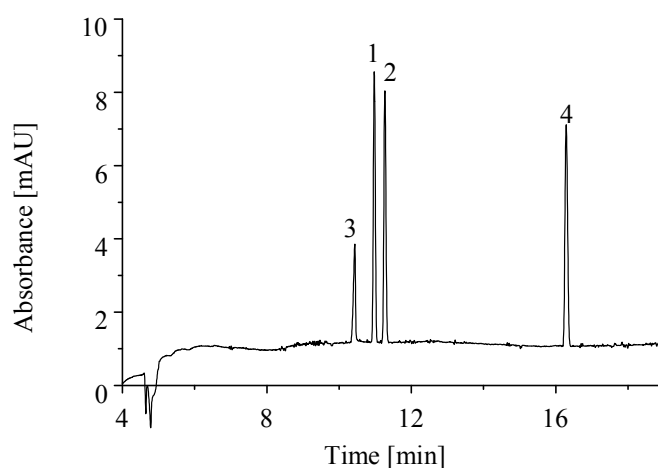


Fig. 17: Electropherogram of a standard sample containing 0.6 mM Fmoc-Met-(O), 0.3 mM Fmoc-Met and 0.4 mM 4-aminobenzoic acid. Experimental conditions: 48/58.2 cm, 50 μ m id, SMIL-coated capillary, 50 mM Tris buffer, pH 8.0, containing 30 mM SDS, 25 kV, 25 $^{\circ}$ C, detection at 214 nm. Peak labeling: 1, Fmoc-Met-S-(O); 2, Fmoc-Met-R-(O); 3, 4-aminobenzoic acid; 4, Fmoc-Met.

4.2.2 EMMA

The presence of SDS in the buffer would impair the Msr enzymes. Therefore, the partial filling mode [141] was selected for the development of an in-capillary assay in order to separate enzyme and substrate solutions from the separation buffer by a bracket of incubation buffer containing 50 mM Tris, pH 8.0, and 20 mM DTT. The mixing of substrate and enzyme zones can be achieved by diffusion [140, 158, 159] or by application of the mixing voltage for a short period of time [126, 139, 160, 161]. Both approaches were tested using 20 μ g/mL Msr enzyme and a concentration of Fmoc-Met(O) of 0.6 mM. The capillary temperature was kept at 37 $^{\circ}$ C. For electrophoretically mediated mixing, 1 kV was applied for 40 s followed with 10 min zero potential incubation. The injection sequences “enzyme-substrate”, “substrate-enzyme” as well as “enzyme-substrate-enzyme” and “substrate-enzyme-substrate” were evaluated. An injection sequence “enzyme-substrate-enzyme” was chosen for the diffusion method to ensure maximum diffusion of enzyme plugs with the substrate plugs. And the diffusion time was set at 10.6 min compared to electrophoretic mixing. The reduction of the substrate was monitored as a response for the mixing efficiency. A decrease of the resolution between the Met(O) diastereomers was observed for the injection sequence “substrate-enzyme-substrate”. Therefore, this injection order was not further investigated. **Fig. 18** shows that mixing by voltage generally resulted in higher substrate reduction, especially when the injection sequence “enzyme-substrate-enzyme” was applied. The injection sequence “enzyme-substrate” led to very low

substrate conversion probably because the substrate migrated faster than the Msrs so that the efficient mixing of zones was not achieved.

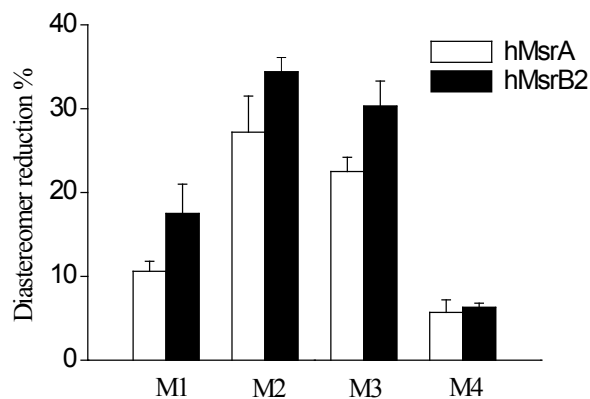


Fig. 18: Evaluation of different mixing methods including (M1) zone diffusion for 10.6 min, with the injection sequence enzyme-substrate-enzyme; (M2) application of 1 kV for 40 s followed with 10 min zero potential incubation, using the injection sequence enzyme-substrate-enzyme; (M3) application of 1 kV for 40 s followed with 10 min zero potential incubation, using the injection sequence substrate-enzyme; (M4) application of 1 kV for 40 s followed with 10 min zero potential incubation using the injection sequence enzyme-substrate.

Since the electrophoretic mobility of the enzymes is not known and cannot be determined in a reliable way, the mixing voltage and the time of voltage application cannot be calculated for known plug lengths of enzyme and substrate in order to ensure maximum plug overlapping [162]. Therefore, the injection sequence "enzyme-substrate-enzyme" was selected instead of optimizing the injection sequence "substrate-enzyme". Because the substrate was sandwiched between enzyme plugs and all the solutions were prepared in incubation buffer, the length of reaction plugs was fixed using an injection pressure of 3.45×10^3 Pa (0.5 psi) for 4 s resulting in plugs of about 7 mm at 37 °C by CE Expert Lite calculator of Beckman Coulter. Different periods of time for the application of the mixing voltage of 1 kV were investigated between 0 and 90 s. The zero potential incubation was set at 10 min. 4-aminobenzoic acid at a concentration of 0.4 mM was included in the substrate solution as internal standard to compensate for injection errors by the CE instrument. **Fig. 19** shows the results of sulfoxide reduction with regard to the time for the application of the mixing voltage, monitoring the corrected peak area ratio of the product Fmoc-Met and the internal standard. The highest substrate conversion was observed for a mixing time of 30 s for both, hMsrA and hMsrB2.

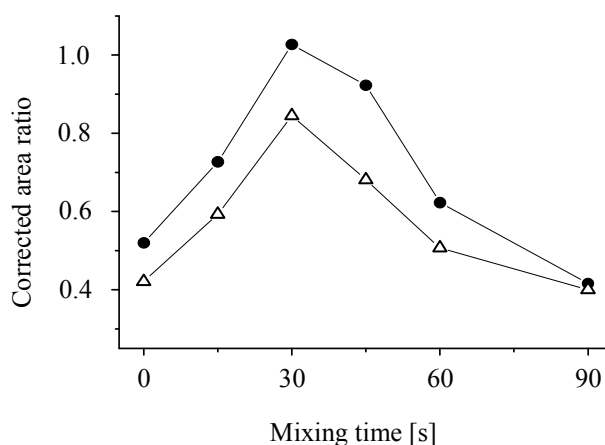


Fig. 19: Time dependence of 1 kV voltage application on the peak formation of Fmoc-Met in the EMMA assay. After mixing, 0.6 mM Fmoc-Met-(O), 20 $\mu\text{g}/\text{mL}$ hMsrA or hMsrB2 and IS were left for 10 min zero potential incubation at 37 $^{\circ}\text{C}$. The ratio of the corrected peak areas of the analytes and the internal standard were used for quantification; triangles, hMsrA; circles, hMsrB2.

Separation of substrate and product at the incubation temperature of 37 $^{\circ}\text{C}$ resulted in frequent breakdown of the electric current. Therefore, a voltage of 25 kV was applied after the incubation for 1 min in order to separate enzyme and substrate before cooling the capillary to 25 $^{\circ}\text{C}$ within 2.5 min with the voltage switched off. Finally, a separation voltage of 25 kV was applied. This procedure resulted in a stable CE system.

Under the optimized EMMA assay conditions, effective reduction of Fmoc-Met(O) with the concomitant formation of Fmoc-Met was observed. The time course of an incubation of 0.6 mM Fmoc-Met(O) with 20 $\mu\text{g}/\text{mL}$ hMsrA is shown in **Fig. 20**. It can be clearly seen that the (*S*)-configured sulfoxide is reduced to Fmoc-Met while the concentration of Fmoc-Met-*R*-(O) remains unaffected illustrating the stereospecificity of the MsrA enzyme. Although not all substrate is converted the data clearly show that the activity of Msr enzymes can be effectively analyzed by the present EMMA assay. The reaction may either be followed by monitoring the decreasing concentrations of the diastereomers of Fmoc-Met(O) or the increase of the Fmoc-Met.

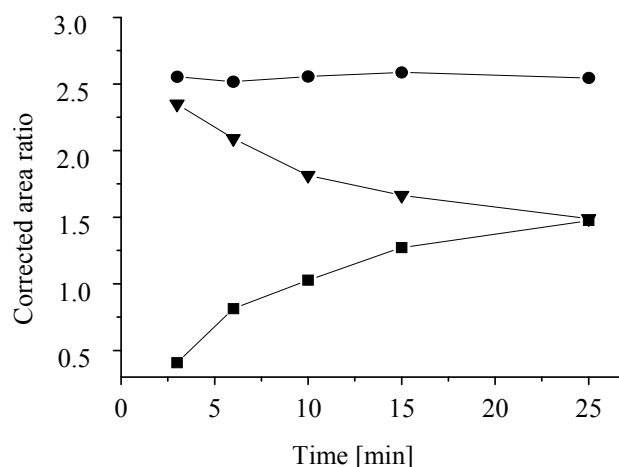


Fig. 20: Analyte concentration as a function of incubation time in the EMMA assay. 600 μM Fmoc-Met-(O) and 20 $\mu\text{g}/\text{mL}$ hMsrA were incubated at 37 $^{\circ}\text{C}$ prior to application of the separation voltage as described in the experimental part. The ratio of the corrected peak areas of the analytes and the internal standard were used for quantification. Triangles, Fmoc-Met-S-(O); circles, Fmoc-Met-R-(O); squares, Fmoc-Met.

Fig. 21A shows representative electropherograms of incubations of Fmoc-Met(O) in the presence of hMsrA (trace c) and hMrsB (trace d), respectively. No interference was observed from matrix components (trace a) and no reduction of the sulfoxide was observed in the absence of enzyme (trace b).

For comparison an offline assay was also developed using the separation system developed for the in-line assay. 0.6 mM Fmoc-Met(O) was incubated with 20 $\mu\text{g}/\text{mL}$ hMsrA or hMsrB2 in Tris buffer, pH 8.0, 20 mM DTT, at 37 $^{\circ}\text{C}$ for 10 min. The reaction was quenched by adding ice-cold methanol and aqueous TFA containing the internal standard 4-aminobenzoic acid to give a concentration of 0.4 mM. The samples were subsequently analyzed by CE. **Fig. 21B** shows electropherograms obtained for both enzymes. Neither interference by endogenous compounds (trace a) nor substrate conversion in the absence of MsrA (trace b) was observed. hMsrA reduced Fmoc-Met-S-(O) (trace c) while hMsrB2 reduced only Fmoc-Met-R-(O) (trace d).

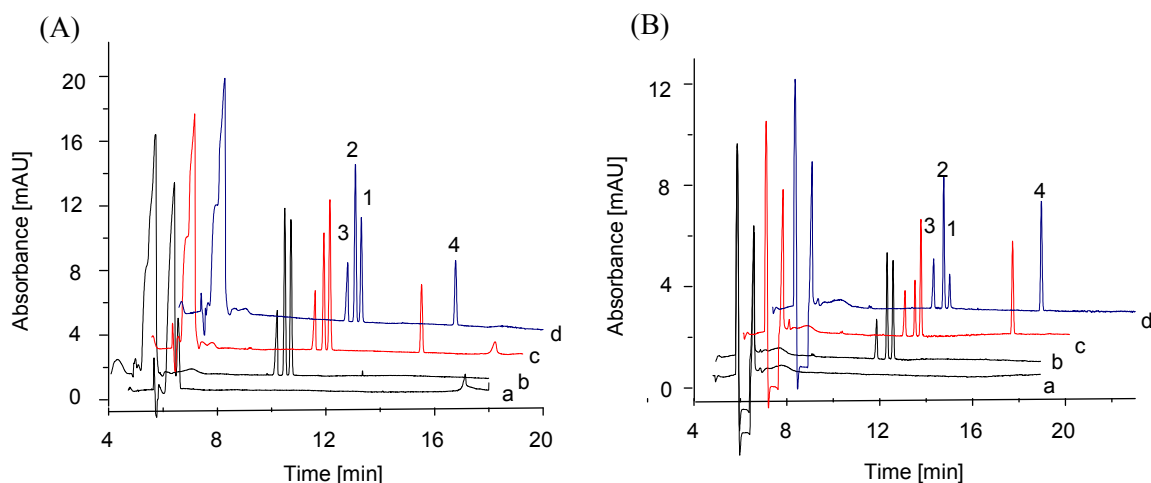


Fig. 21: Electropherograms *Fmoc-Met(O)* incubations in the presence of *Msr* enzymes in (A) the EMMA assay and (B) the offline assay. Blank sample in the absence of analytes (a), control sample in the absence of enzyme (b), incubation with *hMsrA* (c) and incubation with *hMsrB* (d). Peak labeling: 1, *Fmoc-Met-S-(O)*; 2, *Fmoc-Met-R-(O)*; 3, 4-aminobenzoic acid; 4, *Fmoc-Met*. For separation conditions see **Fig. 17**.

4.2.3 Method validation

The EMMA assay was validated according to the ICH guideline Q2(R1) [153] with regard to range, linearity, recovery and precision. The ratio of the corrected peak areas of the analytes and the internal standard were used for quantification. Experiments revealed no difference in peak areas when injecting sample solutions directly or between plugs as described in the EMMA procedure. Therefore, calibration was performed by direct injection of the standard solutions. The accuracy of the off-line assay was estimated by comparison of analytes prepared in enzyme matrix immediately followed by adding 100 μL ice-cold methanol and 10 μL 3% (v/v) TFA aqueous compared to analytes prepared in Tris buffer (pH 8.0). In the EMMA assay, accuracy was estimated by comparison of injections of the plug sequence described for the EMMA method in CE-system 3 in the chapter 3.3 but replacing the enzyme plug by incubation buffer. The validation data are summarized in **Table 4**.

Table 4. Assay validation data using *Fmoc-Met(O)* as substrate.

Parameter	Fmoc-Met	Fmoc-Met-S-(O)	Fmoc-Met-R-(O)
Range [μM]	25 – 500	25 – 500	25 – 500
Linear equation	$y = 0.0070x - 0.0133$	$y = 0.0078x + 0.0088$	$y = 0.0075x + 0.0036$
Coefficient of determination, r^2	0.9993	0.9996	0.9995
Standard deviation of the slope	0.0005	0.0007	0.0007
Standard deviation of the intercept	0.0369	0.0291	0.0300
LOD / LOQ [μM]	10 / 25	5 / 25	5 / 25
Repeatability (n=6)			
Migration time (RSD) [%]	1.5	0.9	1.0
Corrected peak area (RSD) [%]	2.0	1.0	1.4
Interday precision (n=3)			
Migration time (RSD) [%]	1.8	1.0	1.1
Corrected peak area (RSD [%])	1.7	0.9	0.9
Accuracy (mean \pm SD, n=3)			
Off-line assay	99.8 ± 4.0	98.0 ± 3.5	94.7 ± 2.6
EMMA assay	97.1 ± 2.9	97.9 ± 1.3	98.3 ± 4.1

For each analyte, linearity with coefficients of determination, r^2 , of at least 0.9993 were obtained in the range between 25 μM and 700 μM using equally spaced concentrations. The LODs (signal-to-noise ratio = 3) were estimated at 5 μM for each *Fmoc-Met(O)* diastereomer and 10 μM for *Fmoc-Met*, while the LOQs (signal-to-noise ratio = 10) were about 25 μM for all analytes. Intraday and interday precision were estimated by injection of samples containing 600 μM *Fmoc-Met(O)* and 300 μM *Fmoc-Met* six times a day and three times on three consecutive days, respectively. Precision of migration times ranged between 0.9 and 1.5% within one day while interday precision ranged between 1.0 and 1.8%. For corrected peak areas intraday and interday precision varied between 1.0 and 2.0% and between 0.9 and 1.7%, respectively. Accuracy for the assays was estimated at the concentration of 300 μM for each analyte. Values between $94.7 \pm 2.6\%$ and $99.8 \pm 4.2\%$ were found for the offline assay and values between $97.1 \pm 2.9\%$ and $98.3 \pm 1.1\%$ for the EMMA assay.

4.2.4 Enzyme kinetics

The Michaelis-Menten kinetic data were determined for hMsrA and hMsrB2 in the EMMA mode as well as in the off-line assay. Because of the generally lower conversion was observed in EMMA, higher amount of the enzymes were applied in the on-line incubations than in the off-line assay. It should be noted that since the exact volum for an on-line incubation is unknown, the concentration of

the enzyme contributing to the reaction cannot be defined as well. The incubation time of 10 min was identical in both assays. The increase of Fmoc-Met concentrations was determined for the quantification. **Fig. 22** shows the dependence of the initial velocity of the sulfoxide reduction by hMsrA and hMsrB2 as a function of the substrate concentration in the EMMA assay. The Michaelis constants, K_m , and the maximum velocities, v_{max} , were calculated by nonlinear regression and are listed in **Table 5**.

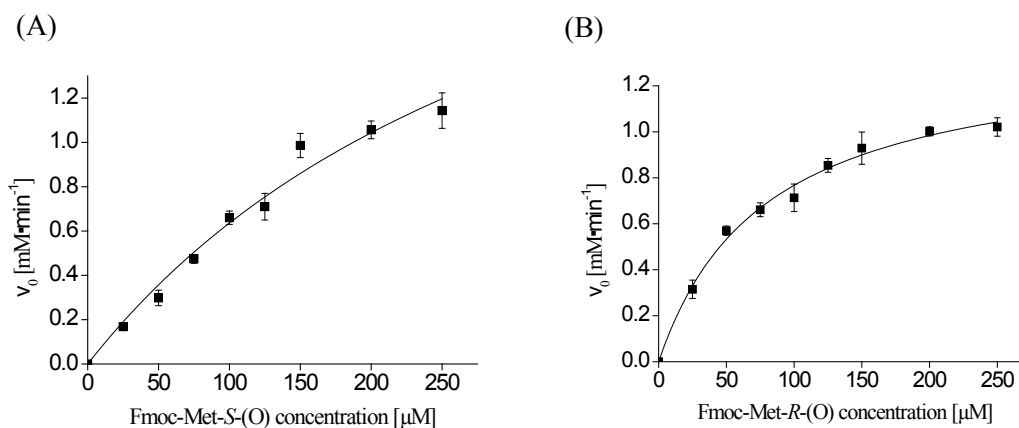


Fig. 22: Initial velocity, v_0 , as function of substrate concentration (A) hMsrA and (B) hMsrB2 obtained from EMMA assay.. Each data point is the mean \pm SD ($n = 3$).

Table 5. Comparison of Michaelis-Menten kinetic parameters of hMsrA and hMsrB2 using Fmoc-Met(O) as substrate in the EMMA and offline assays derived from the increase of Fmoc-Met concentrations. The data are expressed as mean \pm SD ($n = 3$).

Parameter	EMMA assay		Offline assay	
	hMsrA	hMsrB	hMsrA	hMsrB
K_m [μM]	286.7 ± 33.0	115.9 ± 10.0	256.2 ± 27.9	105.7 ± 10.4
v_{max} [$\mu\text{M} \cdot \text{min}^{-1}$]	1.49 ± 0.12	0.97 ± 0.03	1.59 ± 0.11	1.10 ± 0.04
k_{cat} [min^{-1}]	–	–	7.95 ± 0.55	3.74 ± 0.14

Essentially identical values were determined in both assays illustrating the general suitability of the in-capillary assay for the determination of kinetic data of Msr enzymes. Because the exact quantities of the enzymes reacting with the substrates are not known in the case of the EMMA mode, k_{cat} values could not be determined for this assay.

4.3 Off-line CE assay using a diastereomeric peptide substrate

Met(O) derivatives such as dabsyl-Met(O) have been frequently applied as Msr substrates [163, 164]. However, these Met(O) derivatives are not peptides so that they may not reflect the activity of Msr enzymes towards peptide-bound Met(O). Therefore, the aim of the present study was the development of a CE method based on separation of the diastereomers of a Met(O)-containing peptide. The dinitrophenyl (Dnp)-labeled N-acetylated pentapeptide KIFM(O)K was selected because it has been shown to be a substrate for Msr enzymes [149, 165].

4.3.1 Evaluations of initial separation conditions

Since the substrate KIFM(O)K and the reduced peptide KIFMK are basic peptides due to the presence of two Lys residues, the separation of the peptides was attempted in a 43/53.2 cm, 50 μ m id, fused-silica capillary using Tris-based background electrolytes in the pH range 2.5 - 9.5. However, no separation between KIFM(O)K and KIFMK was observed in this pH range. Subsequently, neutral and charged CDs were evaluated as buffer additives at a concentration of 15 mg/mL in a Tris-citric acid buffer, pH 2.5. While partial or baseline separation between KIFM(O)K and KIFMK was observed in the case of β -CD, methyl- β -CD and carboxymethyl- β -CD, the KIFM(O)K diastereomers could not be resolved. The analytes could not be detected within 60 min the presence of 5 mg/mL sulfated β -CD under normal as well as reversed polarity of the applied voltage. Therefore, the pH of the background electrolyte was raised to 8.0 in order to increase the EOF and thereby decrease the migration time and the CD-analyte interaction time. In the presence of 10 mg/mL sulfated β -CD in a 50 mM Tris-HCl buffer, pH 8.0, separation of all analytes was observed with $R_S = 2.5$ for the resolution of KIFMK and KIFM-*R*-(O)K and $R_S = 1.5$ for the separation of the Met(O)-peptide diastereomers under normal polarity conditions. Increasing the concentration of sulfated β -CD to 25 mg/mL resulted in $R_S = 2.5$ for the resolution of the diastereomers but at the expense of long migration times and high currents (above 100 μ A). Addition of 20 mM 15-crown-5 to the Tris buffer, pH 8.0, containing 15 mg/mL sulfated β -CD significantly increased KIFM(O)K diastereomer separation ($R_S = 4.2$). Because migration times of more than 20 min were observed under these conditions, further method optimization was performed using experimental design in order to achieve sufficient peak resolution with short analysis times.

4.3.2 Method optimization by experimental design

In order to identify the significant variables contributing to the separation, a fractional factorial response IV design (2^{6-2} corner experiments, 3 replicates of the center point) was selected based on the preliminary experiments. Buffer pH (6.50 - 8.50), the concentrations of Tris (30 - 80 mM), sulfated β -CD (3 - 16 mg/mL) and 15-crown-5 (2 - 10 mM) as well as the applied voltage (22 - 27 kV) and capillary temperature (18 - 24 °C) were evaluated. Peak resolution between KIFMK and KIFM-R-(O)-K and between KIFM-R-(O)-K and KIFM-S-(O)-K as well as migration time were selected as responses. The matrix of the design and the data obtained for the responses are summarized in **Table 6**. The data were fitted to the model using the partial least squares method. As it can be seen in **Fig. 23**, buffer pH, concentration of sulfated β -CD and capillary temperature were identified as significant variables which were further optimized. The rest factors were identified as insignificant variables because the coefficients included the zero.

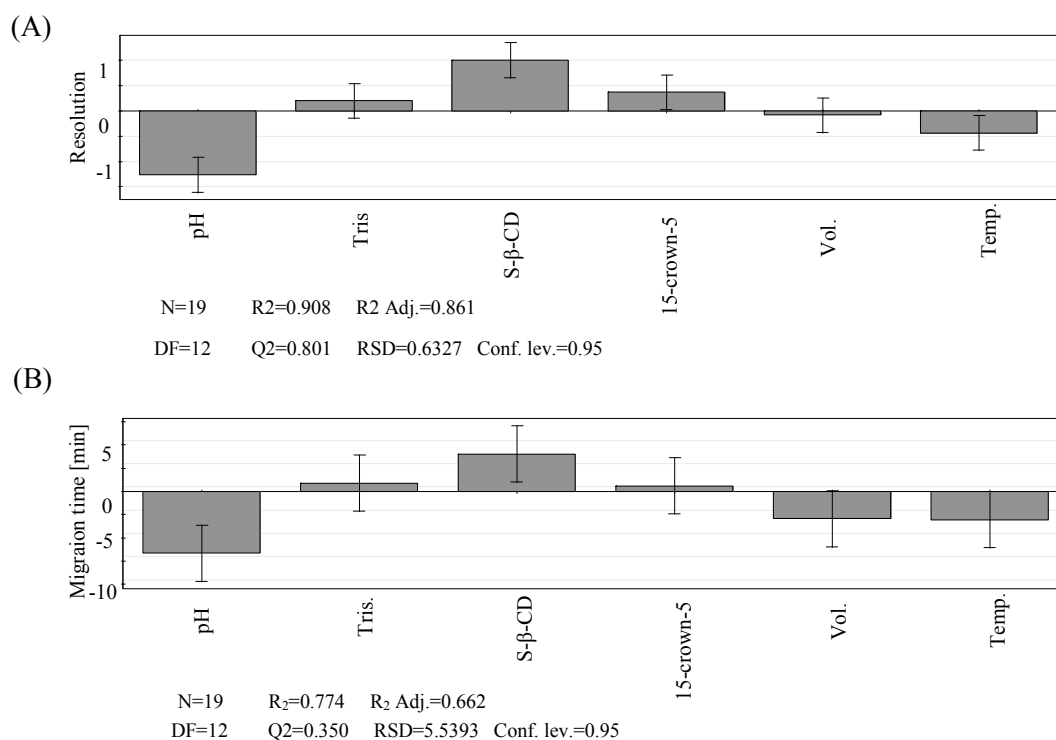


Fig. 23: Regression coefficients plot of screening design of (A) peak resolution between KIFM-R-(O)K and KIFM-S-(O)K and (B) migration time of KIFM-R-(O)K. The error bars represent 95% confidence levels.

Table 6. Matrix of the three level resolution IV fractional factorial design used for factor screening and experimental responses peak resolution, R , and migration time, t . The index numbers refer to the peptide sequences: 1, KIFMK; 2, KIFM-R-(O)-K; 3, KIFM-S-(O)K.

Exp. No.	Run order	pH	Tris [mM]	Sulf. β -CD [mg/mL]	15-crown-5 [mM]	Voltage [kV]	Temp. [$^{\circ}$ C]	$R_{1,2}$	$R_{2,3}$	t_1 [min]	t_2 [min]	t_3 [min]
1	1	6.5	30	3	2	22	18	4.71	3.9	21.95	22.51	22.93
2	10	8.5	30	3	2	27	18	1.3	0.2	6.31	6.5	6.51
3	5	6.5	80	3	2	27	24	3.82	3.33	7.91	8.5	8.81
4	6	8.5	80	3	2	22	24	1.1	0	7.3	7.5	7.5
5	18	6.5	30	16	2	27	24	5.12	4.51	13.62	14.51	15.22
6	19	8.5	30	16	2	22	24	2.31	1.83	8.04	8.33	8.51
7	7	6.5	80	16	2	22	18	6.6	5.6	35.23	39.53	42.4
8	16	8.5	80	16	2	27	18	3.32	2.9	9.29	9.53	9.69
9	9	6.5	30	3	10	22	24	3.8	3.1	13.15	13.8	14.3
10	15	8.5	30	3	10	27	24	1.41	0.35	5.74	5.92	5.97
11	4	6.5	80	3	10	27	18	4.76	4.01	12.87	13.33	13.54
12	14	8.5	80	3	10	22	18	2.93	2.3	11.21	11.5	11.72
13	11	6.5	30	16	10	27	18	6.4	5.7	34.11	35.8	38.32
14	8	8.5	30	16	10	22	18	4.6	4	10.41	11.2	12.3
15	13	6.5	80	16	10	22	24	6.11	5.1	27.21	30.82	32.99
16	3	8.5	80	16	10	27	24	4.11	3.52	7.77	8.23	8.52
17	12	7.5	55	9.5	6	24.5	21	4.99	4.1	10.89	11.4	11.88
18	17	7.5	55	9.5	6	24.5	21	4.66	3.9	10.27	10.9	11.26
19	2	7.5	55	9.5	6	24.5	21	4.93	4.4	11.11	11.74	12.54

Subsequently, a five-level circumscribed central composite design was used to further optimize the significant variables buffer pH (7.6 - 8.4), sulfated β -CD concentration (5 – 15 mg/mL) and capillary temperature (18 – 22 °C), while the insignificant variables were fixed at the medium value of the previously investigated range. The pH range was narrowed compared to the factorial design because severe broadening of the peak of KIFMK was observed below pH 7.5

Again, peak resolution between KIFMK and KIFM-*R*-(*O*)-K and between KIFM-*R*-(*O*)-K and KIFM-*S*-(*O*)-K as well as migration time served as the responses. The design matrix and the experimental results are summarized in **Table 7**. The effect of each of the factors as well as their interactions on the resolution of the diastereomers of KIFM(*O*)K and the migration time of KIFM-*R*-(*O*)-K are shown in **Fig. 24**. The presence of significant square indicated the existence of quadratic behavior and non-linear effects. All R^2 values were higher than 0.95 for the two responses and the Q^2 values of the responses resolution and migration time were 0.88 and 0.62, respectively. This indicates a good fit of the model.

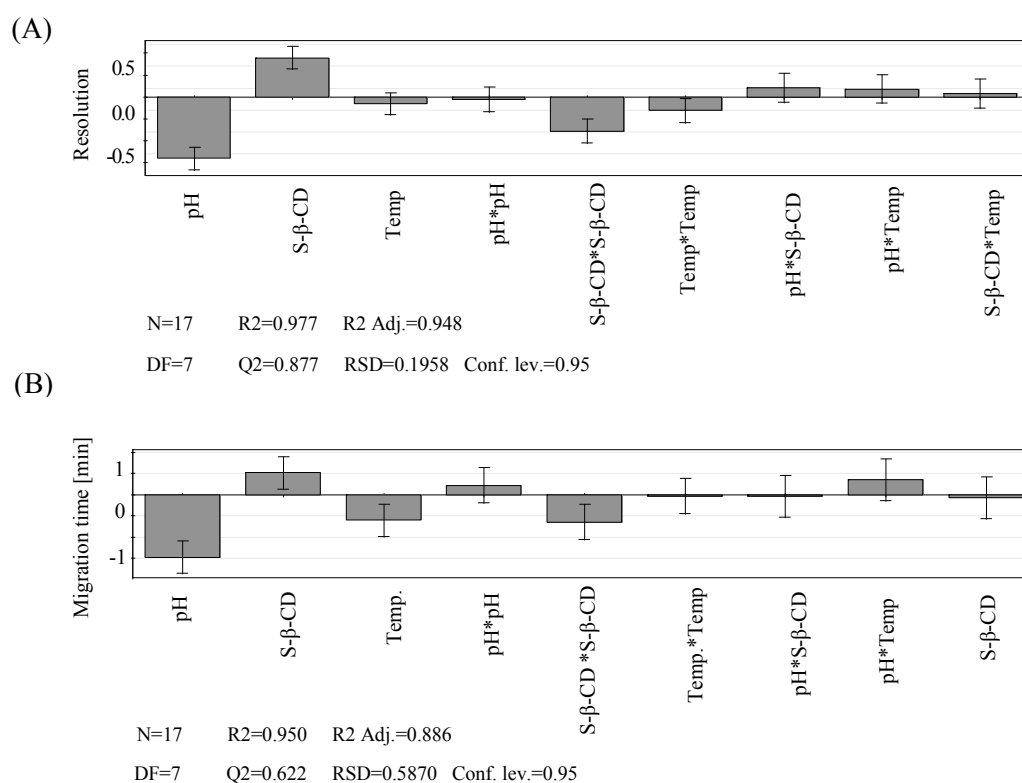


Fig. 24: Regression coefficients plot of response surface design of (A) peak resolution between KIFM-*R*-(*O*) and KIFM-*S*-(*O*)K and (B) migration time of KIFM-*R*-(*O*)K. The error bars represent 95% confidence levels.

Table 7. Response surface design matrix of the five level circumscribed central composite design used for method optimization and experimental responses peak resolution, R , and migration time, t . The index numbers refer to the peptide sequences: 1, KIFMK; 2, KIFM-R-(O)-K; 3, KIFM-S-(O)-K.

Exp. No.	Run order	pH	Sulf. β -CD [mg/mL]	Temp. [$^{\circ}$ C]	$R_{1,2}$	$R_{2,3}$	t_1 [min]	t_2 [min]	t_3 [min]
1	5	7.6	5	18	3.83	3.3	10.89	11.38	11.68
2	7	8.4	5	18	2.25	1.76	8.12	8.32	8.42
3	15	7.6	15	18	6.16	4	11.95	12.51	12.85
4	8	8.4	15	18	4.47	2.7	9.22	9.51	9.68
5	17	7.6	5	22	3.32	2.97	8.98	9.33	9.54
6	2	8.4	5	22	2.37	1.62	7.73	7.91	8.02
7	13	7.6	15	22	5.15	3.65	9.95	10.35	10.6
8	3	8.4	15	22	4.65	2.67	8.33	8.58	8.73
9	1	7.33	10	20	5.85	4.76	13.55	14.33	14.83
10	9	8.67	10	20	3.83	2	7.7	7.9	8.02
11	6	8	1.6	20	2.03	1.61	7.57	7.79	7.95
12	4	8	18.4	20	5.36	3.11	9.25	9.58	9.76
13	11	8	10	16.6	3.75	3.14	10.78	11.2	11.43
14	14	8	10	23.4	3.92	2.9	9.28	9.61	9.8
15	12	8	10	20	4.15	3.23	9.77	10.19	10.31
16	16	8	10	20	4.23	3.43	9.94	10.32	10.52
17	10	8	10	20	4.45	3.71	9.98	10.37	10.58

Buffer pH and the concentration of sulfated β -CD displayed a significant influence on peak resolution while the migration time was mostly determined by buffer pH. Increasing the buffer pH led to a decrease of peak resolution as well as migration time while increasing the concentration of sulfated β -CD resulted in a significant increase of peak resolution and a concomitant increase of migration time. The temperature primarily influenced migration time. The response surface plots of the resolution of the most critical peaks KIFM-R-(O)-K and KIFM-S-(O)-K and the migration time of KIFM-R-(O)-K as a function of the pH and sulfated β -CD concentration are shown in **Fig. 25**.

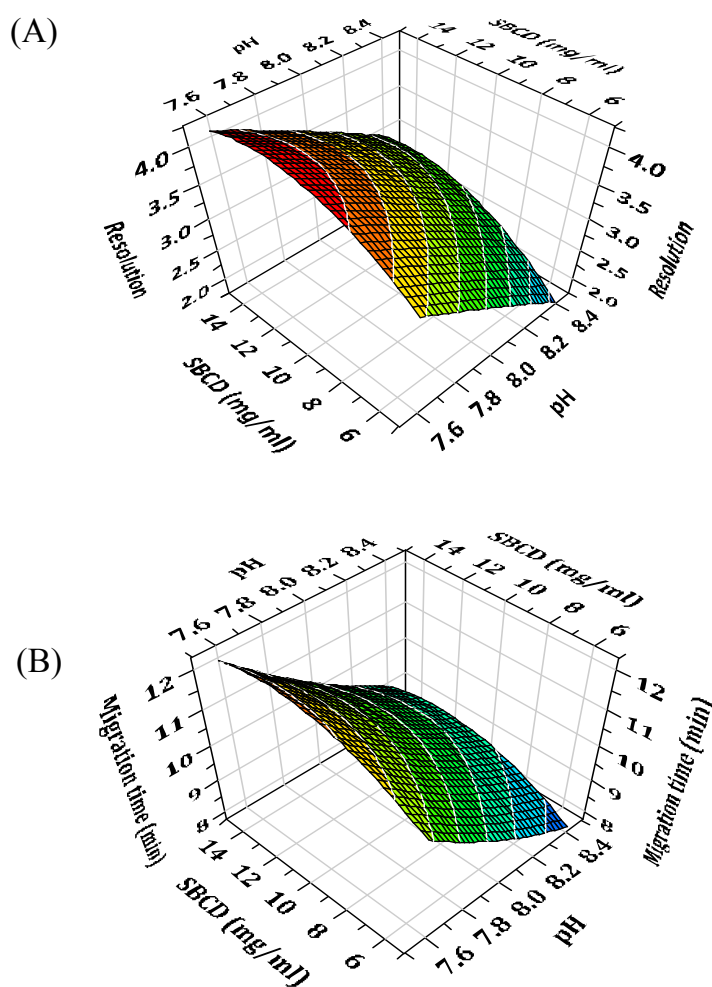


Fig. 25: Response surface plots for (A) the resolution between KIFM-R-(O)K and KIFM-S-(O)K and (B) migration time of KIFM-R-(O)K as a function of buffer pH and sulfated β -CD concentration.

The optimum of the experimental parameters with a high resolution and short migration times were predicted at a buffer pH of 7.85, a sulfated β -CD concentration of 14.3 mg/mL and a capillary temperature of 21.5 °C in combination with the previously fixed parameters of a 50 mM Tris buffer containing 5 mM 15-crown-5 and an applied voltage of 25 kV. $R_S = 3.63$ for the KIFM(O)K diastereomers and a migration time of KIFM-*R*-(O)-K of 10.3 min were predicted. An electropherogram using the selected experimental conditions is shown in **Fig. 26**. The experimentally determined R_S values of 3.14 ± 0.41 ($n = 10$) for the KIFM(O)K diastereomers and a migration time of 10.4 ± 0.08 min ($n = 10$) showed good agreement with the predicted values.

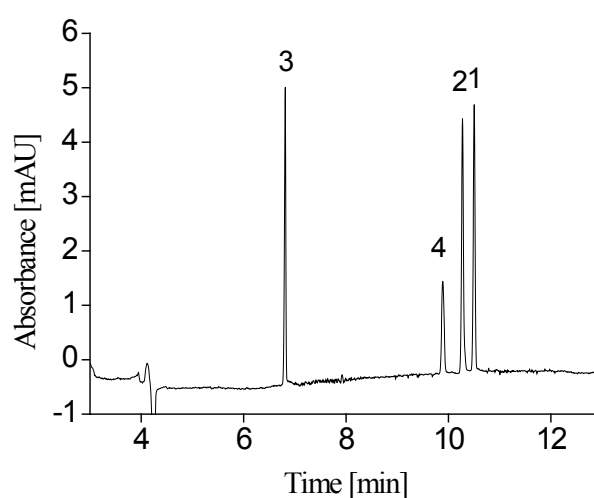


Fig. 26: Electropherogram of a standard sample containing 160 μ M KIFM(O)K, 40 μ M KIFMK and 70 μ M Fmoc- β -Ala. Experimental conditions: 43/53.2 cm, 50 μ m I.D. fused silica capillary, 50 mM Tris buffer, pH 7.85, containing 14.3 mg/mL sulfated β -CD and 5 mM 15-crown-5, 25 kV, 21.5 °C, detection at 214 nm. Peaks: 1, KIFM-S-(O)K; 2, KIFM-*R*-(O)K; 3 Fmoc- β -Ala.; 4 KIFMK,.

4.3.3 Method validation

The optimized method was validated according to ICH guideline Q2(R1) [153] with regard to range, linearity, accuracy, LOD, LOQ and precision. The ratio of corrected peak areas of the analytes and the internal standard (Fmoc- β -Ala) were used for quantitation. The validation data are summarized in **Table 8**.

Table 8. Assay validation data using KIFM(O)K as substrate.

Parameter	KIFMK	KIFM-R-(O)K	KIFM-S-(O)K
Range [μ M]	15 - 220	10 - 220	10 - 220
Linear equation	$y = 0.0099x - 0.0915$	$y = 0.0095x - 0.0061$	$y = 0.0093x - 0.0073$
Coefficient of determination, r^2	0.9945	0.9976	0.9987
Standard deviation of the slope	0.0004	0.0003	0.0002
Standard deviation of the intercept	0.0128	0.0099	0.0077
LOD / LOQ [μ M]	4.3 / 15	3.4 / 10	2.8 / 10
Repeatability (n=6)			
Migration time (RSD) [%]	0.71	0.75	0.76
Corrected peak area (RSD) [%]	4.5	3.6	3.9
Interday precision (n=3)			
Migration time (RSD) [%]	1.8	2.9	3.6
Corrected peak area (RSD [%])	5.2	3.8	4.6
Accuracy (mean \pm SD, n=3)	95.6 \pm 5.2	103.6 \pm 5.7	104.9 \pm 3.3

Eight equally spaced concentrations of KIFMK and KIFM(O)K (each analyzed in triplicate) were used for the construction of the calibration curve. The LODs and LOQs were calculated from the standard deviation of the y -intercepts, σ and the slope of the calibration curve, according to $LOD = 3.3\sigma/Slope$ and $LOQ = 10\sigma/Slope$. Intra- and interday precision were estimated by injection of a standard sample containing 160 μ M KIFM(O)K, 80 μ M KIFMK and 70 μ M internal standard six times a day and three times on three consecutive days, respectively. Accuracy was estimated using also these concentrations by comparison of analyte samples prepared in enzyme matrix without the addition of DTT and immediately frozen at -80 °C with samples prepared in Tris buffer, pH 8.0, without the addition of enzyme or DTT.

4.3.4 Enzyme incubations

The method was applied to evaluate the stereospecificity of the recombinant human Msr enzymes, hMsrA and hMsrB2. 160 μ M KIFM(O)K was incubated in Tris buffer, pH 8.0, containing 20 mM DTT, in the presence of 15 μ g/mL hMsrA or hMsrB2 for 10 min. Control samples were obtained in the absence of enzyme. **Fig. 27A** shows electropherograms of incubations of KIFM(O)K in the presence of hMsrB2 (trace d) and hMsrA (trace c), respectively, indicating the stereospecificity of the sulfoxide reduction by the enzymes. No reduction of the substrate was observed in the absence of enzyme (trace b) and no interference was observed from matrix components (trace a) obtained from an enzyme solution without addition of substrate and internal standard. A time course of the

incubation of 160 μM KIFM(O)K with 1 $\mu\text{g}/\text{mL}$ hMsrA is shown in **Fig. 27B**. KIFM-S-(O)-K decreased with time with the concomitant increase of KIFMK while KIFM-R-(O)-K was not affected.

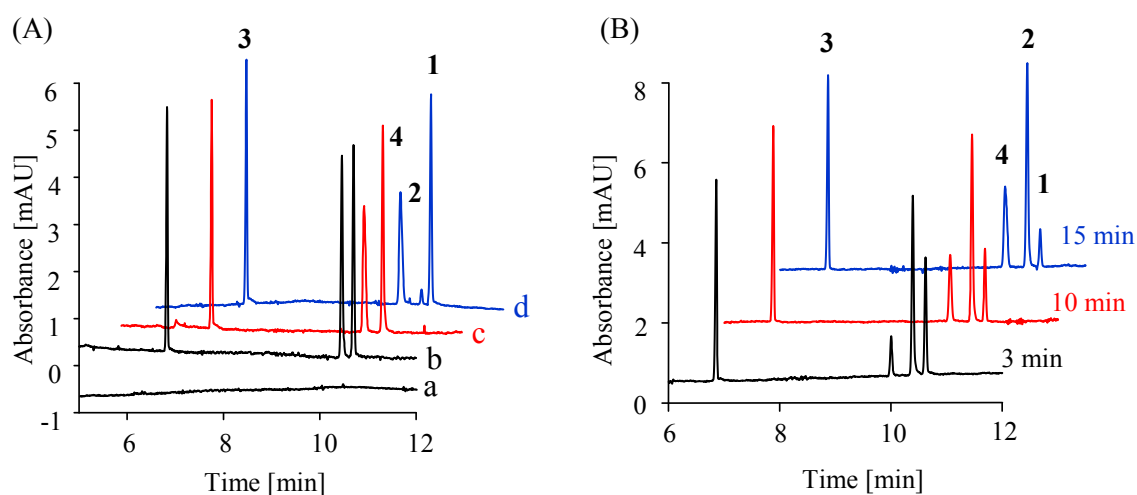


Fig. 27: (A) Electropherograms of Msr stereospecificity, (a) a blank sample in the absence of analytes and (b) a control sample in the absence of enzyme, (c) hMsrA and (d) hMsrB2. 160 μM KIFM(O)K was incubated in the presence of 15 $\mu\text{g}/\text{mL}$ hMsrA or hMsrB2 for 10 min. (B) Electropherograms of the time-dependent reduction of KIFM-S-(O)K by hMsrA. (B) 160 μM KIFM(O)K was incubated in the presence of 1 $\mu\text{g}/\text{mL}$ hMsrA. Peaks: 1, KIFM-S-(O)K; 2, KIFM-R-(O)K; 3, Fmoc- β -Ala; 4 KIFMK. For separation conditions see Fig. 23.

Finally, the Michaelis-Menten kinetics were determined. **Figure 28** shows the dependence of the initial velocity of the sulfoxide reduction by hMsrA or hMsrB2, as a function of the substrate concentration between 20 and 200 μM , corresponding to incubations with the substrate diastereomer mixture in the range 40 - 400 μM . The kinetic data were calculated from the increase of the KIFMK peak and are summarized in **Table 9**.

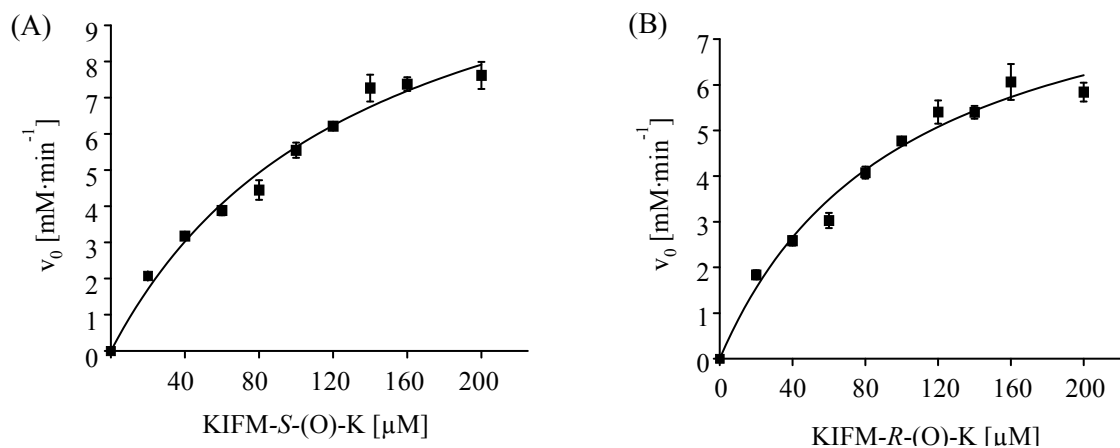


Fig. 28: Initial velocity, v_0 , as a function of substrate concentration for (a) *hMsrA* and (b) *hMsrB2* monitoring the increase of KIFMK. Each data point represents the mean \pm SD ($n = 3$).

Table 9. Kinetic data of Msrs using KIFM(O)K as substrate.

	<i>hMsrA</i>	<i>hMsrB2</i>
K_m [μM]	135.6 ± 25.6	100.5 ± 19.8
v_{max} [$\mu\text{M} \cdot \text{min}^{-1}$]	13.3 ± 1.3	9.3 ± 0.9
k_{cat} [min^{-1}]	331.8 ± 32.5	21.3 ± 2.1
k_{cat}/K_m [$\text{mM}^{-1} \cdot \text{min}^{-1}$]	2447	211

4.4 Off-line assay for recombinant fungal MsrA and mutants using synthetic peptide substrates

A previous study has shown that peptide substrates with positively charged amino acid residues next to Met(O) are preferentially reduced by both human and fungal recombinant MsrA [42]. MsrA contains two highly conserved negatively charged amino acids (Asp 134 and Glu 99) in the active site which may contribute to the observed low conversion rates of peptide substrates with negatively charged amino acids flanking Met(O) [42]. To further confirm the findings, four *N*-acetylated and C-terminally Dnp labeled peptide substrates KDM(O)DK, KDM(O)NK, KNM(O)DK and KFM(O)KK were selected for the evaluation the activity of fungal MsrA and the mutants EQ, DN and DE.

The sequence KDM(O)DK was applied as the substrate possesses two negatively charged amino acids flanking Met(O), while the sequence KFM(O)KK was used as the substrate with one positively charged and one neutral amino acid flanking Met(O). The peptide KDM(O)NK and KNM(O)DK were applied as the substrates carry one neutral amino acid and one negatively charged amino acid flanking Met(O), but the positions for the amino acid residues were reversed. The mutant information refers to **Table 1** in the chapter **3.1**. The wild-type MsrA carries Glu99 (E) and Asp134 (D) and was termed as ED. For the mutant EQ, the acidic Glu 99 in wild-type was replaced by Gln. In the cases of DN and DE mutant, Asp 134 was substituted by Asn and Glu, respectively.

4.4.1 Separation of Met(O) peptide substrates

A 50/60.2 cm, 50 μ m id, fused silica capillary was applied for the separation of Met(O) peptide diastereomers. To ensure a quantitative assay, Fmoc-Ala was applied as the internal standard for all analytes. The separation of KDM(O)DK diastereomers was achieved using a 50 mM Tris-HCl, pH 8.0, containing 15 mM SDS and 15 mg/mL sulfated β -CD. The diastereomers of KFM(O)KK was separated using a 50 mM Tris-HCl buffer with addition of 10 mg/mL sulfated β -CD at pH 7.5. Although the baseline diastereomer separation of KDM(O)NK and KNM(O)DK were achieved using 50 mM Tris-HCl, pH 8.0, containing 10 mg/mL sulfated β -CD and 10 mM Kryptofix[®] 22, long migration times (over 30 min) was observed for the internal standard. As a compromise between peak resolution and analysis time, the separations of diastereomers of KDM(O)NK and KNM(O)DK were conducted with 50 mM Tris-HCl, pH 7.0, containing 12 mg/mL sulfated β -CD. Under these conditions, the diastereomers of KDM(O)NK and KNM(O)DK were separated in 15 min, with a resolution of 1.25 and 1.36, respectively. The methods were not further optimized.

4.4.2 Method validation

The methods were validated according to ICH guideline Q2(R1) [153] with regard to range, linearity, accuracy, LOD, LOQ and precision. The ratio of corrected peak areas of the analytes and the internal standard (Fmoc- β -Ala) were used for quantitation. The validation data for the (*S*)-configured peptide diastereomer are summarized in **Table 10**. Because the method allows the separation of the diastereomers of the substrates, the validation data of the (*R*)-configured sulfoxide diastereomer could also be obtained but were not calculated.

Table 10. Assay validation data using a group of Met(*O*)-containing peptides as substrates.

	KDM- <i>S</i> -(<i>O</i>)DK	KFM- <i>S</i> -(<i>O</i>)KK	KDM- <i>S</i> -(<i>O</i>)NK	KNM- <i>S</i> -(<i>O</i>)DK
Range(μ M)	16.7-184.0	17.2-190.0	15.3-174.6	16.5-182.0
Slope/Intercept	0.0077/-0.0187	0.0063/0.0370	0.0068/-0.0079	0.0073/0.0218
r^2	0.9990	0.9977	0.9980	0.9989
LOD/LOQ (μ M)	5.6/16.7	5.7/17.2	5.1/15.3	5.5/16.5
Repeatability (n=6)				
Migration time (RSD) [%]	2.1	1.7	1.7	1.9
Corrected peak area (RSD) [%]	4.3	2.8	4.2	4.7
Interday precision (n=3)				
Migration time (RSD) [%]	3.9	3.3	4.0	3.8
Corrected peak area (RSD [%])	4.5	3.9	5.4	5.1
Accuracy (mean \pm SD, n=3)	91.5 \pm 6.5	93.5 \pm 6.1	105.5 \pm 9.4	90.7 \pm 8.8

Seven equally spaced concentrations of the respective Met(*O*) peptide (each analyzed in triplicate) in the range of 30-300 μ M were used for the construction of the calibration curve. The concentration of the individual diastereomer was calculated from the ratio of both diastereomers. Intra- and interday precision were estimated by injection of a concentration 200 μ M of the Met(*O*) peptide containing 60 μ M internal standard six times a day and three times on three consecutive days, respectively. Accuracy was estimated using also these concentrations by comparison of analyte samples prepared in enzyme matrix without the addition of DTT and immediately frozen at -80 °C with samples prepared in Tris buffer, pH 8.0, without the addition of enzyme or DTT.

4.4.3 Enzyme incubations

The incubations were conducted in Tris buffer, pH 8.0, in the presence of 20 mM DTT at 37 °C for 15 min. Three enzyme concentrations, i.e., 5 µg/mL, 10 µg/mL and 15 µg/mL, were applied and each concentration was analyzed in triplicate. Control samples were prepared without the addition of enzyme. **Fig. 29** shows representative electropherograms of incubations of the substrates in the presence of wild-type of MsrA. No reduction of the substrate was observed in the control samples and no interference was observed from matrix components obtained from an enzyme solution without addition of substrate and internal standard (data not shown).

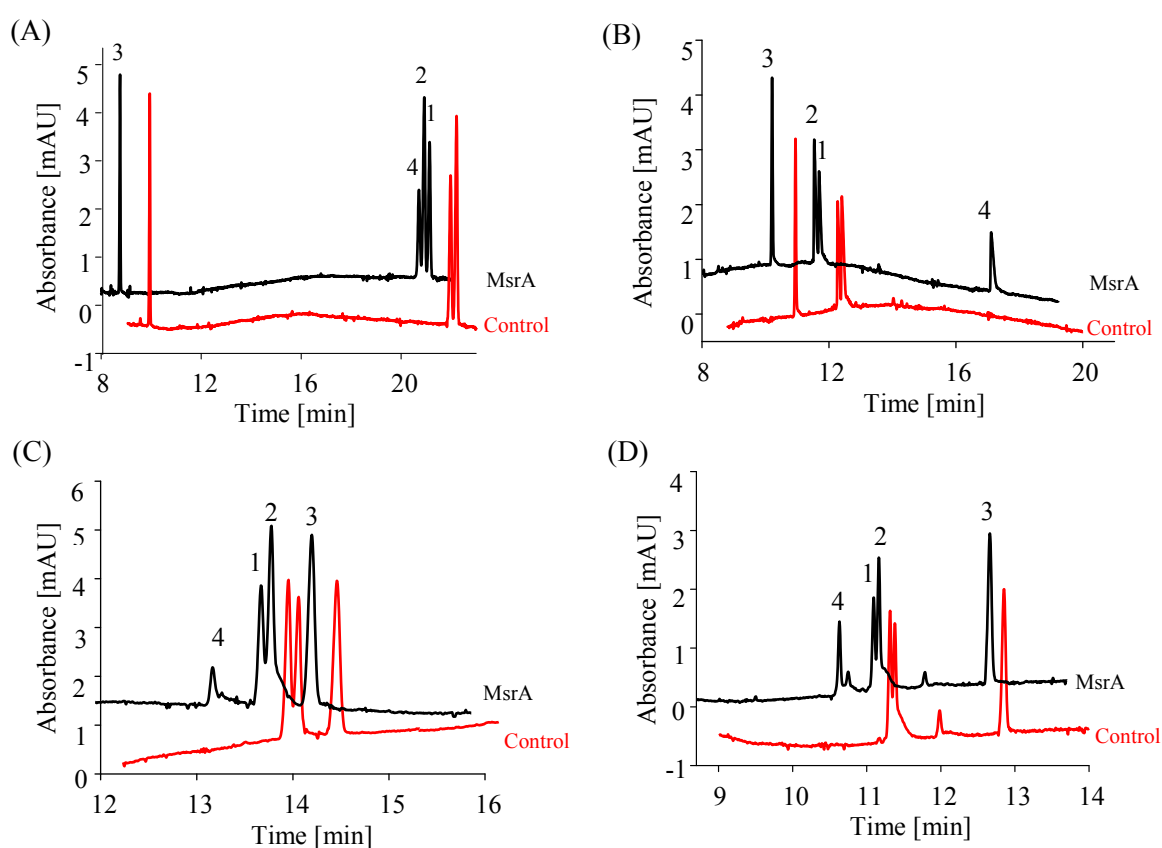


Fig. 29: Electropherograms of incubations. 180 µM Met(O) peptide was incubated in the presence of wild-type MsrA for 15 min at 37 °C. (A) Incubation of KFM(O)KK with 5 µg/mL enzyme. (B) Incubation of KDM(O)DK with 15 µg/mL enzyme. (C) Incubation of KNM(O)DK with 10 µg/mL enzyme. (D) Incubation of KDM(O)NK with 15 µg/mL enzyme. Peaks: 1, Met-S-(O)-containing peptide diastereomer; 2 Met-R-(O)-containing peptide diastereomer; 3, Fmoc-β-Ala; 4, Met-containing peptide; Experimental conditions: (A) 50 mM Tris-HCl, pH 8.0, containing 15 mg/ml sulfated β-CD, 15 mM SDS, 25 kV; (B) 50 mM Tris-HCl, pH 7.5, 10 mg/mL sulfated β-CD, 25 kV; (C) and (D), 50 mM Tris-HCl, pH 7.0, containing 12 mg/ml sulfated β-CD, 20 kV. Other conditions: 50/60.2 cm, 50 µm id, fused silica capillary, 20 °C, detection at 214 nm.

Fig. 30 summarizes the performance of the MsrA mutants compared to the wild-type enzyme of three enzyme concentrations for the four Met(O) peptide substrates. The decrease of Met-S-(O) diastereomer was followed for the activity determination. The values were calculated according to:

$$\text{Reduction (\%)} = \frac{R_{\text{Control}} - R_{\text{MsrA}}}{R_{\text{Control}}} \times 100\% \quad (6)$$

where R_{control} and R_{MsrA} represent the corrected peak area ratio of a control sample and a sample incubated with MsrA, respectively.

At all concentrations of the wild-type enzyme and mutants essentially identical results were obtained. As it can be seen, KFM(O)KK which carries one positively charged amino acid flanking Met(O) appears to be the best substrates for fungal wild-type MsrA as well as the mutants, while KDM(O)DK with two negatively charged aspartic acid residues is the poorest substrate. Literature data also suggest that peptide substrates with amino acids like Asp or Pro adjacent to Met(O) cannot be efficiently reduced by MsrA enzymes [72]. Wild-type MsrA (Glu99, Asp134) showed the highest activity compared to the mutants towards all tested substrates. Furthermore, the mutant EQ (Gln99, Asp134) was the mutant with lowest activity towards all peptides with the exception of the substrate KNM(O)DK, while the mutant DN (Glu99, Asn134) displayed higher activity towards KDM(O)NK than KNM(O)DK. The mutant DE (Glu99, Glu134) was more active than other mutants for all the tested peptide substrates. These findings were generally in agreement with the previously reported results except that the reduction of KDM(O)DK by mutant DE (Glu99, Glu134) was not observed more efficiently than by wild-type fungal MsrA [42].

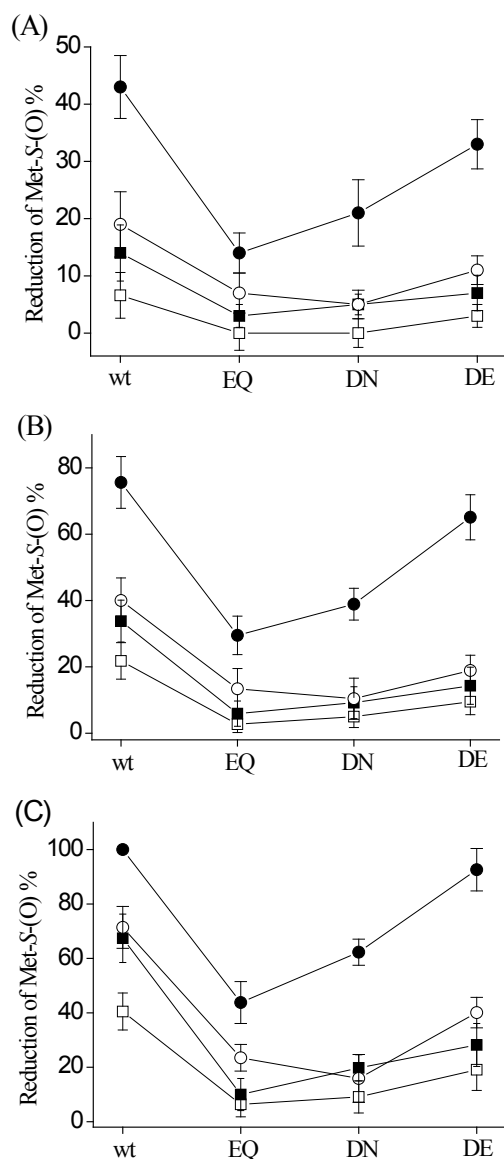


Fig. 30: Reduction of Met-S(O) peptide diastereomer by fungal MsrA wild-type as well as mutated enzymes. 180 μ M of each synthetic peptide containing Met(O) was subjected reduction by fungal MsrA (wt) or the mutated in the presence of 20 mM DTT and 50 mM Tris (pH 8.0) for 15 min at 37 $^{\circ}$ C, with three enzyme concentrations, (A) 5 μ g/ml, (B) 10 μ g/ml and (C) 15 μ g/ml. ●, KFM(O)KK; ○, KNM(O)DK; □, KDM(O)DK; ■, KDM(O)NK.

4.4.4 Molecular modeling

In order to rationalize the various activity of the wild-type enzyme and the mutants toward the substrates, modelling was performed by the group of Prof. W. Sippl (University of Halle, Germany). The model was primary built based on the x-ray structure of Msr from *N. meningitidis* in complex

4.4 Off-line assay for recombinant fungal MsrA and mutants using synthetic peptide substrates

with a substrate [Ac-Met-S-(O)-NHMe] (PDB ID 3bqf). This template shares a 43 % sequence identity with the fungal (*A. nidulans*) wild-type MsrA.

The active site was defined by 6 Å around the substrate in the binding site [Ac-Met-S-(O)-NHMe]. Two types of constraints were set to bias the results towards undergoing the crucial expected interactions. A scaffold constraint was set so that the Met-S-(O) moiety of the peptides are able to adapt a similar position shown in the model (see **Fig. 31A** green). The other was an H-bond constraint with the side chain of E134 for the docking of the mutant DE, as found between the backbone-NH of Met(O) and the protein. Goldscore was used as the scoring function.

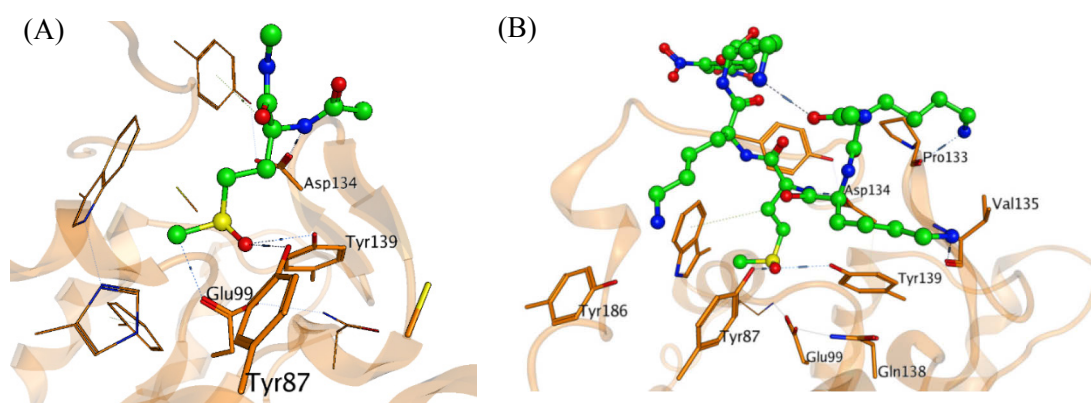


Fig. 31: Generated model of *A. nidulans* MsrA with substrate in binding site. (A) Ac-Met-S-(O)-NHMe and (B) Ac-KKM(O)KK-Dnp. Substrate is colored in green and Msr in orange. H-bond interactions are shown as blue-dashed lines.

Although the docking was successful in placing the Met-S-(O) residue in its predicted position, it was difficult to draw a reasonable conclusion for the substrate preference of the Msr enzymes. The main reason was that the peptide obviously interacted at the surface of the enzyme. Since there are no pronounced binding pockets for the tested peptides, all the residues [except for Met-S-(O)] can only interact on the surface of the protein, some even projected into the solvent (data not shown). In the case of KKM(O)KK, the lysine residues can undergo many interactions with acidic/polar surface groups of the enzyme in which H-bond interactions can be observed between the lysine [KKM(O)KK, red] and the backbone of Pro133, the lysine [KKM(O)KK, red] and the backbone of Val135 and the lysine [KKM(O)KK, red] with the side chain of T186 (**Fig. 31B**).

Nonetheless, the model showed that Glu99 in the active site pocket was buried in the Met-S-(O) binding groove, which might contribute to the right placing of Met-S-(O) and, consequently, to the catalytic activity of Msr. Replacement of Glu99 (wild-type) by Gln (EQ mutant) resulting in loss of enzyme activity supported this hypothesis. Glu134 showed according to the model only H-bond interactions with the backbone of Met-S-(O), and there was no indication that it might also interact with flanking residues from the peptides. No improvement of the enzyme activity was observed when replacing Asp134 by Glu (DE mutant) as well.

4.5 CE separation of Met(O)-containing pentapeptide diastereomers

Although the successful separation of aryl and alkyl sulfoxide enantiomers as well as the sulfoxide enantiomers of the drugs has been accomplished [166-168], the separation of peptide diastereomers containing Met(O) has not been reported expect for the separation of KIFM(O)K described in chapter 4.3. Therefore, the aim of the present study was to further evaluate the separation method for Met(O)-containing pentapeptide diastereomers.

4.5.1 Investigation of dual system of cyclodextrin and achiral crown ether

In chapter 4.3, the diastereomers of KIFM(O)K were resolved by the use of a dual selector system composed of sulfated β -CD and 15-crown-5. In the present part, the dual selector system composed CDs and crown ethers was further investigated.

4.5.1.1 Screening of CDs for diastereomer separation

Evaluation of the separation conditions was performed using the *N*-acetylated and C-terminally Dnp labeled pentapeptides KDM(O)DK, KNM(O)DK, KVM(O)VK, KEM(O)KK and KIFM(O)K. Peptide *pI* values were calculated using the Gen-Script Peptide Property Calculator (www.genscript.com/sslbin/site2/peptide_calculation.cgi). Assuming that the oxidation of Met does not affect the isoelectric point (*pI*) of peptides, KDM(O)DK can be considered a neutral peptide with a *pI* of about 7.0. A *pI* value of 8.9 was calculated for KNM(O)DK, while the values of the remaining peptides were 10.5 [KEM(O)KK] and 10.8 [KVM(O)VK and KIFM(O)K]. Thus, all peptides are positively charged in the acidic pH range and, except for KDM(O)DK, also in the slight alkaline pH range. Therefore, the separation was investigated in a 40/50.2 cm, 50 μ m id, fused-silica capillary in the pH range 2.5-9.5 using 50 mM Tris-citric acid buffers or phosphate-based buffers. However, no separation of the peptide diastereomers was observed under these conditions.

Subsequently, neutral and charged CDs including native β -CD, methyl- β -CD, 2-hydroxypropyl- β -CD, heptakis(2,6-di-*O*-methyl)- β -CD, sulfopropyl- β -CD, sulfobutylether- β -CD, sulfated γ -CD, sulfated β -CD, carboxymethyl- β -CD (CM- β -CD) and CM- β -CD were evaluated as buffer additives at a concentration of 15 mg/mL in a 50 mM Tris-HCl buffer at pH 2.5 and pH 8.0. At pH 2.5, only a very limited partial separation was observed for KIFM(O)K and KVM(O)VK in the presence of CM-

β -CD. None of the analytes could be detected within 100 min under normal polarity of the separation voltage in the presence of sulfated β -CD even when reducing the concentration of the selector to 2 mg/mL. Consequently, the concentration of sulfated β -CD was raised to 30 mg/mL and the polarity of the separation voltage was reversed. Under these conditions, KDM(O)DK and KNM(O)DK could be detected within 10 min but no diastereomer separation was observed. At pH 8.0, partial separation of the diastereomers of KIFM(O)K, KEM(O)KK, KDM(O)DK and KNM(O)DK was noted in the presence of 15 mg/mL sulfated β -CD with normal polarity of the separation voltage. Baseline separation ($R_s > 1.5$) of KIFM(O)K and KEM(O)KK was achieved in a BGE containing 20 mg/mL sulfated β -CD 50 mM Tris-citric acid buffer, pH 7.5. The other peptide diastereomers could not be baseline resolved no matter what sulfated β -CD concentration or buffer pH was investigated. All other investigated CDs proved to be ineffective as BGE additives for achieving at least a partial separation under the experimental screening conditions.

4.5.1.2 Screening of the dual system of CDs and achiral crown ethers

It has been reported in the literature that the addition of achiral crown ethers can enhance enantioseparations of primary amines including amino acids. 18-crown-6 [121, 122, 169] or diaza-crown ethers [124, 125] have been used in combination with native β -CD or neutral β -CD derivatives. Consequently, the crown ethers 18-crown-6 and 15-crown-5 as well as the diaza-crown ethers Kryptofix[®] 22 (4,13-diaza-18-crown-6) and Kryptofix[®] 21 (7,13-diaza-15-crown-5) were studied in combination with β -CD, CM- β -CD and sulfated β -CD using Tris-citric acid buffers with a pH of 2.5 and 8.0 as BGEs. The concentration of the CDs was set at 10 mg/mL, while 18-crown-6 and 15-crown-5 were tested at a concentration of 15 mM and the nitrogen-containing Kryptofix[®] crown ethers at 8 mM. The results in comparison with the sole use of CDs as additives are summarized in **Tables 11** (pH 2.5) and **12** (pH 8.0).

Table 11. Screening of Met(O) peptide diastereomer separation at pH 2.5

Peptide	CD	CD alone		CD + 18-crown-6		CD + 15-crown-5		CD + Kryptofix [®] 22		CD + Kryptofix [®] 21	
		t ₁ / t ₂ [min]	R _S	t ₁ / t ₂ [min]	R _S	t ₁ / t ₂ [min]	R _S	t ₁ / t ₂ [min]	R _S	t ₁ / t ₂ [min]	R _S
KDM(O)DK	β-CD	4.92 / 4.92	0	5.14 / 5.14	0	4.78 / 4.78	0	Np	-	6.55 / 6.55	0
	CM-β-CD	6.57 / 6.57	0	7.70 / 7.70	0	7.31 / 7.31	0	Np	-	8.75 / 8.75	0
	sulf. β-CD	np	-	np	-	Np	-	Np	-	np	-
KVM(O)VK	β-CD	4.91 / 4.91	0	5.35 / 5.35	0	5.12 / 5.12	0	Np	-	12.55 / 12.55	0
	CM-β-CD	8.68 / 8.72	0 ^a	12.65 / 12.72	0.47	10.21 / 10.29	0.35	Np	-	13.77 / 13.85	0.52
	sulf. β-CD	np	-	np	-	Np	-	Np	-	np	-
KIFM(O)K	β-CD	6.82 / 6.82	0	8.73 / 8.73	0	7.55 / 7.55	0	Np	-	18.99 / 19.18	0.87
	CM-β-CD	6.90 / 6.90	0	8.31 / 8.37	0.55	7.87 / 7.91	0 ^a	Np	-	18.35 / 18.43	0.79
	sulf.β-CD	np	-	np	-	Np	-	Np	-	np	-
KEM(O)KK	β-CD	7.12 / 7.12	0	7.83 / 7.83	0	7.63 / 7.63	0	Np	-	13.44 / 13.44	0
	CM-β-CD	7.56 / 7.56	0	8.97 / 9.11	0.63	7.84 / 7.84	0	Np	-	14.33 / 14.46	0.55
	sulf. β-CD	np	-	np	-	Np	-	Np	-	np	-
KNM(O)DK	β-CD	6.32 / 6.32	0	6.91 / 6.91	0	6.71 / 6.71	0	Np	-	13.33 / 13.33	0
	CM-β-CD	7.71 / 7.71	0	8.21 / 8.33	0.58	8.91 / 8.91	0	Np	-	15.38 / 15.55	0.5
	sulf. β-CD	np	-	np	-	Np	-	Np	-	np	-

np, no peak observed within 100 min.

R_S, peak resolution calculated by the 32 Karat™ **Software** according to $R_S = 2(t_2 - t_1) / (w_1 + w_2)$; t₁ and t₂ are the migration times, and w₁ and w₂ are the widths of the peaks at the baseline.

^a peak separation was too low to calculate R_S value

Table 12. Screening of Met(O) peptide diastereomer separation at pH 8.0

Peptide	CD	CD alone		CD + 18-crown-6		CD + 15-crown-5		CD + Kryptofix® 22		CD + Kryptofix® 21	
		t ₁ / t ₂ [min]	R _S	t ₁ / t ₂ [min]	R _S	t ₁ / t ₂ [min]	R _S	t ₁ / t ₂ [min]	R _S	t ₁ / t ₂ [min]	R _S
KDM(O)DK	β-CD	3.23 / 3.23	0	3.86 / 3.86	0	3.52 / 3.52	0	5.63 / 5.63	0	4.93 / 4.93	0
	CM-β-CD	4.55 / 4.55	0	4.99 / 4.99	0	4.81 / 4.81	0	7.84 / 7.84	0	6.65 / 6.65	0
	sulf. β-CD	4.67 / 4.67	0	5.72 / 5.75	0.55	4.63 / 4.69	0.51	7.76 / 7.76	0	6.96 / 6.96	0
KVM(O)VK	β-CD	3.53 / 3.53	0	4.02 / 4.02	0	3.85 / 3.85	0	4.64 / 4.64	0	4.21 / 4.21	0
	CM-β-CD	4.45 / 4.45	0	5.17 / 5.17	0	4.99 / 4.99	0	21.94 / 22.47	1.17	14.17 / 14.38	0.96
	sulf. β-CD	4.74 / 4.74	0	5.28 / 5.28	0	5.12 / 5.12	0	13.39 / 13.39	0	11.53 / 11.53	0
KIFM(O)K	β-CD	3.77 / 3.77	0	4.25 / 4.25	0	3.99 / 3.99	0	10.81 / 10.91	1.21	9.12 / 9.21	1.31
	CM-β-CD	3.89 / 3.89	0	4.66 / 4.66	0	4.32 / 4.32	0	15.45 / 15.74	1.57	11.25 / 11.55	1.29
	sulf.β-CD	8.05 / 8.14	1.34	13.37 / 13.83	2.52	12.63 / 12.95	2.39	29.30 / 30.88	5.73	27.32 / 28.44	5.14
KEM(O)KK	β-CD	3.88 / 3.88	0	4.45 / 4.45	0	4.11 / 4.11	0	10.73 / 10.73	0	8.79 / 8.79	0
	CM-β-CD	4.11 / 4.11	0	4.55 / 4.55	0	4.32 / 4.32	0	15.15 / 15.37	1.21	10.52 / 10.64	1.02
	sulf. β-CD	11.74 / 11.87	1.41	14.89 / 15.07	1.83	13.03 / 13.21	1.62	26.90 / 27.98	4.32	19.91 / 20.34	2.51
KNM(O)DK	β-CD	4.45 / 4.45	0	4.75 / 4.75	0	4.61 / 4.61	0	9.83 / 9.83	0	8.22 / 8.22	0
	CM-β-CD	5.09 / 5.09	0	6.82 / 6.82	0	6.34 / 6.34	0	12.37 / 12.46	0.61	11.11 / 11.22	0.52
	sulf. β-CD	6.84 / 6.84	0.56	9.55 / 9.64	1.02	8.53 / 8.61	0.89	11.86 / 11.95	1.44	10.88 / 10.96	1.39

np, no peak observed within 100 min.

R_S, peak resolution calculated by the 32 Karat™ Software according to $R_S = 2(t_2 - t_1) / (w_1 + w_2)$; t₁ and t₂ are the migration times, and w₁ and w₂ are the widths of their peaks at the baseline.

It should be noted that addition of a crown ether (either regular crown ether or diaza-crown ether) to the BGE in the absence of a CD in concentrations up to 20 mM did not result in any separation. The neutral crown ethers, 18-crown-6 and 15-crown-5, displayed a synergistic effect on the diastereomer separation in combination with CM- β -CD at pH 2.5 and with sulfated β -CD at pH 8.0. Only partial separations were observed at pH 2.5, while baseline separations could be observed for KIFM(O)K and KEM(O)KK with sulfated β -CD and the crown ethers at pH 8.0. Migration times increased in the presence of the crown ethers compared to the sole presence of CDs indicating that a ternary complex may be formed between peptide diastereomers, CDs and crown ethers as derived for amine analytes [121, 170, 171]. No separation could be observed in combination with native β -CD even at concentrations of up to 25 mg/mL of the CD.

The pK_a values of diaza-crown ethers are about 9 [172] so that the compounds are protonated at the pH values studied. Interestingly, none of the analytes could be detected at pH 2.5 in the presence of Kryptofix[®] 22 in CDs-based BGEs under both, normal and reversed polarity of the separation voltage. In contrast, partial diastereomer separation of several peptides were observed for Kryptofix[®] 21-containing BGEs. It may be speculated that the protonated Kryptofix[®] 22 is adsorbed to the capillary wall, thus, modifying the EOF while this occurs to a lesser extend in case of the smaller Kryptofix[®] 21 crown ether. Migration times increased as compared to the presence of the neutral crown ethers despite the fact that the charge of the complexes should be higher in the case of the protonated diaza-crown ethers. This further indicates that the diaza-crown ethers induced an EOF directed towards the anode. Finally, the diastereomers of KIFM(O)K were resolved by the combination Kryptofix[®] 21 and β -CD at pH 2.5.

A significant synergistic effect between the CDs and the diaza-crown ethers was noted at pH 8.0. Except for KDM(O)DK with the approximate pI of 7.0, all other peptide diastereomers were at least partially separated using CM- β -CD. Effective separations were found in the presence of sulfated β -CD with baseline resolution $R_S > 5$ for KIFM(O)K in the presence of both diaza-crown ethers. The diastereomers of this peptide were even resolved when β -CD was used as CD component. **Fig. 32** illustrates the effect of the crown ethers on the diastereomer separation of KEM(O)KK under the screening conditions at pH 8.0 as an example.

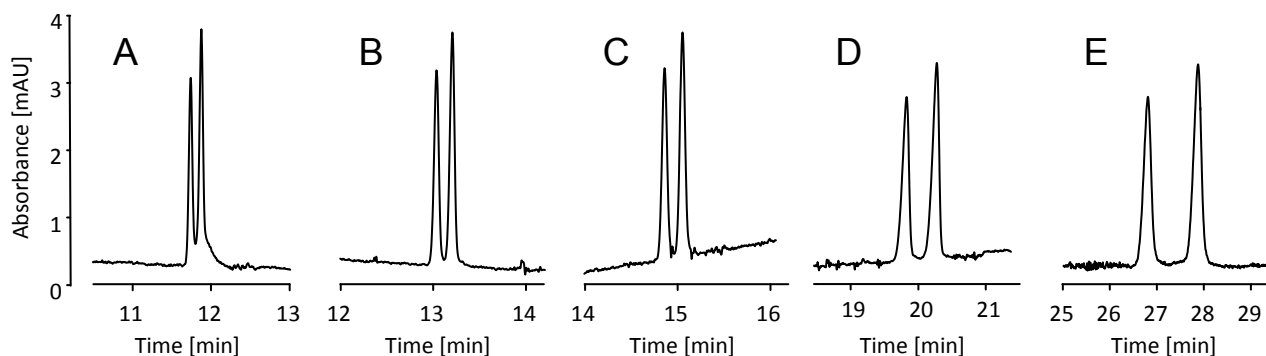


Fig. 32: Effect of CDs and crown ethers as BGE additives on the separation of the diastereomers of KEM(O)KK. Experimental conditions: 40/50.2 cm, 50 μ m id fused silica capillary, 50 mM Tris-citric acid buffer, pH 8.0, 25 kV, 20 $^{\circ}$ C, detection at 214 nm. Buffer additives (A) 10 mg/mL sulfated β -CD, (B) 10 mg/mL sulfated β -CD and 15 mM 15-crown-5, (C) 10 mg/mL sulfated β -CD and 15 mM 18-crown-6, (D) 10 mg/mL sulfated β -CD and 8 mM Kryptofix[®] 21, and (E) 10 mg/mL sulfated β -CD and 8 mM Kryptofix[®] 22.

4.5.1.3 Effect of CD and crown ether concentration in the dual system

The effect of different CD and crown ether concentrations on the separation of the peptide diastereomers was studied using 18-crown-6 and Kryptofix[®] 22 as well as sulfated β -CD, except for KVM(O)VK. In this case, CM- β -CD was applied because it proved to be an effective additive for the diastereomer separation of this peptide in the screening experiments. The experiments were conducted at pH 8.0 because efficient separations were observed at this pH in contrast to pH 2.5. The concentration of one type of selector was fixed while the concentration of the second selector was varied. The results are summarized in **Fig. 33**.

Generally, with a few exceptions, an increase of peak resolution and migration time could be observed upon increasing the concentration of one selector while keeping the other selector constant. In the case of KNM(O)DK an optimum appears to exist for a CD concentration (with constant crown ether concentrations) of about 15 mg/mL because peak resolution decreased when further increasing the CD concentration (**Fig. 33B and 33C**). Only partial resolution of the diastereomers of KDM(O)DK was observed at concentrations of Kryptofix[®] 22 below 10 mM, while no separation was observed at higher concentration.

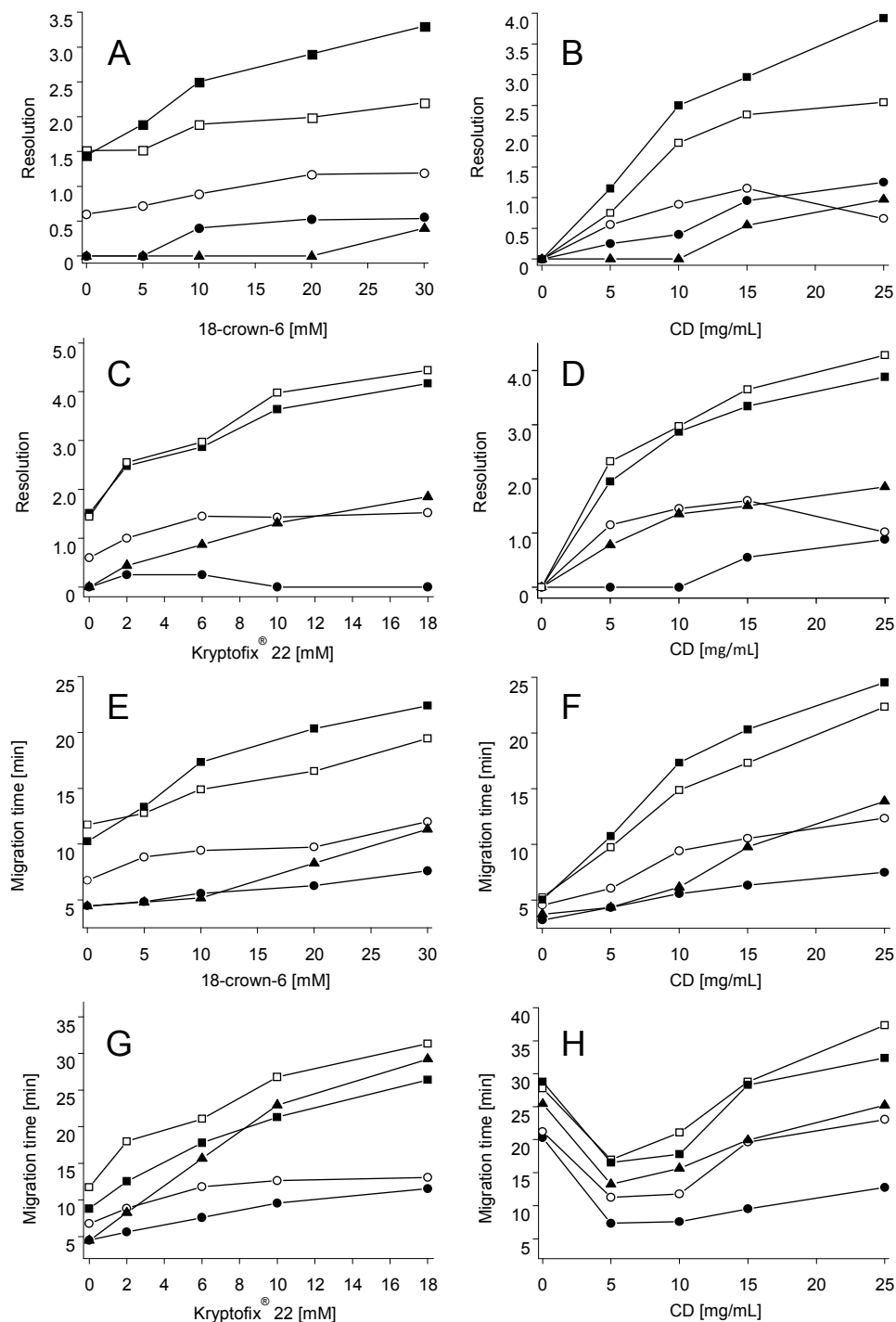


Fig. 33: Effect of the concentration of CDs and the crown ethers, 18-crown-6 and Kryptofix® 22, on (A-D) resolution of Met(O) peptide diastereomers and (E-H) migration time of the first migrating diastereomer. Experimental conditions: 40/50.2 cm, 50 μ m id fused silica capillary, 50 mM Tris-citric acid buffer, pH 8.0, 25 kV, 20 $^{\circ}$ C, detection at 214 nm. CM- β -CD was used for the separation of KVM(O)VK while sulfated β -CD was used for the separation of the other peptides. The concentration of the CD was fixed at 10 mg/mL when varying the crown ether concentrations (A, C, E, G). The concentrations of 18-crown-6 was fixed at 15 mM (B, F) and Kryptofix® 22 at 8 mM (D, H) when varying the CD concentration. ●, KDM(O)DK; ▲, KVM(O)VK; ○, KNM(O)DK; □, KEM(O)KK; ■, KIFM(O)K.

In contrast to the other systems, migration analyte times decreased in case of the Kryptofix[®] 22-based BGE upon addition of 5 mg/mL of the CDs and subsequently increased at higher CD concentrations (**Fig. 33H**). This decrease did not correlate with a general decrease in peak resolution (**Fig. 33D**). It may be speculated that the positively charged diaza-crown ether is adsorbed to the capillary wall resulting in a slow EOF directed toward the anode. This can be counteracted by the presence of negatively charged CDs such as sulfated β -CD or CM- β -CD resulting in a faster migration of the positively charged analytes to the detector at the cathodic end of the capillary. The subsequent increase of the migration times at higher CD concentrations can be explained by the increased analyte complexation and increased viscosity of the buffer at higher CD concentrations.

4.5.1.4 Effect of buffer pH

The effect of the pH of the Tris-citric acid-based electrolyte was studied in a pH range 2.5 to 9.5 with BGEs containing 15 mg/mL CM- β -CD and 20 mM 18-crown-6 or 10 mM Kryptofix[®] 22. The diaza-crown ether is only partially protonated above pH 9.0, while CM- β -CD will be protonated at pH < 3-4. KVM(O)VK was used as model peptide because separations in CM- β -CD-based BGEs have been observed during the screening experiments. The peptide is positively charged over the entire pH range studied (*pI* of approximately 10.8).

Fig. 34A shows the pH-dependent separation of the KVM(O)VK diastereomers using the combination of CM- β -CD and 18-crown-6 in Tris-Citric buffer. Increasing the pH of the BGE resulted in a deterioration of the diastereomer separation with a concomitant decrease of migration times. No separation could be observed at pH values above 4. This may be explained by the increased EOF at higher pH values leading to short migration times, which did not allow sufficient time for analyte-selector interactions.

For the combination CM- β -CD and Kryptofix[®] 22, long migration times were observed at pH values below 6.5. The dependence of the resolution of the diastereomers of KVM(O)VK in the pH range 6.5 – 9.5 is depicted in **Fig. 34B**. The highest resolution was found at pH 7.5 to 8. Further increase of the pH resulted in a loss of resolution. Migration times also significantly decreased, e.g. from about 45 min at pH 7.5 to about 25 min at pH 8.5 with a concomitant decrease of resolution from 2.4 to 2.1. The effect of the change of the charge of the selectors as a function of buffer pH on the formation of the ternary complex with the positively charged peptide could not be concluded from the present data.

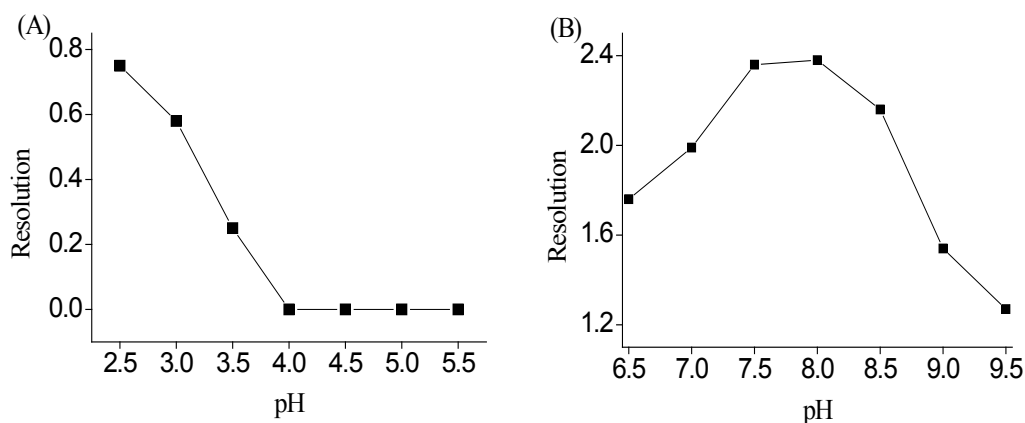


Fig. 34: pH-Dependence of the separation of the KVM(O)VK diastereomers using (A), the combination of 15 mg/mL CM-β-CD and 20 mM 18-crown-6 and (B), the combination of 15 mg/mL CM-β-CD and 10 mM Kryptofix® 22. Experimental conditions: 40/50.2 cm, 50 μm id fused silica capillary, 50 mM Tris-citric acid buffer, 25 kV, 20 °C, detection at 214 nm.

4.5.2 Separation of Met(O)-containing peptide diastereomers by CD-mediated MEKC

The dual system of CDs and achiral crown ethers showed a high ability for the separation Met(O)-containing peptide diastereomers. However, only partial resolution of the diastereomers of KDM(O)DK (neutral peptide) was observed at concentrations of Kryptofix® 22 below 10 mM, and no separation was observed at higher concentrations (Chapter 4.5.1.3). The dual system proved to be ineffective for the further separation of the neutral Met(O) peptide diastereomers NM(O)N and KEM(O)EK. It may be speculated that crown ethers have only weak interaction with neutral peptide diastereomers so that the critical “sandwich complex” contributing to the separation cannot be formed.

As it has been reported, CD-mediated MEKC can be used alternatively for the separations of chiral compounds including peptide enantiomers [173 - 176]. Thus, CD-modified MEKC was investigated using a 50 μm id, 50/60.2 cm fused silica capillary. The diastereomers of KDM(O)DK and NM(O)N showed only low resolution at pH 6.5 and pH 8.0 with a 50 mM Tris buffer, containing 25 mM SDS. The separation was not able to be significantly improved by varying buffer pH and the concentrations of SDS. Only a very limited separation was observed for KDM(O)DK with 10 mg/mL sulfated β-CD in 50 mM Tris-HCl buffer, at pH 8.0. The other two Met(O) peptide diastereomers showed no separation under this condition. Other CDs were not able to separate the tested peptide diastereomers. For the investigation of CD-mediated MEKC, sulfated β-CD was chosen based on the preliminary CD screening results. Native β-CD was also selected as a reference.

The concentration of the CDs was set at 10 mg/mL and SDS was applied at a concentration of 20 mM. Because an unstable baseline and long migration times were observed at a buffer pH below 6.0, the screening pH was set at 6.5 and 8.0. It should be mentioned that all the tested peptides are generally neutral at pH 6.5 while KDM(O)DK and KEM(O)EK are slightly negatively charged at pH 8.0. The screening results are summarized in **Table 13** and **Table 14**.

Table 13. Screening of Met(O) peptide diastereomer separation using CD-MEKC at pH 6.5

Peptide	CD	CD alone		SDS alone		CD + SDS	
		t ₁ / t ₂ [min]	R _S	t ₁ / t ₂ [min]	R _S	t ₁ / t ₂ [min]	R _S
NM(O)N	β-CD	6.15 / 6.15	0	13.13 / 14.23	1.77	10.26 / 11.20	1.77
	sulf. β-CD	8.54 / 8.54	0			18.33 / 20.16	2.82
KDM(O)DK	β-CD	7.00 / 7.00	0	22.63 / 23.93	1.35	18.59 / 20.00	1.29
	sulf. β-CD	15.55 / 15.76	0.25			30.88 / 33.02	2.18
KEM(O)EK	β-CD	7.10 / 7.10	0	30.90 / 32.12	0.58	26.88 / 27.89	0.49
	sulf. β-CD	11.23 / 11.23	1.34			40.78 / 43.12	1.58

Table 14. Screening of Met(O) peptide diastereomer separation using CD-MEKC at pH 8.0

Peptide	CD	CD alone		SDS alone		CD + SDS	
		t ₁ / t ₂ [min]	R _S	t ₁ / t ₂ [min]	R _S	t ₁ / t ₂ [min]	R _S
NM(O)N	β-CD	4.20 / 4.20	0	7.00 / 7.18	1.00	6.12 / 6.26	0.98
	sulf. β-CD	4.53 / 4.53	0			8.87 / 9.13	1.62
KDM(O)DK	β-CD	4.65 / 4.65	0	11.12 / 11.23	0.75	9.88 / 10.00	0.76
	sulf. β-CD	6.23 / 6.26	0			12.91 / 13.33	1.45
KEM(O)EK	β-CD	5.14 / 5.14	0	10.52 / 10.53	0	8.88 / 8.88	0
	sulf. β-CD	6.33 / 6.33	0			16.27 / 16.40	0.78

Effective separations were observed using sulfated β-CD-mediated MEKC. At pH 6.5, baseline separations were achieved for all peptide sequences but with relatively long analysis times. While at pH 8.0, the analysis time was significantly decreased, the resolution between the diastereomers deteriorated as well. This might be attributed to the high EOF generated at a high pH which led to insufficient time for the interactions between analyte and buffer additives. β-CD had little selectivity towards Met(O) peptide diastereomers, but the migration time was shorter in β-CD-mediated MEKC than using a MEKC method in the absence of β-CD. In the case of KDM(O)DK, the migration time was reduced from 11.12 min to 9.87 min with an addition of 10 mg/mL β-CD to 50 mM Tris-HCl buffer containing 20 mM SDS, pH 8.0, while the resolution of the diastereomers was unaffected. A

synergistic effect was observed for sulfated and SDS micelles. This is probably due to the fact that sulfated β -CD itself also displayed weak recognition for Met(O) diastereomers. **Fig. 35** illustrates the effect of the sulfated β -CD-modified MEKC on the diastereomer separation of KDM(O)DK at pH 8.0.

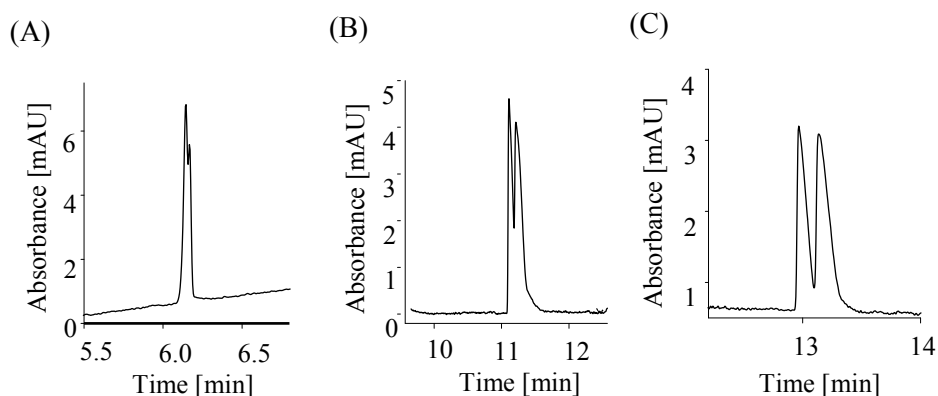


Fig. 35: Electropherograms of the separation of the diastereomers of KDM(O)DK. Experimental conditions: 50/60.2 cm, 50 μ m id fused silica capillary, 50 mM Tris-HCl buffer, pH 8.0, 25 kV, 20 $^{\circ}$ C, detection at 214 nm. Buffer additives (A) 10 mg/mL sulfated β -CD, (B) 20 mM SDS, (C) 10 mg/mL sulfated β -CD and 20 mM SDS.

The study revealed that addition of sulfated β -CD for a SDS-containing BGE was effective for the separation of neutral Met(O) peptide diastereomers. Interestingly, using this system for the basic Met(O) peptide diastereomers resulted in little separation but long migration times (over 60 min). For example, for the separation of KIFM(O)K, no peak was detected within 60 min using a 50 mM Tris-HCl, pH 8.0, containing 10 mg/mL sulfated β -CD and 15 mM SDS. It may be speculated that the positively charged peptide was incorporated into the negatively charged micelles to a great extent by static interactions and, as a consequence, migrated with the SDS micelles towards the anode. Therefore, the overall analyte velocity was reduced.

5 Discussion

Met residues in peptides and proteins are easily oxidized to Met(O). The latter exists as a pair of diastereomers, Met-*S*-(O) and Met-*R*-(O). Reduction of Met(O) diastereomers is catalyzed by Msrs in a stereospecific manner, i.e., MsrA reduces Met-*S*-(O) and MsrB reduces Met-*R*-(O). Separation of Met-*S*-(O) and Met-*R*-(O) is often challenging for the study of the stereospecificity of Msr enzymes. Therefore, the individual diastereomer dabsyl-Met-*S*-(O) and dabsyl-Met-*R*-(O) are most frequently used as substrates in reported stereospecific assays, [36, 73]. Since Met(O) residues are formed as a pair of diastereomers physiologically, the racemic mixture of Met(O) was chosen as the substrate for our study. In order to establish stereospecific CE methods that cover all kinds of substrates, three representative substrates were selected, which were free Met(O), Fmoc-Met(O) and Met(O)-containing pentapeptide. The separation of Met(O) diastereomers was achieved by different CE modes and will be discussed. Subsequently the separation methods were applied to enzyme assays. Both off-line and on-line CE assays were established.

5.1 Separation of substrate diastereomers

5.1.1 Separation of Met(O) derivatives by MEKC

MEKC method was found very effective for the separation of Met(O) derivatives including dabsyl-Met(O) and Fmoc-Met(O). In MEKC, the EOF is directed toward the cathode, while SDS micelles migrate to the anode. As a result, the overall micellar velocity is reduced counteracted by the bulk flow. The Met(O) diastereomers partition into and out of the micelles and, consequently, their migration velocities are affected by this equilibrium. The separation occurs due to the difference of hydrophobic interactions between the diastereomers and the micelles.

The method described by Uthus [99] employed an uncoated fused-silica capillary with a 25 mM KH_2PO_4 buffer, pH 8.0, containing *N*-laurylsarcosine as BGE. In addition, a buffer containing an additional 25 mM SDS in BGE was applied as conditioning solution, which was considered critical for the baseline separation of dabsyl-Met(O) diastereomers. Because SDS is incompatible with potassium ions and leads to the formation of a precipitate [156], KH_2PO_4 was replaced by NaH_2PO_4 in the present assay. Using a 35 mM phosphate buffer, pH 8.0, containing 25 mM SDS resulted in baseline separation of dabsyl-Met(O) diastereomers. This indicated that the presence of *N*-laurylsarcosine was not essential for the separation and no other conditioning buffer was required.

However, using this system a variation of the EOF and consequently shifting migration times of analytes were observed. Performing a dynamic coating by an addition of 0.04% (m/v) polyethylene oxide to the BGE improved precision of the migration times (RSD < 6%) but resulted in long analysis time (more than 30 min).

In order to achieve a stable EOF and shorter analysis times, a SMIL-coated capillary was applied with polybrene as the cationic polymer and dextran sulfate as the anionic polymer. The illustration of coating procedure is shown in **Fig. 36**. The dextran sulfate coating provided a stable and strong cathodic EOF and, consequently, led to a short analysis time.

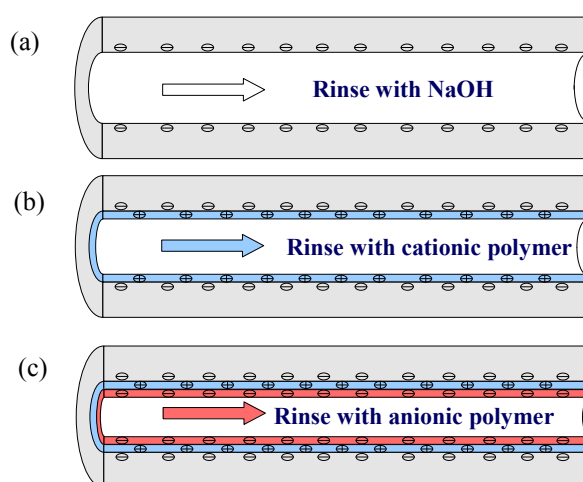


Fig. 36: SMIL coating procedure. (a) Activation of the silanol groups; (b) first layer coating; (c) Second layer coating.

The bi-layer was initially coated by rinsing the capillary with 5% (w/v) aqueous polybrene for 15 min followed by the rinse of 3% (w/v) dextran sulfate solution for 30 min according to Katayama [151, 177]. The procedure was further optimized with an additional rinse of water between the coating reagents, in order to avoid that the two oppositely charged polyelectrolytes interact at the interface of the capillary [178, 179]. This optimization resulted in a more reproducible coating procedure. Application a voltage of 10 kV for 10 min led to a fast capillary condition for a new coated capillary.

The coating efficiency might depend on the static interaction between silanol groups of the fused silica capillary and coating reagent. Katayama et al. further concluded from their study that the coating efficiency primarily depends on the interaction between the ionized silanol groups of the

inner capillary wall and polybrene while dextran sulfate completely covered the polybrene layer [151]. Furthermore, their study shows that capillaries from different sources lead to a variance of the velocity of the EOF in case of a single layer coating, while this variance decreased significantly after dextran sulfate covered on the polybrene layer due to strong interactions between polybrene and dextran sulfate [151]. Therefore, one may speculate that polybrene plays a critical role in the coating efficiency. Unfortunately, when switching from one batch of polybrene to another, a change in the magnitude of EOF was observed. Commercial polybrene is a poorly characterized chemical with regard to polymer size, and this may be the reason for the observed variations. Thus, changing the batch of polybrene in routine analysis of a validated method has to be considered with care. Using dextran sulfate obtained from different batches did not lead to significant changes in migration times, but a dependence of the EOF on the concentration of dextran sulfate coating solution was observed. It may be speculated that complete coverage of the polybrene layer by dextran sulfate is necessary when using MEKC conditions because SDS may also adsorb to the polybrene layer and further change the magnitude of the EOF.

The MEKC method employing a SMIL-coated capillary was found very effective for the separation of Met(O) derivatives, i.e., dabsyl-Met(O) and Fmoc-Met(O) diastereomers. The separation could be conducted in a buffer with a broad pH range. In the separation of dabsyl-Met(O), using a 35 mM phosphate buffer containing 25 mM SDS, resolutions of the diastereomers were found between 2.1 – 2.9 in the pH range 7.0 – 9.0, with migration times from 10.7 – 12.5 min. This might be attributed to the dextran sulfate coating which provided an independent EOF and, therefore, the separation was barely influenced by buffer pH.

5.1.2 Separation of Met(O)-containing pentapeptide diastereomers

A set of synthetic Met(O)-containing peptides was chosen from a previous study [42], which intended to investigate the impact of Met(O)-neighboring amino acids of substrate peptide on the Msr activity. To ensure solubility, lysine residues were incorporated at positions -2 and +2 for most peptides. KIFM(O)K was used in this assay as the standard substrate for enzymatic activity testing. All peptides were N-acetylated with C-terminal Dnp-labeled. Peptides are listed in **Table 15** and can be generally divided into neutral and basic peptides.

Table 15. *Met(O)*-containing peptide diastereomers

Neutral ^(a)	Basic ^(a)
NM(O)N	KIFM(O)K
KDM(O)DK, KEM(O)EK	KNM(O)DK, KDM(O)NK
	KEM(O)KK, KKM(O)EK
	KVM(O)VK, KFM(O)FK
	KFM(O)KK, KKM(O)FK

^(a) All the peptides were N-acetylated, with C-terminal Dnp-labeled.

5.1.2.1 Dual cyclodextrin-achiral crown ether system

Separation of *Met(O)* peptide diastereomers was not possible by MEKC with SDS as micelles. Therefore, alternative separation conditions were investigated. The use of the combination of β -CD and achiral crown ether was initially reported to separate enantiomers of primary amines including amino acids [121, 122, 124, 125]. The separation is assumed to be based on the formation of a sandwich-type complex between the analyte and the respective CD and crown ether [170, 171]. **Fig. 37** shows a possible sandwich complex mode for the separation of the primary amine compounds. It may be speculated that, the primary amino group which is protonated in the acidic buffer that enables the interaction with the crown ether, while the hydrophobic moiety of the molecule is incorporated into the cavity of the cyclodextrin. As a consequence, the transient diastereomeric complexes may become more distinguishable and, as a result, a separation is achieved when the binding constants for the complexes differ between two stereoisomers [170]

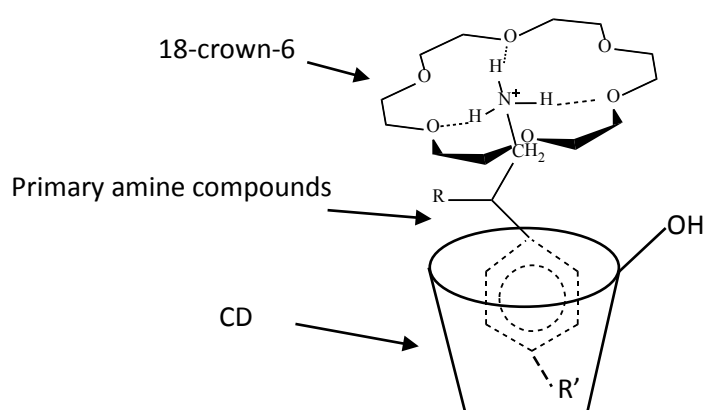


Fig. 37: A sandwiched complex mode (achiral 18-crown-6+cyclodextrin) for separation of chiral primary amino compounds.

Interestingly, this dual system was found also effective for the separation of Met(O) peptide diastereomers even though the molecular size of a peptide is much larger than an amino acid. The positively charged moiety of the peptide may interact with the crown ether while the hydrophobic residue was incorporated into the CD cavity to form the sandwich complex. Molecular modeling studies have also suggested that the binding energy differences between enantiomers in the sandwich complex is the reason for the chiral separation of primary amines [169]. Modeling studies could rationalize the mechanism of the separation Met(O) peptide diastereomers using this dual system.

It should be noted that the addition of a crown ether (either neutral crown ether or diaza-crown ether) to the BGE in the absence of a CD in concentrations up to 20 mM was not able to result in any separation. Thus, it is easy to speculate that the intermediate of the complex formed between a crown ether and the analyte with the CD is the most critical step for the diastereomer separation. Thus, the basic peptide diastereomers with high hydrophobicity such as KIFM(O)KK, KFM(O)FK, KVM(O)VK, KFM(O)KK and KKM(O)FK were separated effectively using this dual system. The synergistic effect between CD and crown ether was not observed for the separation of neutral Met(O)-containing peptide diastereomers. This is probably because the interaction between crown ether and neutral peptide is too weak to form the sandwich complex for the separation.

The effect of neutral crown ether

The data presented in chapter 4.5.1.4 reflects that, the neutral crown ethers, 18-crown-6 and 15-crown-5, displayed a strong synergistic effect on the diastereomer separation in combination with CM- β -CD at pH values < 4.0. Increasing the buffer pH resulted in a deterioration of the diastereomer separation with a concomitant decrease of migration times. This may be explained by the fact that, at low pH primary amino groups were completely protonated so that it be able to interact with neutral crown ethers to form host-guest complexes. The low EOF at low pH that allowed sufficient time for analyte-selector interactions was also beneficial for the separation. For the combination with sulfated β -CD, a slight improvement of the diastereomer separation was even observed at pH 8.0 when the analytes were only partially positively charged.

The effect of diaza-crown ether

In the case of diaza-crown ethers, more significant synergistic effect was observed in a broad pH range. For instance, in combination with sulfated β -CD, baseline separation of the KIFM(O)K diastereomers with a $R_s > 5$ was found in the presence of either Kryptofix[®] 22 or Kryptofix[®] 21 in a

pH range 7.0 - 10.0. The diastereomers of KIFM(O)K were even resolved by the combination of Kryptofix[®] 21 and native β -CD at pH 2.5.

Interestingly, none of the analytes could be detected at pH 2.5 in the presence of Kryptofix[®] 22 under both, normal and reversed polarity of the separation voltage. A similar behavior has also been observed by Iványi and colleagues when they attempted the enantioseparation of Trp by the combination of Kryptofix[®] 22 and neutral CD derivatives [124]. In contrast, partial diastereomer separation of several peptides was observed for Kryptofix[®] 21. It may be speculated that the Kryptofix[®] 22 which is protonated below pH 9.0 is adsorbed to the capillary wall, thus, modifying the EOF while this occurs to a lesser extent in case of the smaller Kryptofix[®] 21 crown ether. Diaza-crown ethers have been used for EOF modification and reversal for the separation of inorganic ions as bifunctional modifiers [180, 181]. The adsorption of Kryptofix[®] 22 can be counteracted by the presence of negatively charged CDs such as sulfated β -CD or CM- β -CD, resulting in a faster migration of the positively charged analytes to the detector at the cathodic end of the capillary. This explains that the migration times decreased in case of the Kryptofix[®] 22-based BGEs upon addition of 5 mg/mL of sulfated β -CD or CM- β -CD (see **Fig. 33H**). The subsequent increase of the migration times at higher CD concentrations can be explained by increased analyte complexation and increased viscosity of the buffer at higher CD concentrations. Migration times increased compared to the presence of the neutral crown ethers despite the fact that the charge of the complexes should be higher in the case of the protonated diaza-crown ethers. This further indicates that the diaza-crown ethers induced an EOF directed towards the anode.

The combination of CM- β -CD and Kryptofix[®] 22 provided the highest resolution at pH 7.5 to 9.0 for the separation of the KVM(O)VK diastereomers. A further increase of the pH from 7.5 to 8.5 led to a decrease of resolution from 2.4 to 2.1 with a concomitant significant decrease of migration time from 45 min to 25 min. Thus, the recommended pH for the separation would be 8.0 to 8.5 as a compromise between resolution and analysis time. One may assume that the decrease of the migration times (and loss of resolution) is due to the fact that Kryptofix[®] 22 is less protonated at pH 8 - 8.5. In this case, the interaction of the crown ether with the capillary wall is weakened resulting in a change of the EOF directed towards the cathode. However, the synergistic effect was still observed at pH 9.5 when Kryptofix[®] 22 was barely protonated to affect the EOF (**Fig. 38**).

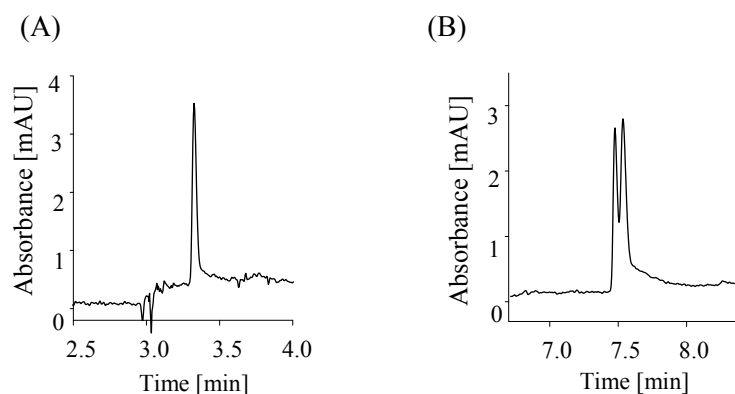


Fig. 38: Electropherograms of the diastereomer separation of KVM(O)VK. Experimental conditions: 40/50.2 cm, 50 μm id fused silica capillary, 25 kV, 20 $^{\circ}\text{C}$, detection at 214 nm. 50 mM Tris-citric acid buffer, pH 9.5. Buffer additives (A) 15 mg/mL CM- β -CD, (B) 15 mg/mL CM- β -CD, 10 mM Kryptofix[®] 22.

5.1.2.2 Cyclodextrin-mediated MEKC

As a further separation study for the Met(O) peptide diastereomers, CD-mediated MRKC was employed. The combination of micelles and CD is often used when the sole system is ineffective [173 - 175]. The separation is considered to be based on the analyte distribution in the system consisting of the micelle, CD and aqueous buffer [182, 183]. The equilibrium of a CD-mediated MEKC system is illustrated in **Fig. 39**. Micelles and CDs coexist in the aqueous buffer. Since CD has a hydrophilic outer surface, there is little driving force for micellar incorporation [183]. A surfactant molecule may, however, be included into the CD cavity [184, 185].

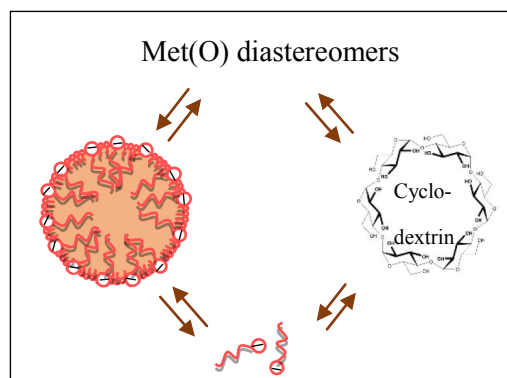


Fig. 39: Illustration of the equilibrium of a CD mediated-MEKC system.

In chapter 4.5.2, for the neutral β -CD-MEKC system, the peptide molecules that were included in the SDS micelles migrated towards anode, while the analyte complexed with β -CD migrated towards cathode. As a consequence, the migration times of the peptide diastereomers were reduced without loss of peak resolution between the diastereomers. Further increase of the concentration of β -CD may lead to a decrease of peak resolution. In case of using negatively charged CD-mediated MEKC, the addition of sulfated β -CD to SDS-based BGE resulted in an increase of resolution as well as migration times. This was because sulfated β -CD displayed slight recognition between the diastereomers which contributed to an improved peak resolution. The peptide incorporated by the negatively charged CD migrated to the anode, thus the analysis times was prolonged.

The substitution of sulfated β -CD with sulfated γ -CD in CD-mediated MEKC resulted in a slight improvement of diastereomer separation. **Fig. 40** shows electropherograms of the separation of KDM(O)DK by sulfated γ -CD-mediated MEKC. It seems that the large cavity of the γ -CD better accommodates the analyte with the surfactant monomers [184, 186].

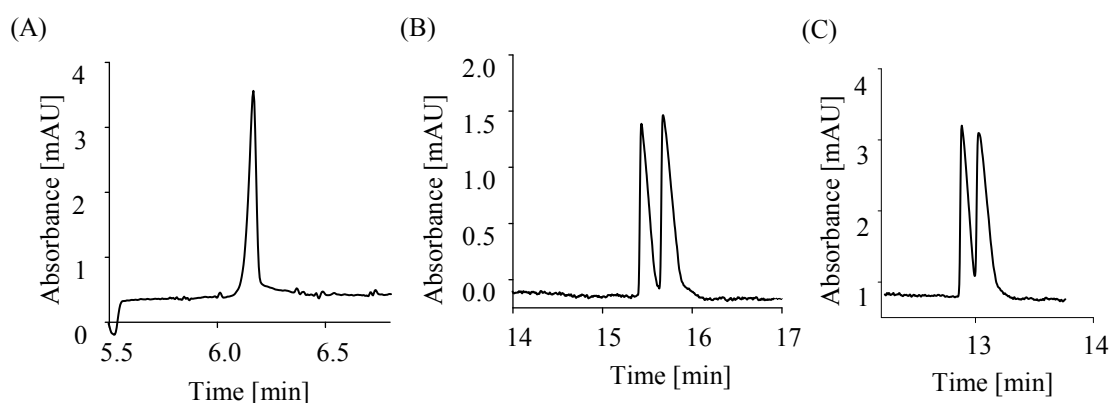


Fig 40: Electropherograms of diastereomer separation of KDM(O)DK. Buffer additives (A) 10 mg/mL sulfated γ -CD (B) 10 mg/mL sulfated γ -CD and 20 mM SDS and (C) 10 mg/mL 10 mg/mL sulfated β -CD and 20 mM SDS. Experimental conditions see **Fig. 35**.

All neutral peptide diastereomers were baseline or close to be baseline resolved using sulfated β -CD-mediated MEKC. For the basic peptides, however, strong electrostatic interactions exist between the positively charged peptide and the negatively charged SDS micelles. As a result, they are preferentially incorporated into the micellar phase, which does not allow the separation principle of CD-mediated MEKC to be effectively realized.

5.2 Assays for Msr enzymes

5.2.1 Off-line assay using free Met(O) as substrate

The MEKC method allowed the baseline separation of dabsyl-Met(O) and dabsyl-Met and was successfully applied to the determination of the stereospecificity of hMsrA and fungal fRMsr enzymes toward Met(O) diastereomers as substrates. The method was highly repeatable with regard to migration time of the analytes. An internal standard ensured the repeatability of the assay. This method can be used for the screening of the stereospecificity of Met(O) reductases as well as for the determination of enzyme kinetic data. An advantage of the assay is the fact that free Met(O) can be used as substrate. In contrast to commonly used coupled reactions involving Trx and Trx reductase, no additional enzymes are required.

Enzyme kinetic data of human MsrA with Met(O) as substrate have not been published. However, Kwak et al. recently reported a K_m value of $350 \pm 60 \mu\text{M}$ for mouse MsrA toward free Met(O) as substrate [164], which is in the same order of magnitude as found for hMsrA in the present study. K_m values in the range between $240 \pm 30 \mu\text{M}$ and $2100 \pm 200 \mu\text{M}$ and K_{cat} values in the range 0.30 ± 0.03 to $7.71 \pm 0.03 \text{ s}^{-1}$ have been found for MsrA of microorganisms [163].

5.2.2 Electrophoretically mediated microanalysis (EMMA)

In on-line assays, the enzyme is either immobilized on the surface of the capillary wall or present in solution. Since the SDS in the MEKC BGE would impair the activity of Msr enzymes, the partial filling mode was selected using a bracket of incubation buffer in order to separate enzyme and substrate solution from the separation buffer. The efficient mixing of substrate and enzyme is an important issue. This can be achieved by diffusion during injection and/or incubation depending on the injection process. Longitudinal and transverse diffusion contribute to the mixing process [140, 158, 159]. The second approach is based on the electrophoretic mobilities of substrate and/or enzyme so that mixing is achieved by application of a mixing voltage for a short period of time [126, 139, 160]. The electrophoretically mediated mixing using the injection sequence “enzyme-substrate-enzyme” showed the maximum sulfoxide reduction among all the tested mixing methods including diffusion. It can be concluded that electrophoretic mixing provided higher mixing efficiency than simple plug diffusion in the present assay.

The duration of the application of the mixing voltage was evaluated at a 1 kV in case not to impair the enzyme. The on-line incubation was conducted at 37 °C. Separation at the same temperature

resulted in a decrease of resolution between the Fmoc-Met(O) diastereomers. More importantly, frequent breakdowns of the electric current were observed when separating at 37 °C due to generation of Joule heating. Therefore, a voltage of 25 kV was applied for 1 min in order to separate enzyme and substrate before cooling the capillary to 25 °C.

Since the exact volume for an on-line incubation is unknown, the exact concentration of the enzyme working for the on-line reaction cannot be defined as well. Compared to the off-line assay, a higher amount of enzyme was applied to obtain comparable enzymatic reduction (20 µg/mL versus 5 µg/mL). This could be mainly attributed to the incomplete overlap of the reactant plugs [187, 188]. Depending on the efficiency of plug mixing by diffusion and electrokinetic transport, the enzyme plug is assumed to be diluted as well.

In order to monitor the performance of the EMMA method, the kinetic parameters of Msrs were determined and compared to the data obtained with off-line assay. As is shown in **Table 5**, essentially identical values were determined in both assays. With the on-line incubation, it is important to mention that quantities of the enzyme that contributed directly to the reaction is not exactly known, so that the K_{cat} values cannot be determined. Compared to the literature data, using comparable incubation conditions, i.e., Tris buffer, pH 8.0 and DTT as reducing agent, K_m values in the low millimolar range (1.10 ± 0.12 to 2.12 ± 0.36 mM) were observed for MsrA enzymes from the Arabidopsis family [77] using Fmoc-Met(O) as substrate. The present data for human enzymes are about 10-fold lower, which can be explained by species differences. However, the data reported in the present study for Fmoc-Met(O) as substrate are in the same range as K_m values reported for mammalian Msr enzymes in assays that employed dabsyl-Met(O) as substrate and DTT as reducing agents. A K_m value of 51 ± 38 µM was described for MsrA [164], while values ranging between 15 ± 6 µM and 1.3 ± 0.2 mM were observed for MsrB [164, 189]. This clearly demonstrates the usefulness of the EMMA assay for the determination of the stereospecific reduction of Met(O) by Msr enzymes. Furthermore, it is interesting to note that Fmoc-Met-*R*-(O) is a substrate for MsrB enzymes, which has not been reported before. Whether this is only true for mammalian enzymes or also applies to MsrB from other species will have to be elucidated in the future. It has been shown that Fmoc-Met(O) is a substrate for plant MsrA in *Pisum sativum L.*, but neither the stereoselectivity nor enzyme kinetic data has been determined for this enzyme [76].

Compared to the off-line assay, the EMMA assay can be completed in a shorter period of time for screening the activity of Msr enzymes because no sample workup is required. Moreover, the assay is fully automated and requires smaller amounts of enzyme and substrates, which reduces the overall

cost of the assay. On the other hand, off-line assays are generally easier to establish because buffer compatibility between incubation buffer and separation buffer do not have to be considered.

5.2.3 Off-line assays using Met(O)-containing pentapeptides as substrates

Dabsyl-Met(O) has been frequently applied as the mimics of peptide substrates [163, 164]. However, Met(O) derivatives are not peptide so that they may not reflect the activity of Msr enzymes towards peptide-bound Met(O). Therefore, Met(O)-containing peptide substrate was applied. KIFM(O)K was used as the standard substrate for the activity test in the previous studies [42, 149, 165] so it was chosen in our assay. The separation of KIFM(O)K diastereomers as well as the reduced peptide KIFMK was optimized under the help of the design of experiment. The method was successfully applied for the enzyme assay. **Table 16** shows the kinetic data obtained using KIFM(O)K as substrate as well as the data using free Met(O) and Fmoc-Met(O) as substrates, and the literature data with dabsyl-Met(O) or oxidized Met-rich proteins as substrates. It should be noted that for a Trx reduction system, the enzymatic activity reflects the complete enzymatic system including Trx reductase and Msr [58, 163, 164, 190]. For a DTT system, using different concentrations of DTT can result in various enzyme activities [191]. Furthermore, the kinetic performance for a specific Msr from different species can differ as well [163].

The K_m values observed for KIFM(O)K in our assay as well as reported data of protein substrates [84] for both enzymes in different organisms are lower compared to the data obtained from Met(O) derivatives, i.e., Fmoc-Met(O) and dabsyl-Met(O) [58, 164]. In contrast, the K_{cat} values of peptide and protein substrates are higher, which results in a significantly higher K_{cat}/K_m quotient. It appears that peptide-bound and protein substrates are better substrates which can be efficiently reduced by both, MsrA and MsrB, compared to free Met(O) and its derivatives. Studies on the substrate specificity of MsrA and MsrB from *N. Meningitidis* [192 - 194] also support the idea that the active sites of both Msrs are rather adapted for binding protein-bound Met(O) more tightly than free Met(O) or small molecule Met(O)-containing compounds.

Table 16. *Msr* kinetic data obtained with the substrate KIFM(O)K compared to free Met(O), Fmoc-Met(O) as well as the literature data using various substrates.

Organism	Substrate	Reduction system	K_{cat} (S ⁻¹)	K_m (μM)	K_{cat}/K_m (mM ⁻¹ ·min ⁻¹)	Ref.
<i>MsrA</i>						
Human	Free Met(O)	DTT	5.5 ± 0.3	390 ± 47.3	840	Results
Human	Fmoc-Met(O)	DTT	0.13 ± 0.01	256 ± 27.9	31	Results
Human	KIFM(O)K ^(a)	DTT	5.5 ± 0.5	135.6 ± 25.6	2447	Results
Mouse	dabsyl-Met(O)	DTT	0.28 ± 0.02	340 ± 40	49	[58]
<i>E.coli</i>	MRP4	Trx	13.0 ± 5.4	137 ± 76	5693	[84]
<i>E.coli</i>	β-Casein	Trx	1.13 ± 0.11	45 ± 13	1500	[84]
<i>MsrB</i>						
Mouse	Free Met(O)	Trx	8E-4 ± 3E-5	36 ± 17	1.4	[164]
Human	Fmoc-Met(O)	DTT	0.06 ± 0.002	105.7 ± 10.4	35	Results
Human	KIFM(O)K ^(a)	DTT	0.36 ± 0.04	100.5 ± 19.8	211	Results
Human	dabsyl-Met(O)	Trx	0.07 ± 0.008	190 ± 20	23	[164]
<i>E.coli</i>	MRP4	Trx	1.04 ± 0.16	70 ± 20	894	[84]
<i>E.coli</i>	β-Casein	Trx	0.78 ± 0.05	54 ± 9	864	[84]

^(a)The peptide is N-acetylated, with C-terminal Dnp-labeled.

5.2.4 Activity determination for fungal MsrA and the mutants

The data of the present study suggest that peptide substrates with positively charged residues adjacent to Met(O) are preferentially reduced by fungal MsrA as well as the mutants, which supports the findings in the previous study [42]. This is also in accordance with the literature which also reported that peptide substrates with amino acids such as Asp or Pro adjacent to Met(O) cannot be efficiently reduced by MsrA enzyme [72].

Wild-type MsrA (Glu99, Asp134) displayed the highest activity for all substrate compared to the mutants. Substitution of Glu99 by Gln (mutant EQ) resulted in the lowest activity towards all substrate except for KNM(O)DK, while replacement of Asp134 by Asn134 (mutant DN) lead to a higher activity towards KDM(O)NK than KNM(O)DK. It might be speculated that asymmetric negative charges in the enzyme active center correspond to the reversed substrate preference. The mutant DE (Glu99, Glu134) showed higher activity towards all the substrates than other mutants but was not found more active than wild-type fungal MsrA in the reduction of peptide substrate with negatively charged amino acids flanking Met(O) as described in the previous study [42].

In an attempt to rationalize the activity towards the peptide substrates, molecular modelling studies were conducted. The docking was successful in placing the Met-S-(O) residue in its predicted position. However, there was no pronounced binding pockets for the tested peptides, which may be explained by that the peptide substrate was too short to dock into the right place in the enzyme. Nonetheless, the model showed that Glu99 in the active site pocket was buried in the Met-S-(O) binding site and probably served as a conserved residue that contributed to the right placing of Met-S-(O). Consequently, the wild-type fungal MsrA showed the higher activity than the EQ mutant, in which Glu99 was substituted with a Gln residue. While Glu134 showed only H-bond interactions with the backbone of Met-S-(O) peptide. There were no indications that it might also interact with Met(O) flanking residues.

6 Conclusion

Within this thesis stereospecific CE assays including off-line and in-capillary assays have been established for the study of stereospecificity of Msr enzymes. The substrates composed free Met(O), Met(O) derivative as well as Met(O)-containing peptides. Upon establishment of the separation conditions, the methods were validated and successfully applied for analyzing recombinant human and fungal MsrA and MsrB enzymes. Since the successful separation of Met(O) diastereomers, the stereospecificity of Msr enzymes was clearly demonstrated. Besides, the established methods could also be used for the determination of the Michaelis-Menten kinetic data.

An off-line assay was developed using free Met(O) as substrate. The advantage of the assay over existing assays is the fact that free Met(O) can be used as the natural substrate. In the assay, DTT was used as reducing agent for Msr recycling instead of using the coupled reaction involving Trx and Trx reductase so that no additional enzymes were required. An in-capillary EMMA assay was established using Fmoc-Met(O) as substrate. Compared to the off-line assay, the EMMA assay was fully automated and required smaller amounts of enzyme and substrates, thus, reducing the overall cost of the assays. The first stereospecific assay employed a peptide substrate [KIFM(O)K] which appeared to be a better substrate than Met(O) derivatives such as dabsyl-Met(O) and Fmoc-Met(O). Thus, it may represent enzyme activities towards protein-bound Met(O) in a better way compared to simple amino acid derivative-based assay. A group of synthetic Met(O)-containing peptide was applied in order to investigate the preference of recombinant MsrA enzymes including enzyme mutants towards peptide substrates. Molecular modelling was attempted to rationalize the importance of amino acid in the active site of MsrA for the binding of the substrate. In the final part, the separation of Met(O)-containing peptide diastereomers was studied in a systematic way with regard to buffer additives such as cyclodextrins and crown ethers. While basic Met(O)-containing peptides were resolved by the dual system composed of cyclodextrins and crown ethers, the separation of the diastereomers of neutral peptides was achieved by cyclodextrin-mediated MEKC.

Reference

1. Imlay, J.A., *Cellular defenses against superoxide and hydrogen peroxide*. *Annu Rev Biochem*, 2008. **77**: p. 755-776.
2. Hohn, A., J. König, T. Grune, *Protein oxidation in aging and the removal of oxidized proteins*. *J Proteomics*, 2013. **92**: p. 132-159.
3. Shi, X., Dalal, N.S., *On the hydroxyl radical formation in the reaction between hydrogen peroxide and biologically generated chromium (V) species*. *Arch Biochem Biophys*. 1990. **277**: p. 342-350.
4. Albrich, J.M., McCarthy, C.A., Hurst, J.K., *Biological reactivity of hypochlorous acid: Implications for microbicidal mechanisms of leukocyte myeloperoxidase*, *PNAS USA*. 1981. **78**: p. 210-214.
5. Kelley, E.E., Khoo, N.K.H., Hundley, N.J., Malik, U.Z., Freeman, B.A., Tarpey, M.M., *Hydrogen peroxide is the major oxidant product of xanthine oxidase*. *Free Radic Biol Med*, 2010. **48**: p. 493-498.
6. Cash, T.P., Y. Pan, M.C. Simon, *Reactive oxygen species and cellular oxygen sensing*. *Free Radic Biol Med*, 2007. **43**: p. 1219-25.
7. Ray, P.D., B.W. Huang, Y. Tsuji, *Reactive oxygen species (ROS) homeostasis and redox regulation in cellular signaling*. *Cell Signal*, 2012. **24**: p. 981-90.
8. Jain, M., Rivera, S., Monclus, E.A., Synenki, L., Zirk, A., Eisenbart, J., Feghali-Bostwick, C., Mutlu, G.M., Budinger, G.R.S., Chandel, N.S., *Mitochondrial reactive oxygen species regulate transforming growth factor-beta signaling*. *J Biol Chem*, 2012. **288**: p. 770-7.
9. Dickinson, B.C., Chang, C.J., *Chemistry and biology of reactive oxygen species in signaling or stress responses nature chemical biology*. *Nat Chem Biol*, 2011. **7**: p. 504-511.
10. Sies, H., *Physiological society symposium: impaired endothelial and smooth muscle cell function in oxidative stress*. *Exp Physiol*, 1997. **82**: p. 291-295.
11. Jones, D.P., *Redefining oxidative stress*. *Antioxid Redox Sign*, 2006. **8**: p.1865-1879.
12. Matés, J.M., Pérez-Gómez, C., Castro, I.N.D., *Antioxidant enzymes and human diseases*. *Clin Biochem*, 1999. **8**: p. 595-603.
13. Hurst, R., Bao, Y., Jemth, P., Mannervik, B., Williamson, G., *Phospholipid hydroperoxide glutathione peroxidase activity of rat class theta glutathione transferase T2-2*. *Biochem Soc T*, 1997. **25**: p, S559.
14. Silva, E.L., Piskula, M.K., Yamamoto, N., Moon, J-H., Terao, J., *Quercetin metabolites inhibit copper ion-induced lipid peroxidation in rat plasma*. *FEBS Lett*, 1998. **430**: p 405-408.
15. Stadtman, E.R., *Metal ion-catalyzed oxidation of proteins: biochemical mechanism and biological consequences*. *Free Radical Bio Med*, 1990. **9**: p. 315-325.

16. Dean, R.T., Fu, S., Stocker, R., Davies, M.J., *Biochemistry and pathology of radical-mediated protein oxidation*. Biochem J, 1997. **324**: p, 1-18.
17. Stadtman, E.R., *Protein oxidation and aging*. Free Radical Res, 2006. **40**: p, 1250-1258.
18. Fucci, L., Oliver, C.N., Coon, M.J., Stadtman, E.R., *Inactivation of key metabolic enzymes by mixed-function oxidation reaction: Possible implication in protein turnover and ageing*. PNAS USA, 1983. **80**: p, 1521-1525.
19. Hazell, L.J., van den Berg, J.J.M., Stocker, R., *Oxidation of low-density lipoprotein by hypochlorite causes aggregation that is mediated by modification of lysine residues rather than lipid oxidation*. Biochem J, 1994. **302**: p 297-304.
20. Martínez, A., Portero-Otin, M., Pamplona, R., Ferrer, I., *Protein targets of oxidative damage in human neurodegenerative diseases with abnormal protein aggregates*. Brain Pathol, 2010. **20**: p. 281-297
21. Mohsenzagegan, M., Mirschafiey, A., *The immunopathogenic role of reactive oxygen species in Alzheimer disease*. Iran J Allergy Asthma Immunol, 2012. **11**: p 203-216.
22. Schöneich, C., *Methionine oxidation by reactive oxygen species: reaction mechanisms and relevance to Alzheimer's disease*. Biochim Biophys Acta, 2005. **1703**: p 111-119.
23. Smith, C.D., Carney, J.M., Starke-Reed, P.E., Oliver, C.N., Stadtman, E.R., Floyd, R.A., Markesbery, W.R., *Excess brain protein oxidation and enzyme dysfunction in normal aging and in Alzheimer disease*. PNAS USA, 1991. **88**: p 10540-10543.
24. Levine, R.L., Stadtman, E.R., *Oxidative modification of proteins during aging*. Exp Gerontol, 2001. **36**: p 1495-1502.
25. Baralbar, M.A., Llu, L., Ahmed, E.K., Frlguet, B., *Protein oxidative damage at the crossroads of cellular senescence, aging and age-related disease*. Oxid Med Cell Longev, 2012. **2012**: p 1-8.
26. Radi, R., Bush, K.M., Cosgrove, T.P., Freeman, B.A., *Reaction of xanthine oxidase-derived oxidants with lipid and protein of human plasma*. Arch Biochem Biophys, 1991. **286**: p 117-125.
27. Vogt, W., *Oxidation of methionyl residues in proteins: tools, targets, and reversal*. Free Radical Bio Med, 1995. **18**: p 93-105.
28. Shechter, Y., Burstein, Y., Patchornik, A., *Selective oxidation of methionine residues in proteins*. Biochem, 1975. **14**: p 4497-4503.
29. Levine, R.L., Berlett, B.S., Moskovitz, J., Mosoni, L., Stadtman, E.R., *Methionine residues may protect proteins from critical oxidative damage*. Mech Ageing Dev, 1999. **107**: p 323-332.
30. Ripp, S.L., Itagaki, K., Philpot, R.M., Elfarra, A.A., *Methionine S-oxidation in human and rabbit liver microsomes: evidence for a high-affinity methionine S-oxidase activity that is distinct from flavin-containing monooxygenase 3*. Arch Biochem Biophys, 1999. **367**: p 322-332.
31. Dever, J.T., Elfarra, A.A., *In vivo metabolism of L-methionine in mice: evidence for*

- stereoselective formation of methionine-d-sulfoxide and quantitation of other major metabolites.* Drug Metab Dispos, 2006. **34**: p 2036-2043.
32. Nakao, L.S., Iwai, L.K., Kalil, J., Augusto, O., *Radical production from free and peptide-bound methionine sulfoxide oxidation by peroxyxynitrite and hydrogen peroxide/iron (II).* FEBS lett, 2003. **547**: p 87-91.
 33. Moskovitz, J., Bar-Noy, S., Williams, W.M., Requena, J., Berlett, B.S., Stadtman, E.R., *Methionine sulfoxide reductase (MsrA) is a regulator of antioxidant defense and lifespan in mammals.* PNAS USA, 2001. **98**: p 12920-12925.
 34. Kim, H-Y., Gladyshev, V.N., *Methionine sulfoxide reductases: selenoprotein forms and roles in antioxidant protein repair in mammals.* Biochem J, 2007. **407**: p 321-329.
 35. Lowther, W.T., Weissbach, H., Etienne, F., Brot, N., Matthew, B.W., *The mirrored methionine sulfoxide reductases of Neisseria gonorrhoeae pilB.* Nat Struct Biol, 2002. **9**: p 348-352.
 36. Moskovitz, J., Poston, J.M., Berlett, B.S., Nosworthy, N.J., Szezepanowski, R., Stadtman, E.R., *Identification and characterization of a putative active site for peptide methionine sulfoxide reductase (MsrA) and its substrate stereospecificity.* J Bio Chem, 2000. **275**: p 14167-14172.
 37. Sharov, V.S., Ferrington, D.A., Squier, T.C., Schöneich, C., *Diastereoselective reduction of protein-bound methionine sulfoxide by methionine sulfoxide reductase.* FEBS lett, 1999. **455**: p 247-250.
 38. Boschi-Muller, S., Gand, A., Branlant, G., *The methionine sulfoxide reductases: catalysis and substrate specificities.* Arch Biochem Biophys, 2008. **474**: p 266-273.
 39. Lee, B., Gladyshev, V.N., *The biological significance of methionine sulfoxide stereochemistry.* Free Radical Bio Med, 2011. **50**: p 221-227.
 40. Lin, Z., Johnson, L.C., Weissbach, H., Brot, N., Lively, M.O., Lowther, W.T., *Free methionine-(R)-sulfoxide reductase from Escherichia coli reveals a new GAF domain function.* PNAS USA, 2007. **104**: p 9597-9602.
 41. Gruez, A., Libiad, M., Boschi-Muller, S., Branlant, G., *Structural and biochemical characterization of free methionine-R-sulfoxide reductase from Neisseria meningitidis.* J Biol Chem, 2010. **285**: p 25033-25043.
 42. Abdelaleem, R.G.H., (2014). *Methionine sulfoxide reductases of Aspergillus nidulans* (Doctoral dissertation). Retrieved from Digitale Bibliothek Thüringen database (Document 25079).
 43. Hansel, A., Heinemann, S.H., Hoshi, T., *Heterogeneity and function of mammalian MSRs: enzymes for repair, protection and regulation.* Biochim Biophys Acta, 2005. **1703**: p 239-247.
 44. Stadtman, E.R., Moskovitz, J., Berlett, B.S., Levine, R.L., *Cyclic oxidation and reduction of protein methionine residues is an important antioxidant mechanism.* Mol Cell Biochem, 2002. **234**: p 3-9.
 45. Gabbita, S.P., Aksenov, M.Y., Lovell, M.A., Markesbery, W.R., *Decrease in peptide methionine*

- sulfoxide reductase in Alzheimer's disease brain*. J Neurochem, 1999. **73**: p 1660-1666.
46. Krishnan S., Chi E.Y., Wood, S.J., Kendrick, B.S., Li, C., Garzon-Rodriguez, W., Wypych, J., Randolph, T.W., Narhi, L.O., Biere, A.L., Citron, M., Carpenter, J.F., *Oxidative dimer formation is the critical rate-limiting step for Parkinson's disease α -synuclein fibrillogenesis*. Biochem, 2003. **42**: 829-837.
 47. Ruan, H., Tang, X., Chen, M., Joiner, M-L., Sun, G., Brot, N., Weissbach, H., Heinemann, S.H., Iverson, L., Wu, C., Hoshi, T., *High-quality life extension by the enzyme peptide methionine sulfoxide reductase*. PNAS USA, 2002. **99**: p 2748-2753.
 48. Erickson, J.R., Joiner, M.A., Guan, X., Kutschke, W., Yang, J., Oddis, C.V., Bartlett, R.K., Lowe, J.S., O'Donnell, S.E., Aykin-Burns, N., Zimmerman, M.C., Zimmerman, K., Ham, A-J., Weiss, R.M., Spitz, D.R., Shea, M.A., Colbran, R.J., Mohler, P.J., Anderson, M.E., *A dynamic pathway for calcium-independent activation of CaMKII by methionine oxidation*. Cell, 2008. **133**: p 462-474.
 49. Su, Z., Limberis, J., Martin, R.L., Xu, R., Kolbe, K., Heinemann, S.H., Hoshi, T., Cox, B.F., Gintant, G.A., *Functional consequences of methionine oxidation of hERG potassium channels*. Biochem Pharmacol, 2007. **74**: p 702-711.
 50. Ezraty, B., Grimaud, R., Hassouni, M.E., Moinier, D., Barras, F., *Methionine sulfoxide reductase protect Ffh from oxidative damages in Escherichia coli*. J EMBO, 2004. **23**: p 1868-1877.
 51. Lim, J.C., You, Z., Kim, G., Levine, R.L., *Methionine sulfoxide reductase A is a stereospecific methionine oxidase*. PNAS USA, 2011. **108**: p10472-10477.
 52. Lim, J.C., Kim, G., Levine, R.L., *Stereospecific oxidation of calmodulin by methionine sulfoxide reductase A*. Free Raducal Bio Med, 2013. **61**: p 257-264.
 53. Kumar, R.A., Koc, A., Cerny, R.L., Gladyshev, V.N., *Reaction mechanism, evolutionary analysis, and role of zinc in Drosophila methionine-R-sulfoxide reductase*. J Biol Chem, 2002. **277**: p 37527-37535.
 54. Zhao, H., Kim, G., Levine, R.L., *Methinone sulfoxide reductase contributes to meeting dietary methionine requirements*. Arch Biochem Biophy, 2012. **522**: p 37-43.
 55. Kim, H-Y., *The methionine sulfoxide reduction system: selenium utilization and methionine sulfoxide reductase enzymes and their functions*. Antioxid Redox Sign, 2013. **19**: p 958-969.
 56. Kim, H-Y, Gladyshev, V.N., *Methionine sulfoxide reduction in mammals: characterization of methionine-R-sulfoxide reductases*. Mol Biol Cell, 2004. **15**: p 1055-1064.
 57. Vouquier, S., Mary, J., Friguet, B., *Subcellular localization of methionine sulphoxide reductase A (MsrA); evidence for mitochondrial and cytosolic isoforms in rat liver cells*. Biochem J, 2003. **373**: p 531-537.
 58. Kim, H-Y., Gladyshev, V.N., *Role of structural and functional elements of mouse methionine-S-Sulfoxide reductase in its subcellular distribution*. Biochemistry, 2005. **44**: p 8059-8067.

59. Picot, C.R., Perichon, M., Cintrat, J-C., Friguet, B., Petropoulos, I., *The peptide methionine sulfoxide reductase, MsrA and MsrB (hCBS-1), are downregulated during replicative senescence of human WI-38 fibroblasts*. FEBS Lett, 2004. **558**: p 74-78.
60. Picot, C.R., Petropoulos, I., Perichon, M., Moreau, M., Nizard, C., Friguet, B., *Overexpression of MsrA protects WI-38 SV40 human fibroblasts against H₂O₂-mediated oxidative stress*. Free Radical Bio Med, 2005. **39**: p 1332-1314.
61. Boschi-Muller, S., Olry, A., Antoine, M., Branlant, G., *The enzymology and biochemistry of methionine sulfoxide reductases*. Biochim Biophys Acta, 2005. **1703**: p 231-238.
62. Brot, N., Weissbach, H., *Biochemistry and physiological role of methionine sulfoxide residues in proteins*. Arch Biochem Biophys, 1983. **223**: p 271-281.
63. Ma, X., Guo, P., Shi, W., Luo, M., Tan, X., Chen, Y., Zhou, C., *Structure plasticity of the thioredoxin recognition site of Yeast methionine S-sulfoxide reductase Mxr1*. J Biol Chem, 2011. **286**: p 13430-13437.
64. Olry, A., Boschi-Muller, S., Branlant, G., *Kinetic characterization of the catalytic mechanism of methionine sulfoxide reductase B from Neisseria meningitidis*. Biochemistry, 2004. **43**: p 11616-11611.
65. Drazic, A., Winter, J., *The physiological role of reversible methionine oxidation*. Biochi Biophys Acta, 2014. **1844**: p 1367-1382.
66. Russel M., Model, P., *The role of thioredoxin in filamentous phage assembly*. J Biol Chem, 1986. **261**: p 14997-15006.
67. Boschi-Muller, S., Azza, S., Sanglier-Cianferani, S., Talfournier, F., Van, D.A., Branlant, G., *A sulfenic acid enzyme intermediate is involved in the catalytic mechanism of peptide methionine sulfoxide reductase from Escherichia coli*. J Biol Chem, 2000. **275**: p 35908-35913.
68. Tarrago, L., Laugier, E., Rey, P., *Protein-repairing methionine sulfoxide reductases in photosynthetic organisms: gene organization, reduction mechanisms, and physiological roles*. Mol Plant, 2009. **2**: p 202-217.
69. Lee, B.C., Dikiy, A., Kim, H.-Y., Gladyshev, V.N., *Functions and evolution of selenoprotein methionine sulfoxide reductases*. Biochim Biophys Acta, 2009. **1790**: p 1471-1477.
70. Arner, E.S., *Selenoproteins-what unique properties can arise with selenocysteine in place of cysteine?* Exp Cell Res, 2010. **316**: p 1296-1303.
71. Kauffmann, B., Aubry, A., Favier, F., *The three-dimensional structures of peptide methionine sulfoxide reductase: current knowledge and open questions*. Biochi Biophys Acta, 2005. **1703**: p 249-260.
72. Ghesquière, B., Jonckheere, V., Colaert, N., Van Durme, J., Timmerman, E., Goethals, M., Schymkowitz, J., Rousseau, F., Vandekerckhove, J., Gevaert, K., *Redox proteomics of protein-bound methionine oxidation*. Mol Cell Proteomics, 2011. 10 (5): M110.006866. DOI: 10.1074/mcp.M110.006866.

73. Minetti, G., Balduini, C., Brovelli, A., *Reduction of DABS-L-methionine-DL-sulfoxide by protein methionine sulfoxide reductase from polymorphonuclear leukocytes: stereospecificity towards the L-sulfoxide*. Ital J Biochem, 1994. **43**: 273-283.
74. Weissbach, H., Etienne, F., Hoshi, T., Heinemann, S.H., Lowther, B., John, G.S., Nathan, C., Brot, N., *Peptide methionine sulfoxide reductase: structure, mechanism of action, and biological function*. Arch Biochem Biophys, 2002. **397**: p 172-178.
75. Moskovitz, J., Weissbach, H., Brot, N., *Cloning and expression of a mammalian gene involved in the reduction of methionine sulfoxide residues in proteins*. PNAS USA, 1996. **93**: p 2095-2099.
76. Ferguson, D.L., Burke, J.J., *A new method of measuring protein-methionine-S-oxide reductase activity*. Plant Physiol, 1992. **100**: p 529-532.
77. Romero, H.M., Pell, E.J., Tien, M., *Expression profile analysis and biochemical properties of the peptide methionine sulfoxide reductase A (PMSRA) gene family in Arabidopsis*. Plant Sci, 2006. **170**: p 705-714.
78. Weissbach, H., Resnick, L., Brot, N., *Methionine sulfoxide reductases: history and cellular role in protecting against oxidative damage*. Biochim Biophys Acta, 2005. **1703**: p 203-212.
79. Brunell, D., Weissbach, H., Hodder, P., Brot, N., *A high-throughput screening compatible assay for activators and inhibitors of methionine sulfoxide reductase A*. Assay Drug Dev Techn, 2010. **8**: p 615-620.
80. Lee, B.C., Le, D.T., Gladyshev, V.N., *Mammals reduce methionine-S-sulfoxide with MsrA and are unable to reduce methionine-R-sulfoxide, and this function can be restored with a yeast reductase*. J Biol Chem, 2008. **283**: p 28361-28369.
81. Le, D.T., Lee, B.C., Marino, S.M., Zhang, Y., Fomenko, D.E., Kaya, A., Hacıoglu, E., Kwak, G.-H., Koc, A., Kim, H.-Y., Gladyshev, V.N., *Functional analysis of free methionine-R-sulfoxide reductase from Saccharomyces cerevisiae*. J Biol Chem, 2009. **284**: p 4354-4364.
82. Oien, D.B., Moskovitz, J., *Substrates of the methionine sulfoxide reductase system and their physiological relevance*. Curr Top Dev Biol, 2007. **80**: p 93-133.
83. Xiong, Y., Chen, B., Smallwood, H.S., Urbauer, R.J.B., Markille, L.M., Galeva, N., Williams, T.D., Squier, T.C., *High-affinity and cooperative binding of oxidized Calmodulin by methionine sulfoxide reductase*. Biochemistry, 2006. **45**: p 14642-14654.
84. Tarrago, L., Kaya, A., Weerapana, E., Marino, S.M., Gladyshev, V.N., *Methionine sulfoxide reductases preferentially reduce unfolded oxidized proteins and protect cells from oxidative protein unfolding*. J Biol Chem, 2012, **287**: p 24448-24459.
85. Baillie, T.A., *Metabolism and toxicity of drugs. Two decades of progress in industrial drug metabolism*. Chem Res Toxicol, 2008. **21**: p 129-137.
86. Bentley, R., *Role of sulfur chirality in the chemical process of biology*. Chem Soc Rev, 2005. **34**: 609-624.

87. Beedham, C., *The role of non-P450 enzymes in drug oxidation*. Pharm World Sci, 1997, **19**: 255-263.
88. Lynch, T., *The effect of cytochrome P450 metabolism on drug response, interactions, and adverse effect*. Am Fam Physican, 2007. **76**: p 391-396.
89. Brot, N., Werth, J., Koster, D., Weissbach, H., *Reduction of N-acetyl methionine sulfoxide: A simple assay for peptide methionine sulfoxide reductase*. Anal Biochem, 1982. **122**: p 291-294.
90. Moskovitz, J., Berlett, B.S., Poston, J.M., Stadtman, E.R., *The yeast peptide-methionine sulfoxide reductase functions as an antioxidant in vivo*. PNAS USA, 1997. **94**: p 9585-9589.
91. Sagher, D., Brunell, D., Brot, N., Vallee, B.L., Weissbach, H., *Selenocompounds can serve as oxidoreductants with the methionine sulfoxide reductase enzymes*. J Biol Chem, 2006. **281**: 31184-31187.
92. Sagher, D., Brunell, D., Hejtmancik, J.F., Kantorow, M., Brot, N., Weissbach, H., *Thionein can serve as a reducing agent for the methionine sulfoxide reductases*. PNAS USA, 2006. **103**: p 8656-8661.
93. Morand, K., Talbo, G., Mann, M., *Oxidation of peptides during electrospray ionization*. Rapid Commun Mass Sp, 1993. **7**: p 738-743.
94. Chen, M., Cook, K.D., *Oxidation artifacts in the electrospray mass spectrometry of a peptide*. Anal Chem, 2007. **79**: p 2031-2036.
95. Guan, Z., Yates, N.A., Bakhtiar, R., *Detection and characterization of methionine oxidation in peptides by collision-induced dissociation and electron capture dissociation*. J Am Soc Mass Spectr, 2003. **14**: p 605-613.
96. Wang, X., Shao, B., Oda, M.N., Heinecke, J.W., Mahler, S., Stocher, R., *A sensitive and specific ELSA detects methionine sulfoxide-containing apolipoprotein A-I in HDL*. J Lipid Res, 2009. **50**: p 586-594.
97. Le, D.T., Liang, X., Fomenko, D.E., Raza, A.S., Chong, C.-K., Carlson, B.A., Hatfield, D.L., Gladyshev, V.N., *Analysis of methionine/ selenomethionine oxidation and methionine sulfoxide reductase function using methionine-rich protein and antibodies against their oxidized forms*. Biochemistry, 2008. **47**: p 6685-6694.
98. Liang, X., Kaya, A., Zhang, Y., Le, D.T., Hua, D., Gladyshev, N., *Characterization of methionine oxidation and methionine sulfoxide reduction using methionine-rich cysteine-free proteins*. BMC Biochem, 2012. **13**: p 1-10.
99. Uthus, E.O., *Determination of the specific activities of methionine sulfoxide reductase A and B by capillary electrophoresis*. Anal Biochem, 2010. **401**: p 68-73.
100. Grossman, P.D., Colburn, J.C., *Capillary electrophoresis: Theory and practice*. Academic Press, Inc., San Diego, California, USA, 1992.
101. Tarabe, S., Otsuka, K., Ichikawa, K., Tsuchiya, A., Ando, T., *Electrokinetic separation with micellar solutions and open-tubular capillaries*. Anal Chem, 1984. **56**: p 111-113.

102. Terabe, S., *Micellar electrokinetic chromatography for high-performance analytical separation*. Chem Rec, 2008. **8**: p 291-301.
103. Fanali, S., *Chiral separations by CE employing CDs*. Electrophoresis, 2009. **30**: p 5203-5210.
104. Chankvetadze, B., *Separation of enantiomers with charged chiral selectors in CE*. Electrophoresis, 2009. **30**: p 5211-5221.
105. Scriba, G.K.E., *Chiral recognition of mechanisms in analytical separation sciences*. Chromatographia, 2012. **75**: p 815-838.
106. Prokhorova, A.F., Shapovalova, E.N., Shpigun, O.A., *Chiral analysis of pharmaceuticals by capillary electrophoresis using antibiotics as chiral selectors*. J Pharmaceut Biomed, 2010. **53**: p 1170-1179.
107. Kuhn, R., *Enantiomeric separation by capillary electrophoresis using a crown ether as chiral selector*. Electrophoresis, 1999. **20**: p 2605-2613.
108. Zhang, H., Qi, L., Mao, L., Chen, Y., *Chiral separation using capillary electromigration techniques based on ligand exchange principle*. J Sep Sci, 2012. **35**: p 1236-1248.
109. Haginaka, J., *Enantiomer separation of drugs by capillary electrophoresis using proteins as chiral selectors*. J Chromatogr A, 2000. **875**: p 235-254.
110. Chankvetadze, B., *Capillary electrophoresis in chiral analysis*. WILEY, 1997. ISBN 0-471-97415-3.
111. Amin, N.C., Blanchin, M.-D., Aké, M., Fabre, H., *Capillary electrophoresis methods for the analysis of antimalarials. Part I. Chiral separation methods*. J Chromatogr A, 2012. **1264**: p 1-12.
112. Nigović, B., Vegar, I., *Capillary electrophoresis determination of pravastatin and separation of its degradation products*. Croatica Chemica Acta, 2008. **81**: p 615-622.
113. Hlaváček, J., Vítovcová, M., Sázelová, P., Pícha, J., Vaněk., Buděšinský, M., Jiráček, J., Gillner, D.M., Holz, R.C., Mikšík, I., Kašička, V., *Mono-N-acyl-2,6-diaminopimelic acid derivatives: analysis by electromigration and spectroscopic methods and examination of enzyme inhibitory activity*. Anal Biochem, 2014. **467**: P 4-13.
114. Biwer, A., Antranikian, G., Heinzle, E., *Enzymatic production of cyclodextrins*. App Microbiol Biotechnol, 2002. **59**: p 607-617.
115. Scriba, G.K.E., 2008. *Cyclodextrins in capillary electrophoresis enantioseparations-Recent developments and applications*. J Sep Sci, 2008. **31**: p1991-2011.
116. Behr, J.-P., Lehn, J.-M., Vierling, P., *Molecular receptors. Structurel effects and substraee recognition in binding of raganic and biogenic ammonium ions by chrial polyfunctional macrocyclic polyethers bearing amino-acid and other side-chains*. Helvetica Chimica Acta. 1982. **65**: p 1853-1867.
117. Kuhn, R., Stoecklin, F., Erni, F., *Chiral separation by host-guest complexation with cyclodextrin and crown ether in capillary zone electrophoresis*. Chromatographia, 1992. **33**: p

- 32-36.
118. Kuhn, R., Wagner, J., Walbroehl, Y., Bereuter, T., *Potential and limitations of an optically active crown ether for chiral separation in capillary zone electrophoresis*. *Electrophoresis*, 1994. **15**: p 828-834.
119. Kuhn, R., Hoffstetter-Kuhn, S., *Chiral separation by capillary electrophoresis*. *Chromatographia*, 1992. **34**: p 505-512.
120. Huang, W., Xu, H., Fazio, S.D., Vivilecchia, R.V., *Chiral separation of primary amino compounds using a non-chiral crown ether with β -cyclodextrin by capillary electrophoresis*. *J Chromatogr B*, 1997. **695**: p 157-162.
121. Huang, W., Fazio, S.D., Vivilecchia, R.V., *Achievement of enantioselectivity of non-polar primary amines by a non-chiral crown ether*. *J Chromatogr A*, 1997. **781**: p 129-137.
122. Armstrong, D.W., Chang, L.W., Chang, S.S.C., *Mechanism of capillary electrophoresis enantioselectivity using a combination of an achiral crown ether plus cyclodextrins*. *J Chromatogr A*, 1998. **793**: p 115-134.
123. Huang, W., Xu, H., Fazio, S.D., Vivilecchia, R.V., *Enhancement of chiral recognition by formation of a sandwiched complex in capillary electrophoresis*. *J Chromatogr A*, 2000. **875**: p 361-369.
124. Iványi, T., Pál, K., Lázár, I., Massart, D.L., Heyden, Y.V., *Application of tetraoxadiazacrown ether derivatives as chiral selector modifiers in capillary electrophoresis*. *J Chromatogr A*, 2004. **1028**: p 325-332.
125. Elek, J., Mangelings, D., Iványi, T., Lázár, I., Heyden, Y.V., *Enantioselective capillary electrophoretic separation of tryptophan- and tyrosine-methylesters in a dual system with a tetra-oxadiazacrown-ether derivative and a cyclodextrin*. *J Pharmaceut Biomed*, 2005. **38**: p 601-608.
126. Fan, Y., Scriba, G.K.E., *Advances in-capillary electrophoretic enzyme assays*. *J Pharmaceut Biomed*, 2010. **53**: p 1076-1090.
127. Glatz, Z., *Determination of enzymatic activity by capillary electrophoresis*. *J Chromatogr B*, 2006. **841**: p 23-27.
128. Wang, X., Li, K., Adams, E., Van Schepdael, A., *Recent advances in CE-mediated microanalysis for enzyme study*. *Electrophoresis*, 2014. **35**: p 119-127.
129. Shanmuganathan, M., Britz-Mckibbin, P., *High quality drug screening by capillary electrophoresis: A review*. *Anal Chim Acta*, 2012. **773**: p 24-36.
130. Hai, X., Yang, B., Van Schepdael, A., *Recent developments and applications of EMMA in enzymatic and derivatization reactions*. *Electrophoresis*, 2012. **33**: p 211-227.
131. Krueger, R.J., Hobbs, T.R., Mihal, K.A., Tehrani, J., Zeece, M.G., *Analysis of endoproteinase Arg C action on adrenocorticotrophic hormone by capillary electrophoresis and reversed-phase high-performance liquid chromatography*. *J Chromatogr*, 1991. **543**: p 451-461.

132. Bao, J., Regnier, F.E., *Ultramicro enzyme assays in a capillary electrophoretic system. J Chromatogr*, 1992. **608**: p 217-224.
133. Urban, P.L., Goodall, D.M., Bruce, N.C., *Enzymatic microreactors in chemical analysis and kinetic studies. Biotechnol Adv*, 2006. **24**: p 42-57.
134. Iqbal, J., Iqbal, S., Müller, C.E., *Advances in immobilized enzyme microreactors in capillary electrophoresis. Analyst*, 2013. **138**: p 3104-3116.
135. Nowak, P., Woźniakiewicz, M., Kościelniak, P., *An overview of on-line systems using drug metabolizing enzymes integrated into capillary electrophoresis. Electrophoresis*, 2013. **34**: p 2604-2614.
136. Křenková, J., Foret, F., *Immobilized microfluidic enzymatic reactors. Electrophoresis*, 2004. **25**: p 3550-3563.
137. Harmon, B.J., Patterson, D.H., Regnier, F.E., *Mathematical treatment of electrophoretically mediated microanalysis. Anal Chem*, 1993. **65**: p 2655-2662.
138. Avila, L.Z., Whitesides, G.M., *Catalytic activity of native enzymes during capillary electrophoresis: An enzymatic "Microreactor". J Org Chem*, 1993. **58**: p 5508-5512.
139. Zhang, J., Hoogmartens, J., Van Schepdael, A., *Advances in CE-mediated microanalysis: An update. Electrophoresis*, 2008. **29**: p 56-65.
140. Krylova, S.M., Okhonin, V., Evenhuis, C.J., Krylov, S.N., *The inject-Mix-React-Separate-and-Quantitate (IMReSQ) approach to studying reactions in capillaries. Trend Anal Chem*, 2009. **28**: p 987-1010.
141. Van Dyck, S., Van Schepdael, A., Hoogmartens, J., *Michaelis-Menten analysis of bovine plasma amine oxidase by capillary electrophoresis using electrophoretically mediated microanalysis in a partially filled capillary. Electrophoresis*, 2001. **22**: p 1436-1442.
142. Liu L., Chen, Y., Yang, L., *Inhibition study of alanine aminotransferase enzyme using sequential online capillary electrophoresis analysis. Anal Biochem*, 2014. **467**: p 28-30.
143. Asensi-Bernardi, L., Martín-Biosca, Y., Escuder-Gilabert, L., Sagrado, S., Medina-Hernández, M.J., *In-line capillary electrophoretic evaluation of the enantioselective metabolism of verapamil by cytochrome P3A4. J Chromatogr A*, 2013. **1298**: p 139-145.
144. Nehmé, H., Nehmé, R., Lafite, P., Routier, S., Morin, P., *In-capillary reactant mixing for monitoring glycerol kinase kinetics by CE. J Sep Sci*, 2013. **36**: p 2151-2157.
145. Zhao, W., Tian, M., Nie, R., Wang, Y., Guo, L., Yang, L., *Online enzyme discrimination and determination of substrate enantiomers based on electrophoretically mediated microanalysis. Anal Chem*, 2012. **84**: p 6701-6706.
146. Pochet, L., Servais, A.-C., Farcas, E., Bettonville, V., Bouckaert, C., Fillet, M., *Determination of inhibitory potency of of argatroban toward thrombin by electrophoretically mediated microanalysis. Talanta*, 2013. **116**: p 719-725.
147. Fuessl, S., Trapp, O., *Integration of on-column catalysis and EKC analysis: Investigation of*

- Enantioselective sulfoxidations*. Electrophoresis, 2012. **33**: p 1060-1067.
148. Kuschel, L., Hansel, A., Schönherr, R., Weissbach, H., Brot, N., Hoshi, T., Heinemann, S.H., *Molecular cloning and functional expression of a human peptide methionine sulfoxide reductase (hMsrA)*. FEBS Lett, 1999. **456**: p 17-21.
149. Jung, S., Hansel, A., Kasperczyk, H., Hoshi, T., Heinemann, S.H., *Activity, tissue distribution and site-directed mutagenesis of a human peptide methionine sulfoxide reductase of type B: hCBS1*. FEBS Lett, 2002. **527**: p 91-94.
150. Hansel, A., Kuschel, L., Hehl, S., Lemke, C., Agricola, H.-J., Hoshi, T., Heinemann, S.H., *Mitochondrial targeting of the human peptide methionine sulfoxide reductase (MSRA), an enzyme involved in the repair of oxidized proteins*. FASEB J, 2002. **16**: p 911-913.
151. Katayama, H., Ishihama, Y., Asakawa, N., *A stable capillary coating with successive multiple ionic polymer layers*. Anal Chem, 1998. **70**: p 2254-2260.
152. Vendrell, J., Avilés, F.X., *Complete amino acid analysis of proteins by dabsyl derivatization and reversed-phase liquid chromatography*. J Chromatogr, 1986. **358**: p 401-413.
153. International Conference on Harmonization (ICH) guideline Q2(R1) (2005). www.ich.org
154. Eriksson, L., Johansson, E., Kettaneh-Wold, N., Wikström, C., Wold, S., *Design of Experiments-Principles and Applications*, Learnways AB, Stockholm 2000.
155. Jones, G., Willett, P., Glen, R.C., Leach, A.R., Taylor, R., *Development and validation of a genetic algorithm for flexible docking*. J Mol Biol, 1997. **267**: p 727-748.
156. Deeb, S.E., Iriban, M.A., Gust, R., *MEKC as a powerful growing analytical technique*. Electrophoresis, 2011. **32**: p 166-183.
157. Jansen, E.J.M., Van Denberg, R.H., Both-Miedema, R., Doorn, L., *Advantages and limitations of pre-column derivatization of amino acids with dabsyl chloride*. J Chromatogr, 1991. **553**: p 123-133.
158. Okhonin, V., Wong, E., Krylow, S.N., *Mathematical model for mixing reactants in a capillary microreactor by transverse diffusion of laminar flow profiles*. Anal Chem, 2008. **80**: p 7482-7486.
159. Wong, E., Okhonin, V., Berezovski, M.V., Nozaki, T., Waldmann, H., Alexandrov, K., Krylov, N., *“Inject-Mix-React-Separate-and-Quantitate” (IMReSQ) method for screening enzyme inhibitors*. J Am Chem Soc. 2008. **130**: 11862-11863.
160. Fan, Y., Scriba, G.K.E., *Electrophoretically mediated microanalysis assay for sirtuin enzymes*. Electrophoresis, 2010. **31**: p 3874-3880.
161. Zhang, J., Hoogmartens, Van Schepdael, A., *Recent developments and applications of EMMA in enzymatic and derivatization reactions*. Electrophoresis, 2010. **31**: p 65-73.
162. Zhang, J., Hoogmartens, J., Van Schepdael, A., *Kinetic study of cytochrome P450 by capillary electrophoretically mediated microanalysis*. Electrophoresis, 2008. **29**: p 3694-3700.

163. Tarrago, L., Gladyshev, V.N., *Recharging oxidative protein repair: Catalysis by methionine sulfoxide reductases towards their amino acid, protein, and model substrates*. Biochemistry (Moscow), 2012. **77**: p 1324-1336.
164. Kwak, G.-H., Hwang, K.Y., Kim, H.-Y., *Analyses of methionine sulfoxide reductase activities towards free and peptidyl methionine sulfoxides*. Arch Biochem Biophys, 2012. **527**: p 1-5.
165. Haenold, R., Wassef, R., Hansel, A., Heinemann, S.H., Hoshi, T., *Identification of a new functional splice variant of the enzyme methionine sulphoxide reductase A (MSRA) expressed in rat vascular smooth muscle cells*. Free Radical Res, 2007. **41**: p 1233-1245.
166. Hadley, M.R., Decrette, M., Guillore, G., Rosini, C., Donnoli, M.I., Superchi, S., Hutt, A.J., *Capillary electrophoretic resolution of chiral aryl alkyl and aryl benzyl sulphoxides using sulphated β -cyclodextrins as chiral selectors*. J Sep Sci, 2001. **24**: p766-776.
167. Prost, F., Caslavská, J., Thormann, W., *Chiral analysis of albendazole sulfoxide enantiomers in human plasma and saliva using capillary electrophoresis with on-column absorption and fluorescence detection*. J Sep Sci, 2002. **25**: p 1043-1054.
168. Rodriguez, M.A., Liu Y., Mcculla, R., Jenks, W.S., Armstrong, D.W., *Enantioseparation of chiral sulfoxides and sulfinate esters by capillary electrophoresis*. Electrophoresis, 2002. **23**: p 1561-1570.
169. Elbashir, A.A., Suliman, F.O., *Computational modeling of capillary electrophoretic behavior of primary amines using dual system of 18-crown-6 and β -cyclodextrin*. J Chromatogr A, 2011. **1218**: p 5344-5351.
170. Zhang, C., Huang, W., Chen, Z., Rustom, A.M., *Separation of chiral primary amino compounds by forming a sandwiched complex in reversed-phase high performance liquid chromatography*. J Chromatogr A, 2010. **1217**: p 4965-4970.
171. Koide, T., Ueno, K., *Mechanistic study of enantiomeric recognition of primary amino compounds using an achiral crown ether with cyclodextrin by capillary electrophoresis and nuclear magnetic resonance*. J Chromatogr A, 2001. **923**: p 229-239.
172. Dantz, D.A., Buschmann, H.-J., Schollmeyer, E., *Protonation of noncyclic and cyclic diamines in aqueous solution*. Thermochim Acta, 1997. **294**: p 133-138.
173. Desilva, K., Jiang, Q., Kuwana, T., *Chiral separation of naphthalene-2,3-dialdehyde labelled peptide by cyclodextrin-modified electrokinetic chromatography*. Biomed Chromatogr, 1995. **9**: 295-301.
174. Chen, Y., Zhang, J., Zhang, L., Chen, G., *Separation of dipeptides with two chiral centers using 2-hydroxypropyl- β -CD-modified MEKC*. Electrophoresis, 2010. **31**: p 1493-1497.
175. Kitagawa, F., Otsuka, K., *Recent progress in capillary electrophoretic analysis of amino acid enantiomers*. J Chromatogr B, 2011. **879**: p 3078-3095.
176. Sutcliffe, N., Corran, P.H., *Comparison of selectivities of reversed-phase high-performance liquid chromatography, capillary zone electrophoresis and micellar capillary electrophoresis in the separation of neurohypophyseal peptides and analogues*. J Chromatogr, 1993. **636**: 95-103.

177. Lucy, C.A., MacDonald, A.M., Gulcev, M.D., Non-covalent capillary coatings for protein separations in capillary electrophoresis. *J Chromatogr A*, 2008. **1184**: p 81-105.
178. Graul, T.W., Schlenoff, J.B., *Capillaries modified by polyelectrolyte multipayers for electrophoretic separations*. *Anal Chem*, 1999. **71**: p 4007-4013.
179. Kitagawa, F., Kamiya, M., Okamoto, Y., Taji, H., Onoue, S., Tsuda, Y., Otsuka, K., *Electrophoretic analysis of proteins and enantiomers using capillaries modified by a successive multiple ionic-polymer layer (SMIL) coating technique*. *Anal Bioanal Chem*, 2006. **386**: 594-601.
180. Chiou, C.-S., Shih, J.-S., *Bifunctional cryptand modifier for capillary electrophoresis in separation of inorganic/organic anions and inorganic cations*. *Analyst*, 1996. **121**: p 1107-1110.
181. Mori, M., Tsue, H., Tanaka, S., Tanaka, K., Haddad, P., *A new and selective capillary column coated with cationic diazacrown ether for separation of organic and inorganic anions by capillary electrophoresis*. *Electrophoresis*, 2003. **24**: p 1944-1950.
182. Luong, J.H.T., *Mixed-mode capillary electrokinetic separation of positional explosive isomers using sodium dodecyl sulfate and negative- β -cyclodextrin derivatives*. *J Chromatogr A*, 1998. **811**: p 225-232.
183. Terabe, S., Miyashita, Y., Shibata, O., *Separation of highly hydrophobic compounds by cyclodextrin-modified micellar electrokinetic chromatography*. *J Chromatogr*, 1990. **516**: p 23-31.
184. Funasaki, N., Yodo, H., Hada, S., Neya, S., *Stoichiometries and equilibrium constants of cyclodextrin-surfactant complexations*. *Bull Chem Soc Jpn*, 1992. **65**: p 1323-1330.
185. Astray, G., Cid, A., García-Río, L., Lodeiro, C., Mejuto, J.C., Moldes, O., Morales, J., *Cyclodextrin-surfactant mixed systems as reaction media*. *Prog React Kinet Mec*, 2010. **35**: p105-129.
186. Nishi, H., Matsuo, M., *Separation of corticosteroids and aromatic hydrocarbons by cyclodextrin-modified micellar electrokinetic chromatography*. *J Liq Chromatogr*, 1991. **14**: p 973-986.
187. Kwan, H.Y., Thormann, W., *Electrophoretically mediated microanalysis for characterization of the enantioselective CYP3A4 catalyzed N-demethylation of ketamine*. *Electrophoresis*, 2012. **33**: p 3299-3305.
188. Nehme, H., Nehme, R., Lafite, P., Routier, S., Morin, P., *New development in in-capillary electrophoresis techniques for kinetic and inhibition study of enzymes*. *Anal Chim Acta*, 2012. **722**: p127-135.
189. Kim, H.-Y., Gladyshev, V.N., *Different catalytic mechanisms in mammalian selenocysteine- and cysteine- containing methionine-R-sulfoxide reductases*. *PLoS Biology*, 2005. **3**: 2080-2089.
190. Kim, H.-Y., Fomenko, D.E., Yoon, Y.-E., Gladyshev, V.N., *Catalytic advantages provided by selenocysteine in methionine-S-sulfoxide reductases*. *Biochemistry*, 2006. **45**: p 13697-13704.

191. Wu, P., Zhang, Z., Guan, X., Li, Y., Zeng, J., Zhang, J., Long, Li., Hu, Z., Wang, F., Chen, J., *A specific and rapid colorimetric method to monitor the activity of methionine sulfoxide reductase A*. *Enzyme Microb Tech*, 2013. **53**: p 391-397.
192. Olry, A., Boschi-Muller, S., Marraud, M., Sanglier-Cianferani, S., Van Dorsselaar, A., Branlant, G., *Characterization of the methionine sulfoxide reductase activities of PILB, a probable virulence factor from Neisseria meningitidis*. *J Biol Chem*, 2002. **277**: p 12016-12022.
193. Antoine, M., Boschi-Muller, S., Branlant, G., *Kinetic characterization of the chemical steps involved in the catalytic mechanism of methionine sulfoxide reductase A from Neisseria meningitidis*. *J Biol Chem*, 2003. **278**: p 45352-45357.
194. Olry, A., Boschi-Muller, S., Branlant, G., *Kinetic characterization of the catalytic mechanism of methionine sulfoxide reductase B from Neisseria meningitidis*. *Biochemistry*, 2004. **43**: p 11616-11622.

Abbreviations

Ac	acetyl
Asp	aspartic acid
Asn	asparagin
BGE	background electrolyte
Ca²⁺/CaM	calcium/calmodulin
CD	cyclodextrin
CE	capillary electrophoresis
CEC	capillary electrochromatography
CEKC	capillary electrokinetic chromatography
CMC	critical micelle concentration
CM-β-CD	carboxymethyl-β-cyclodextrin
Cys	cysteine
CZE	capillary zone electrophoresis
dabsyl	4- <i>N,N</i> -dimethylaminoazobenzene-4'-sulfonyl
DTT	dithiothreitol
Dnp	2,4-dinitrophenyl
EOF	electroosmotic flow
EMMA	electrophoretically mediated microanalysis
ER	endoplasmic reticulum
FRMsr	free methionine-(<i>R</i>)-sulfoxide reductase
Fmoc	9-fluorenylmethoxycarbonyl
Gln	glutamine
Glu	glutamic acid
Grx	glutaredoxin
HPLC	high performance liquid chromatography
hMsrA	human methionine sulfoxide reductase
id	internal diameter
LOD	limit of detection

LOQ	limit of quantification
Lys	lysine
od	out diameter
MEKC	micelle electrokinetic chromatography
Met	L-methionine
Met(O)	L-methionine sulfoxide
Met-<i>R</i>-(O)	L-methionine- <i>R</i> -sulfoxide
Met-<i>S</i>-(O)	L-methionine- <i>S</i> -sulfoxide
Msr	methionine sulfoxide reductase
pI	isoelectric point
ROS	reactive oxygen species
RSD	relative standard deviation
SD	standard deviation
SDS	sodium dodecyl sulfate
Sec	Selenocysteine
SMIL	successive multiple ionic polymer layer
S/N	signal to noise ratio
TDLFP	trimethanolamine
TFA	trifluoroacetic acid
Tris	transverse diffusion of laminar flow profiles
Trx	thioredoxin
UV	ultraviolet
β-Ala	β-alanine

List of Publications and Presentations

Journal article

Capillary electrophoresis separation of peptide diastereomers that contain methionine sulfoxide by dual cyclodextrin-crown ether systems.

Q. Zhu, S.H. Heinemann, R. Schönherr, G. K. E. Scriba, *J. Sep. Sci.* 2014, 00, 1.

Experimental design-guided development of a stereospecific capillary electrophoresis assay for methionine sulfoxide reductase enzymes using a diastereomeric pentapeptide substrate.

Q. Zhu, X. Huo, S.H. Heinemann, R. Schönherr, R. El-Mergawy, G. K.E. Scriba, *J. Chromatogr. A* 2014, 1359, 224.

Stereospecific electrophoretically mediated microanalysis assay for methionine sulfoxide reductase enzymes.

Q. Zhu, R. G. El-Mergawy, S.H. Heinemann, R. Schönherr, P. Jáč, G. K. E. Scriba, *Anal. Bioanal. Chem.* 2014, 406, 1723.

Stereospecific micellar electrokinetic chromatography assay of methionine sulfoxide reductase enzymes employing a multiple layer coated capillary.

Q. Zhu, R. G. El-Mergawy, S.H. Heinemann, R. Schönherr, P. Jáč, G. K. E. Scriba, *Electrophoresis* 2013, 34, 2712.

16-Morpholino quaternary ammonium steroidal derivatives as neuromuscular blocking agents: Synthesis, biological evaluation and in silico probe of ligand-receptor interaction.

H. Hu, Z. Rao, J. Xu, **Q. Zhu**, H-J. Altenbach, H. Chen, D. Zhou, Y. Xiao, X. Ke, H. Guo, Z. Wu, P. Liu, X. Hu, *Euro. J. Med. Chem.* 2012 ,56, 332.

Book chapter

Enantiomer Separations by Capillary Electrophoresis. Book title: Capillary Electrophoresis: Method and Protocols. G. K. E. Scriba, H. Harnisch, **Q. Zhu**, Submitted, 2014

Oral presentations

25th Doktorandenseminar des AK Separation Science, 2015 in Hohenroda, title “Capillary electrophoresis-based Study of Methionine Sulfoxide Reductase”

Q. Zhu, S. H. Heinemann, R. Schönherr, G. K. E. Scriba

CE-Forum 2014, in Marburg, title “Stereospecific Capillary Electrophoresis Assay for Determination of Activities of Methionine Sulfoxide Reductase”

Q. Zhu, S. H. Heinemann, R. Schönherr, G. K. E. Scriba

GCCCD 2012 conferences, in Bonn, title “Capillary Electrophoresis-Based Study of Methionine Sulfoxide Reductase.

Q. Zhu, R. G. El-Mergawy, S. H. Heinemann, R. Schönherr, P. Jáč, G. K. E. Scriba

Poster presentations

CE-Forum 2013, in Jena, poster, title “Capillary Electrophoresis-Based Study of Methionine Sulfoxide Reductase”,

Q. Zhu, R. G. El-Mergawy, S. H. Heinemann, R. Schönherr, P. Jáč, G. K. E. Scriba

20th International Symposium on Separation Sciences, 2014 in Prague, poster, title “Experimental Design-guided Development of a Capillary Electrophoresis Assay for Methionine Sulfoxide Reductase using a Pentapeptide Substrate”

Q. Zhu, S. H. Heinemann, R. Schönherr, P. Jáč, G. K. E. Scriba

Curriculum Vitae

- Personal details:** Name: Qingfu Zhu
Date of birth/Nationality: October 16, 1985/ Chinese
Marital status: Married
- Education:**
- | | |
|----------------|-----------------------------------------------------------------------------|
| Since Nov 2011 | PhD candidate, School of Pharmacy,
Friedrich-Schiller University Jena; |
| 2011 | M.Sc.in School of Pharmacy, Wuhan University |
| 2008 | B.Ag. in Plant Science and Technology,
Huazhong Agricultural University; |
| 2008 | B.Sc. in School of Pharmacy,
Wuhan University (minor); |
- Fellowship:**
- | | |
|-------------------|-------------------------------------------------------|
| Oct 2014-Sep 2015 | Wissenschaftlicher Mitarbeiter at University of Jena; |
| Nov 2011-Sep 2014 | Scholarship from China Scholarship Council; |
- Work experience:**
- | | |
|--------------------|-------------------------------------------------------------------------------------------------------------------------------------------------------------------|
| Since October 2014 | Teaching assistant at Department of
Pharmaceutic Chemisty, University of Jena;
(Praktikum: Quantitative Bestimmung von Arznei-,
Hilfs- und Schadstoffen) |
|--------------------|-------------------------------------------------------------------------------------------------------------------------------------------------------------------|
- Membership:**
- | | |
|--------------------|------------------------------------------------------------------------------------------------|
| Since October 2014 | Board member of Gesellschaft Chinesischer
Chemiker und Chemieingenieure in Deutschland e.V. |
|--------------------|------------------------------------------------------------------------------------------------|

Eigenständigkeitserklärung

Hiermit erkläre ich, dass mir die geltende Promotionsordnung der Fakultät bekannt ist, und ich die vorliegende Arbeit selbstständig und nur unter Verwendung der angegebenen Hilfsmittel und Literatur angefertigt und bisher keiner anderen Hochschule als Dissertation oder Prüfungsarbeit vorgelegt habe. Ich habe weder die Hilfe eines Promotionsberaters in Anspruch genommen, noch unmittelbar oder mittelbar geldwerte Leistungen in Zusammenhang mit dem Inhalt meiner Dissertation an Dritte erbracht.

Jena, den

Ort, Datum

Qingfu Zhu

